LBNL-57952

ECO2N: A TOUGH2 Fluid Property Module for Mixtures of Water, NaCl, and CO_2

Karsten Pruess

Earth Sciences Division, Lawrence Berkeley National Laboratory
University of California, Berkeley, CA 94720

August 2005

This work was supported by the Director, Office of Science, Office of Basic Energy Sciences of the U.S. Department of Energy and by the Zero Emission Research and Technology project (ZERT) under Contract No. DE-AC03-76SF00098.

Abstract

ECO2N is a fluid property module for the TOUGH2 simulator (Version 2.0) that was designed for applications to geologic sequestration of CO_2 in saline aquifers. It includes a comprehensive description of the thermodynamics and thermophysical properties of H_2O - NaCl - CO_2 mixtures, that reproduces fluid properties largely within experimental error for the temperature, pressure and salinity conditions of interest (10 $^{\circ}C \leq T \leq 110\ ^{\circ}C$; $P \leq 600$ bar; salinity up to full halite saturation). Flow processes can be modeled isothermally or non-isothermally, and phase conditions represented may include a single (aqueous or CO_2-rich) phase, as well as two-phase mixtures. Fluid phases may appear or disappear in the course of a simulation, and solid salt may precipitate or dissolve. This report gives technical specifications of ECO2N and includes instructions for preparing input data. Code applications are illustrated by means of several sample problems, including problems that had been previously investigated in a code intercomparison study.

TABLE OF CONTENTS

LIST OF FIGURES vii

LIST OF TABLES xi

1. INTRODUCTION 1

2. FLUID PHASES AND THERMODYNAMIC VARIABLES IN THE SYSTEM WATER-NaCl-CO_2 3

2.1 Phase Composition 7

2.2 Phase Change 10

2.3 Conversion of Units 11

3. THERMOPHYSICAL PROPERTIES OF WATER-NaCl-CO_2 Mixtures 13

3.1 Density 14

3.2 Viscosity 16

3.3 Specific Enthalpy 16

4. PREPARATION OF INPUT DATA 18

4.1 Initialization Choices 18

4.2 Permeability Change from Precipitation and Dissolution of Salt 20

4.3 Choice of Program Options 22

5. SAMPLE PROBLEMS 24

5.1 Problem No. 1 (*rtab*) - Demonstration of Initialization Options 24

5.2 Problem No. 2 (*rcc3*) - Radial Flow from a CO_2 Injection Well 28

5.3 Problem No. 3 (*r1dv*) - CO_2 Discharge Along a Fault Zone 37

5.4 Problem No. 4 (*rtp7*) - CO_2 Injection into a 2-D Layered Brine Formation 46

6. CONCLUDING REMARKS 56

ACKNOWLEDGEMENT 56

REFERENCES 57

APPENDIX A. Code Intercomparison Problem 3: Radial Flow from a CO_2 Injection Well 59

APPENDIX B. Code Intercomparison Problem 4: CO_2 Discharge Along a Fault Zone 61

APPENDIX C. Code Intercomparison Problem 7: CO_2 Injection into a 2-D Layered Brine Formation 63

LIST OF FIGURES

Figure 1. Possible phase combinations in the system water-CO_2 3

Figure 2. Phase states of CO_2 4

Figure 3. Dissolved CO_2 mass fractions at T = 30 ˚C for pure water (0m) and 4-molar NaCl brine 8

Figure 4. H_2O mass fractions in gas at T = 30 ˚C for pure water (0m) and 4-molar NaCl brine 8

Figure 5. Concentration of water in gas and CO_2 in the liquid (aqueous) phase for salinities ranging from zero to fully saturated 9

Figure 6. CO_2 phase partitioning in the system H_2O - NaCl - CO_2 10

Figure 7. Schematic of the temperature-pressure tabulation of CO_2 properties 14

Figure 8. Model for converging-diverging pore channels 20

Figure 9. Porosity-permeability relationship for tubes-in-series model 21

Figure 10. TOUGH2/ECO2N input file for sample problem 1 - demonstration of initialization options 24

Figure 11. Primary variables internally used in ECO2N for the INCON data given in Fig. 10 26

Figure 12. Output data for sample problem 1 27

Figure 13. Schematic of sample problem 2 28

Figure 14. TOUGH2 input file for grid generation for radial injection problem 29

Figure 15. Modified MESH file for radial injection problem 29

Figure 16. TOUGH2 input file for radial injection problem 30

Figure 17. Part of printed output for radial flow problem 31

Figure 18. Simulated pressures as a function of the similarity variable 33

Figure 19. Simulated gas saturations 34

Figure 20. Simulated solid saturations 34

Figure 21. Simulated CO_2 mass fraction in aqueous phase 35

Figure 22. Simulated NaCl mass fraction in aqueous phase 35
Figure 23. Simulated water mass fraction in CO_2-rich phase 36
Figure 24. TOUGH2 input file for fault zone problem 38
Figure 25. Part of printed output for fault leakage problem 40
Figure 26. Simulated CO_2 fluxes at bottom and top of fault zone 42
Figure 27. Simulated water flux at top of fault zone 43
Figure 28. Gas saturation profiles at times of 10^7 and 10^9 seconds 43
Figure 29. Pressure profiles at times of 10^7 and 10^9 seconds 44
Figure 30. Dissolved CO_2 mass fraction in aqueous phase (top) and dissolved water mass fraction in gas (bottom) after 10^7 s 45
Figure 31. Code fragment of subroutine GXYZ, modified for sand-shale medium 46
Figure 32. TOUGH2 input file for CO2 injection into a 2-D layered brine formation 48
Figure 33. Part of printed output for problem of CO2 injection into a layered brine formation 49
Figure 34. Time evolution of pressures in two grid blocks and time stepping 51
Figure 35. Gas flow rates at the well block 51
Figure 36. Gas saturations at the well block and its neighbors 52
Figure 37. Phase saturations at the well block 52
Figure 38. Absolute values of aqueous phase flow rates between the well block and neighboring grid blocks 53
Figure 39. Solid saturations in the well block and its neighbors 53
Figure 40. Contour map of fluid pressures after 2 years of CO_2 injection 54
Figure 41. Contour map of gas saturations after 2 years of CO_2 injection 54
Figure 42. Contour map of dissolved CO_2 mass fractions after 2 years of CO_2 injection 55
Figure B.1 Schematic of the fault zone model (a) and applied boundary conditions (b) 61
Figure C.1 Schematic representation of geometry for CO_2 injection in Utsira Formation 64

LIST OF TABLES

Table 1.	Summary of ECO2N	6
Table 2.	Molecular weights in the system H_2O–NaCl–CO_2	12
Table 3.	Parameters for molar volume of dissolved CO_2	15
Table 4.	PVT properties at a temperature of 45 ˚C at selected pressures, as used in the TOUGH2/ECO2N simulation	39
Table 5.	CO_2 inventory	41
Table 6.	MESHMAKER input data for grid generation	47
Table 7.	CO_2 inventory for injection into a saline 2-D layered system	55
Table A.1	Hydrogeologic parameters	60
Table A.2	Initial conditions and injection specifications	60
Table C.1	Initial conditions and injection specifications	64
Table C.2	Hydrogeologic parameters	66

1. Introduction

Injection of CO_2 into saline formations has been proposed as a means whereby emissions of heat-trapping greenhouse gases into the atmosphere may be reduced. Such injection would induce coupled processes of multiphase fluid flow, heat transfer, chemical reactions, and mechanical deformation. Several groups have developed simulation models for subsets of these processes. The present report describes a fluid property module "ECO2N" for the general-purpose reservoir simulator TOUGH2 (Pruess et al., 1999; Pruess, 2004), that can be used to model non-isothermal multiphase flow in the system H_2O - NaCl - CO_2. TOUGH2/ECO2N represents fluids as consisting of two phases: a water-rich aqueous phase, herein often referred to as "liquid," and a CO_2-rich phase referred to as "gas." In addition, solid salt may also be present. The only chemical reactions modeled by ECO2N include equilibrium phase partitioning of water and carbon dioxide between the liquid and gaseous phases, and precipitation and dissolution of solid salt. The partitioning of H_2O and CO_2 between liquid and gas phases is modeled as a function of temperature, pressure, and salinity, using the recently developed correlations of Spycher and Pruess (2005). Dissolution and precipitation of salt is treated by means of local equilibrium solubility. Associated changes in fluid porosity and permeability may also be modeled. All phases - gas, liquid, solid - may appear or disappear in any grid block during the course of a simulation. Thermodynamic conditions covered include a temperature range from ambient to 100 ˚C (approximately), pressures up to 600 bar, and salinity from zero to fully saturated. These parameter ranges should be adequate for most conditions encountered during disposal of CO_2 into deep saline aquifers.

ECO2N is written in Fortran 77 and is "plug-compatible" with TOUGH2, Version 2.0. The code is intrinsically single-precision, but requires 64-bit arithmetic, which on 32-bit processors (PCs and workstations) may be realized by using compiler options for generating 64-bit arithmetic. For example, on an IBM RS/6000 computer, this may be accomplished with the compiler option "-qautodbl=dblpad". ECO2N may be linked with standard TOUGH2 modules like any of the fluid property modules included in the TOUGH2 V 2.0 package. As an example, we list the linking instruction that would be used on an IBM RS/6000 workstation.

```
f77 -o zco2n t2cg22.o meshm.o eco2n.o t2f.o t2solv.o ma28.o
```

Execution of an input file *rcc3* would be made with the command

```
zco2n <rcc3 >rcc3.out
```

The present report is a user's guide for the TOUGH2/ECO2N simulator. Information provided in the TOUGH2 users' guide (Pruess et al., 1999) is not duplicated here. We begin with a discussion of phase conditions and thermodynamic variables in the system H_2O - NaCl - CO_2, for conditions of interest in geologic sequestration of CO_2. This is followed by a discussion of our thermophysical property model, and guidance for preparing input data. Several sample problems are provided which document code performance and serve as a tutorial for applications.

2. Fluid Phases and Thermodynamic Variables in the System Water-NaCl-CO_2

In the two-component system water-CO_2, at temperatures above the freezing point of water and not considering hydrate phases, three different fluid phases may be present: an aqueous phase that is mostly water but may contain some dissolved CO_2, a liquid CO_2-rich phase that may contain some water, and a gaseous CO_2-rich phase that also may contain some water. Altogether there may be seven different phase combinations (Fig. 1). If NaCl ("salt") is added as a third fluid component, the number of possible phase combinations doubles, as in each of the seven phase combinations depicted in Fig. 1 there may or may not be an additional phase consisting of solid salt. Liquid and gaseous CO_2 may coexist along the saturated vapor pressure curve of CO_2, which ends at the critical point (T_{crit}, P_{crit}) = (31.04 ˚C, 73.82 bar; Vargaftik, 1975), see Fig. 2. At supercritical temperatures or pressures there is just a single CO_2-rich phase.

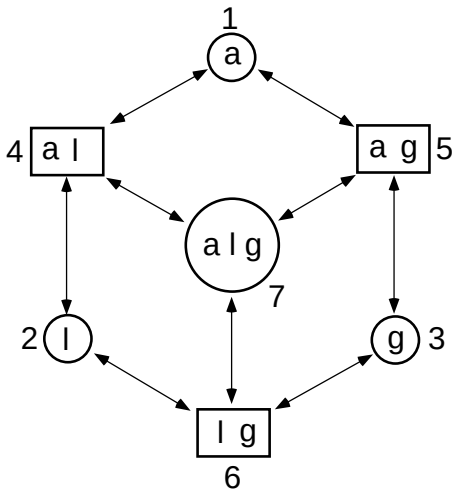

Figure 1. Possible phase combinations in the system water-CO_2. The phase designations are a - aqueous, l - liquid CO_2, g - gaseous CO_2. Separate liquid and gas phases exist only at subcritical conditions.

The present version of ECO2N can only represent a limited subset of the phase conditions depicted in Fig. 1. Thermophysical properties are accurately calculated for gaseous as well as for liquid CO_2, but no distinction between gaseous and liquid CO_2 phases is made in the treatment of flow, and no phase change between liquid and gaseous CO_2 is treated. Accordingly, of the seven phase combinations shown in Fig. 1, ECO2N can represent the ones numbered 1 (single-phase aqueous with or without dissolved CO_2 and salt), 2 and 3 (a single CO_2-rich phase that may be either liquid or gaseous CO_2, and may include dissolved water), and 4 and 5 (two-phase conditions consisting of an aqueous and a single CO_2-rich phase, with no distinction being made as to whether the CO_2-rich phase is liquid or gas). ECO2N cannot represent conditions 6 (two-phase mixture of

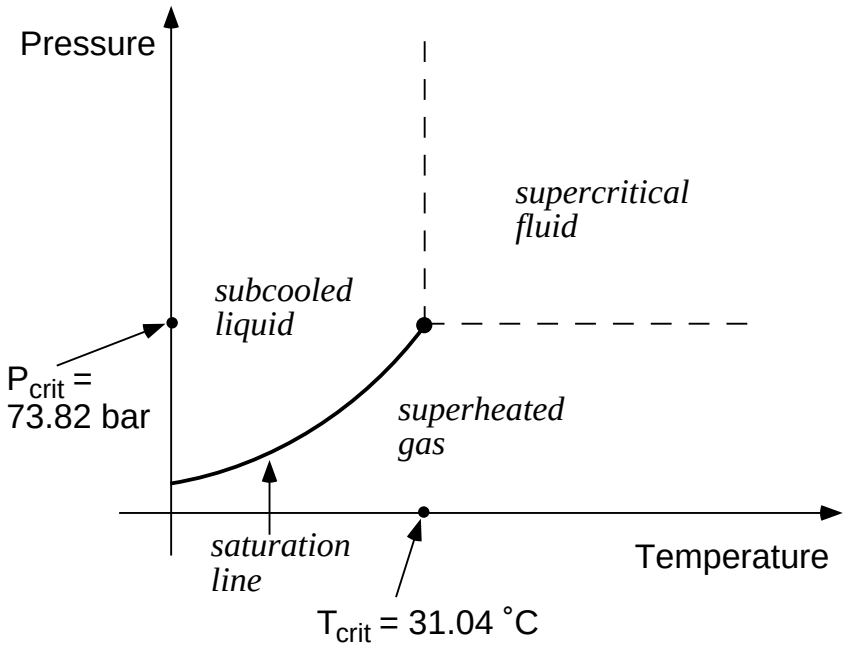

Figure 2. Phase states of CO_2.

liquid and gaseous CO_2) and 7 (three-phase). All sub- and super-critical CO_2 is considered as a single non-wetting phase, that will henceforth be referred to as "gas." ECO2N may be applied to sub- as well as super-critical temperature and pressure conditions, but applications that involve sub-critical conditions are limited to systems in which there is no change of phase between liquid and gaseous CO_2, and in which no mixtures of liquid and gaseous CO_2 occur.

Numerical modeling of the flow of brine and CO_2 requires a coupling of the phase behavior of water-salt-CO_2 mixtures with multiphase flow simulation techniques. Among the various issues raised by such coupling is the choice of notation. There are long-established notational conventions in both fields, which may lead to conflicts and misunderstandings when they are combined. In an effort to avoid confusion, we will briefly discuss notational issues pertaining to partitioning of CO_2 between an aqueous and a gaseous phase.

Phase partitioning is usually described in terms of mole fractions of the two components, which are denoted by x and y, respectively, where $x_1 = x_{H2O}$ and $x_2 = x_{CO2}$ specify mole fractions in the aqueous phase, while $y_1 = y_{H2O}$ and $y_2 = y_{CO2}$ give mole fractions in the gas phase (Prausnitz et al., 1986; Spycher et al., 2003). We follow this notation, except that we add the subscript "eq" to emphasize that these mole fractions pertain to equilibrium partitioning of water and CO_2 between co-existing aqueous and gas phases. Accordingly, we denote the various mole

fractions pertaining to equilibrium phase partitioning as $x_{1,eq}$, $x_{2,eq}$, $y_{1,eq}$, and $y_{2,eq}$, while the corresponding mass fractions are denoted using upper-case X and Y. Mass fractions corresponding to single-phase conditions, where water and CO_2 concentrations are not constrained by phase equilibrium relations, are denoted by X_1 (for water) and X_2 (for CO_2) in the aqueous phase, and by Y_1 and Y_2 in the gas phase.

In the numerical simulation of brine-CO_2 flows, we will be concerned with the fundamental thermodynamic variables that characterize the brine-CO_2 system, and their change with time in different subdomains (grid blocks) of the flow system. Four "primary variables" are required to define the state of water-NaCl-CO_2 mixtures, which according to conventional TOUGH2 useage are denoted by X1, X2, X3, and X4. A summary of the fluid components and phases modeled by ECO2N, and the choice of primary thermodynamic variables, appears in Table 1. Different variables are used for different phase conditions, but two of the four primary variables are the same, regardless of the number and nature of phases present. This includes the first primary variable X1, denoting pressure, and the fourth primary variable X4 which is temperature. The second primary variable pertains to salt and is denoted X_{sm} rather than X2 to avoid confusion with X_2, the CO_2 mass fraction in the liquid phase. Depending upon whether or not a precipitated salt phase is present, the variable X_{sm} has different meaning. When no solid salt is present, X_{sm} denotes X_s, the salt mass fraction referred to the two-component system water-salt. When solid salt is present, X_s is no longer an independent variable, as it is determined by the equilibrium solubility of NaCl, which is a function of temperature. In the presence of solid salt, for reasons that are explained below, we use as second primary variable the quantity "solid saturation plus ten," $X_{sm} = S_s + 10$. Here, S_s is defined in analogy to fluid saturations and denotes the fraction of void space occupied by solid salt.

The physical range of both X_s and S_s is (0, 1); the reason for defining X_{sm} by adding a number 10 to S_s is to enable the presence or absence of solid salt to be recognized simply from the numerical value of the second primary variable. As had been mentioned above, the salt concentration variable X_s is defined with respect to the two-component system H_2O - NaCl. This choice makes the salt concentration variable independent of CO_2 concentration, which simplifies the calculation of the partitioning of the H_2O and CO_2 components between the aqueous and gas phases (see below). In the three-component system H_2O - NaCl - CO_2, the total salt mass fraction in the aqueous phase will for given X_s of course depend on CO_2 concentration. Salt mass fraction in the two-component system H_2O - NaCl can be expressed in terms of salt molality (moles m of salt per kg of water) as follows.

Table 1. Summary of ECO2N

Components	# 1: water # 2: NaCl # 3: CO_2
Parameter choices	
(NK, NEQ, NPH, NB) =	(3, 4, 3, 6) water, NaCl, CO_2, nonisothermal (default) (3, 3, 3, 6) water, NaCl, CO_2, isothermal molecular diffusion can be modeled by setting NB = 8
Primary Variables	
single fluid phase (only aqueous, or only gas)#	(P, X_{sm}, X3, T)
P - pressure	
X_{sm} - salt mass fraction X_s in two-component water-salt system, or solid saturation S_s+10	
X3 - CO_2 mass fraction in the aqueous phase, or in the gas phase, in the three-component system water-salt-CO_2	
T - temperature	
two fluid phases (aqueous and gas)#	(P, X_{sm}, S_g+10, T)
P - pressure	
X_{sm} - salt mass fraction X_s in two-component water-salt system, or solid saturation S_s+10	
S_g - gas phase saturation	
T - temperature	

When discussing fluid phase conditions, we refer to the potentially mobile (aqueous and gas) phases only; in all cases solid salt may precipitate or dissolve, adding another active phase to the system.

$$X_s = \frac{m M_{NaCl}}{1000 + m M_{NaCl}} \tag{1}$$

Here M_{NaCl} = 58.448 is the molecular weight of NaCl, and the number 1000 appears in the denominator because molality is defined as moles per 1000 g of water. For convenience we also list the inverse of Eq. (1).

$$m = \frac{1000 X_s / M_{NaCl}}{1 - X_s} \tag{2}$$

The third primary variable X3 is CO_2 mass fraction (X_2) for single-phase conditions (only aqueous, or only gas) and is "gas saturation plus ten" ($S_g + 10$) for two-phase (aqueous and gas) conditions. The reason for adding 10 to S_g is analogous to the conventions adopted for the second primary variable, namely, to be able to distinguish single-phase conditions ($0 \leq X3 \leq 1$) from two-phase conditions ($10 \leq X3 \leq 11$). In single-phase conditions, the CO2 concentration variable X_2 is "free," i.e., it can vary continuously within certain parameter ranges, while in two-phase aqueous-gas conditions, X_2 has a fixed value $X_{2,eq}$ that is a function of temperature, pressure, and salinity (see below). Accordingly, for single-phase conditions X_2 is included among the independent primary variables (= X3), while for two-phase conditions, X_2 becomes a "secondary" parameter that is dependent upon primary variables (T, P, X_s). "Switching" primary variables according to phase conditions present provides a very robust and stable technique for dealing with changing phase compositions; see Section 2.2, below.

Initialization of a simulation with TOUGH2/ECO2N would normally be made with the internally used primary variables as listed in Table 1. For convenience of the user, additional choices are available for initializing a flow problem; see Section 4, below.

2.1 Phase Composition

The partitioning of H_2O and CO_2 among co-existing aqueous and gas phases is calculated from a slightly modified version of the correlations developed in (Spycher and Pruess, 2005). These correlations were derived from the requirement that chemical potentials of all components must be equal in different phases. For two-phase conditions, they predict the equilibrium composition of liquid (aqueous) and gas (CO2-rich) phases as functions of temperature, pressure, and salinity, and are valid in the temperature range 12 ˚C ≤ T ≤ 110 ˚C, for pressures up to 600 bar, and salinity up to saturated NaCl brines. In the indicated parameter range, mutual solubilities of H_2O and CO_2 are calculated with an accuracy typically within experimental uncertainties. The modification made in ECO2N is that CO_2 molar volumes are calculated using a tabular EOS based on Altunin's correlation (1975), instead of the Redlich-Kwong equation of state used in (Spycher and Pruess, 2005). This was done to maintain consistency with the temperature and pressure conditions for phase change between liquid and gaseous conditions used elsewhere in ECO2N. Altunin's correlations yield slightly different molar volumes than the Redlich-Kwong EOS whose parameters were fitted by Spycher and Pruess (2005) to obtain the best overall match between observed and predicted CO_2 concentrations in the aqueous phase. The (small) differences in Altunin's molar volumes cause predictions for the mutual solubility of water and CO_2 to be somewhat different also. However, the differences are generally small, see Figs. 3-5.

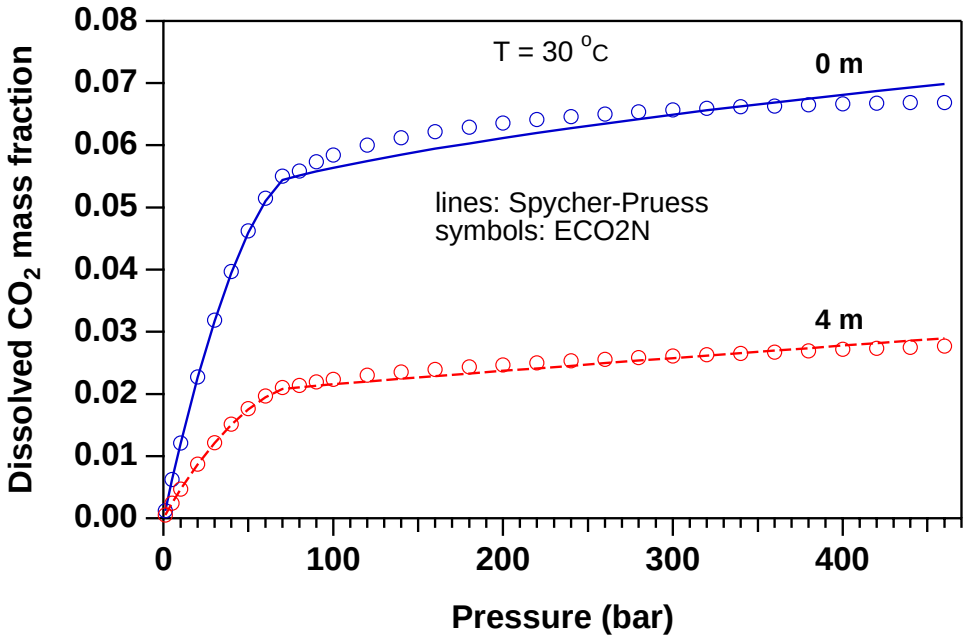

Figure 3. Dissolved CO_2 mass fractions in two-phase system at T = 30 ˚C for pure water (0m) and 4-molal NaCl brine. Lines represent the original correlation of Spycher and Pruess (2005) that uses a Redlich-Kwong EOS for molar volume of CO_2. Symbols represent data calculated by ECO2N in which the molar volume of CO_2 is obtained from the correlations of Altunin (1975).

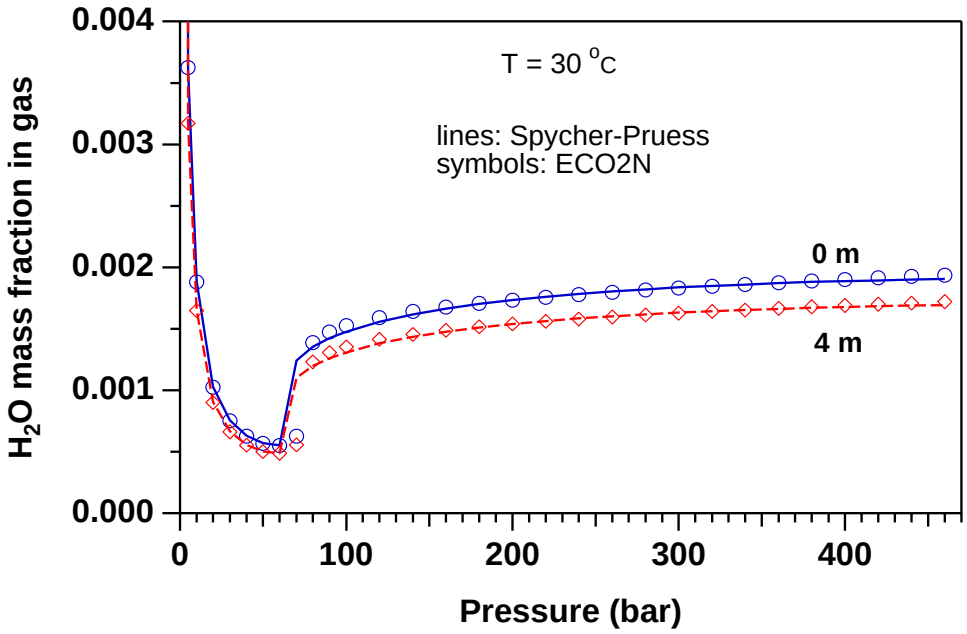

Figure 4. H_2O mass fractions in gas in two-phase system at T = 30 ˚C for pure water (0m) and 4-molal NaCl brine. Lines represent the original correlation of Spycher and Pruess (2005) that uses a Redlich-Kwong EOS for molar volume of CO_2. Symbols represent data calculated by ECO2N in which the molar volume of CO_2 is obtained from the correlations of Altunin (1975).

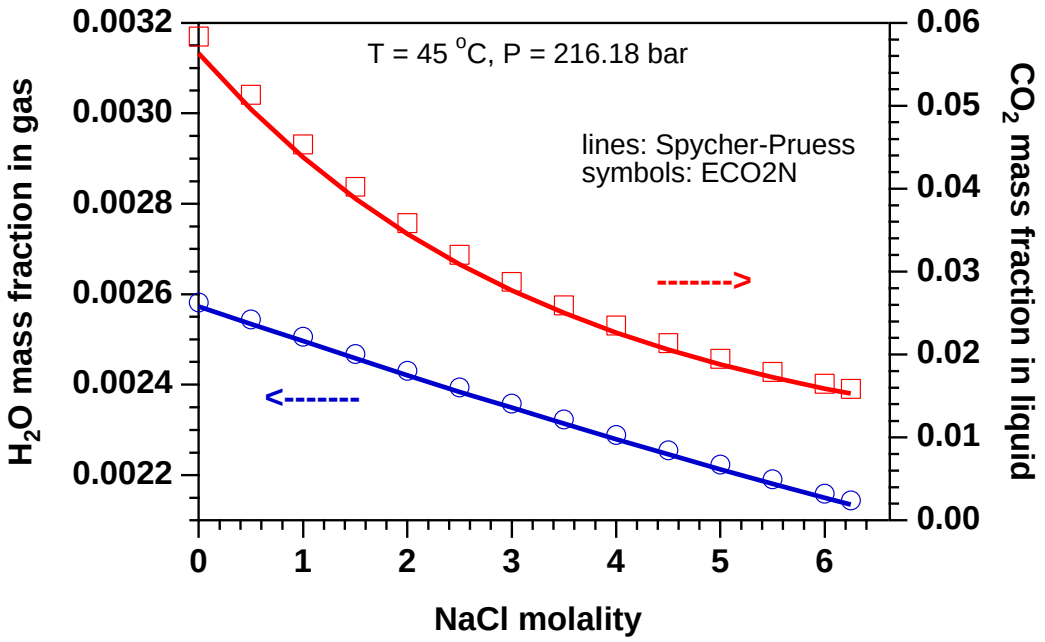

Figure 5. Concentration of water in gas and CO_2 in the liquid (aqueous) phase at (T, P) = (45 ˚C, 216.18 bar), for salinities ranging from zero to fully saturated. Lines were calculated from the correlation of Spycher and Pruess (2005) that uses a Redlich-Kwong EOS for molar volume of CO_2. Symbols represent data calculated by ECO2N from a modified correlation in which the molar volume of CO_2 is obtained from the correlations of Altunin (1975).

For conditions of interest to geologic dispoal of CO_2, equilibrium between aqueous and gas phases corresponds to a dissolved CO_2 mass fraction in the aqueous phase, $X_{2,eq}$, on the order of a few percent, while the mass fraction of water in the gas phase, $Y_{1,eq}$, is a fraction of a percent, so that gas phase CO_2 mass fraction $Y_{2,eq} = 1 - Y_{1,eq}$ is larger than 0.99. The relationship between CO_2 mass fraction X3 and phase composition of the fluid mixture is as follows (see Fig. 6)

- $X3 < X_{2,eq}$ corresponds to single-phase liquid conditions;
- $X3 > Y_{2,eq}$ corresponds to single-phase gas;
- intermediate values ($X_{2,eq} \le X3 \le Y_{2,eq}$) correspond to two-phase conditions with different proportions of aqueous and gas phases.

Dissolved NaCl concentrations may for typical sequestration conditions range as high as 6.25 molal. This corresponds to mass fractions of up to X_{sm} = 26.7 % in the two-component system water-salt. Phase conditions as a function of X_{sm} are as follows.

- $X_{sm} \le$ XEQ corresponds to dissolved salt only;
- $X_{sm} >$ XEQ corresponds to conditions of a saturated NaCl brine and solid salt.

Here XEQ denotes the equilibrium solubility of NaCl, which in ECO2N is evaluated as in EWASG (Battistelli et a., 1997) as a function of temperature, using an equation by Potter cited in Chou (1987). No dependence of XEQ on CO_2 concentration is taken into account.

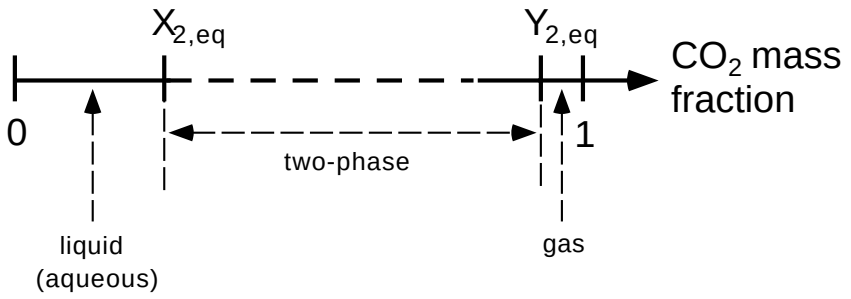

Figure 6. CO_2 phase partitioning in the system H_2O - NaCl - CO_2. The CO_2 mass fraction in brine-CO_2 mixtures can vary in the range from 0 (no CO_2) to 1 (no brine). $X_{2,eq}$ and $Y_{2,eq}$ denote, respectively, the CO_2 mass fractions in aqueous and gas phases corresponding to equilibrium phase partitioning in two-phase conditions. Mass fractions less than $X_{2,eq}$ correspond to conditions in which only an aqueous phase is present, while mass fractions larger than $Y_{2,eq}$ correspond to single-phase gas conditions. Mass fractions intermediate between $X_{2,eq}$ and $Y_{2,eq}$ correspond to two-phase conditions with different proportions of aqueous and gas phases.

2.2 Phase Change

In single-phase (aqueous or gas) conditions, the third primary variable X3 is the CO_2 mass fraction in that phase. In single-phase aqueous conditions, we must have $X3 \leq X_{2,eq}$, while in single-phase gas conditions, we must have $X3 \geq Y_{2,eq}$. The possibility of phase change is evaluated during a simulation by monitoring X3 in each grid block. The criteria for phase change from single-phase to two-phase conditions may be written as follows.

- single-phase aqueous conditions: a transition to two-phase conditions (evolution of a gas phase) will occur when $X3 > X_{2,eq}$;
- single-phase gas conditions: a transition to two-phase conditions (evolution of an aqueous phase) will occur when $X3 < Y_{2,eq} = 1\text{-}Y_{1,eq}$.

When two-phase conditions evolve in a previously single-phase grid block, the third primary variable is switched to $X3 = S_g+10$. If the transition occurred from single-phase liquid conditions, the starting value of S_g is chosen as 10^{-6}; if the transition occurred from single-phase gas, the starting value is chosen as $1 - 10^{-6}$.

In two-phase conditions, the third primary variable is $X3 = S_g+10$. For two-phase conditions to persist, X3 must remain in the range $(10, 11 - S_s)$. Transitions to single-phase conditions are recognized as follows.

- if X3 < 10 (i.e., $S_g < 0$): gas phase disappears; make a transition to single-phase liquid conditions;
- if X3 > 11 - S_s (i.e., $S_g > 1 - S_s$): liquid phase disappears; make a transition to single-phase gas conditions.

Phase change involving (dis-)appearance of solid salt is recognized as follows. When no solid salt is present, the second primary variable X_{sm} is the concentration (mass fraction referred to total water plus salt) of dissolved salt in the aqueous phase. The possibility of precipitation starting is evaluated by comparing X_{sm} with XEQ, the equilibrium solubility of NaCl at prevailing temperature. If $X_{sm} \leq$ XEQ no precipitation occurs, whereas for $X_{sm} >$ XEQ precipitation starts. In the latter case, variable X_{sm} is switched to S_s+10, where solid saturation S_s is initialized with a small non-zero value (10^{-6}). If a solid phase is present, the variable $X_{sm} = S_s$+10 is monitored. Solid phase disappears if $X_{sm} < 10$, in which case primary variable X_{sm} is switched to salt concentration, and is initialized as slightly below saturation, $X_{sm} =$ XEQ - 10^{-6}.

2.3 Conversion of Units

The Spycher and Pruess (2005) model for phase partitioning in the system H_2O–NaCl–CO_2 is formulated in molar quantities (mole fractions and molalities), while TOUGH2/ECO2N describes phase compositions in terms of mass fractions. This section presents the equations and parameters needed for conversion between the two sets of units. The conversion between various concentration variables (mole fractions, molalities, mass fractions) does not depend upon whether or not concentrations correspond to equilibrium between liquid and gas phases; accordingly, the relations given below are valid regardless of the magnitude of concentrations.

Let us consider an aqueous phase with dissolved NaCl and CO_2. For a solution that is m-molal in NaCl and n-molal in CO_2, total mass per kg of water is

$$M = 1000\ (\text{g } H_2O) + m\ M_{NaCl}\ (\text{g NaCl}) + n\ M_{CO2}\ (\text{g } CO_2) \tag{3}$$

where M_{NaCl} and M_{CO2} are the molecular weights of NaCl and CO_2, respectively (see Table 2). Assuming NaCl to be completely dissociated, the total moles per kg of water are

$$m_T = 1000/M_{H2O} + 2m + n \tag{4}$$

The Spycher and Pruess (2005) correlations provide CO_2 mole fraction x_2 in the aqueous phase and H_2O mole fraction y_1 in the gas phase as functions of temperature, pressure, and salt

concentration (molality). For a CO_2 mole fraction x_2 we have $n = x_2 m_T$ from which, using Eq. (4), we obtain

$$n = \frac{x_2\left(2m + 1000/M_{H2O}\right)}{1 - x_2} \tag{5}$$

CO_2 mass fraction X_2 in the aqueous phase is obtained by dividing the CO_2 mass in n moles by the total mass,

$$X_2 = \frac{n M_{CO2}}{1000 + m M_{NaCl} + n M_{CO2}} \tag{6}$$

Water mass fraction Y_1 in the CO_2-rich phase is simply

$$Y_1 = \frac{y_1 \cdot M_{H2O}}{y_1 \cdot M_{H2O} + (1 - y_1) M_{CO2}} \tag{7}$$

The molecular weights of the various species are listed in Table 2 (Evans, 1982).

Table 2. Molecular weights in the system H_2O–NaCl–CO_2.

species	mol. weight
H_2O	18.016
Na	22.991
Cl	35.457
NaCl	58.448
CO_2	44.0

3. Thermophysical Properties of Water-NaCl-CO_2 Mixtures

Thermophysical properties needed to model the flow of water-salt-CO_2 mixtures in porous media include density, viscosity, and specific enthalpy of the fluid phases as functions of temperature, pressure, and composition, and partitioning of components among the fluid phases. Many of the needed parameters are obtained from the same correlations as were used in the EWASG property module of TOUGH2 (Battistelli et al., 1997). EWASG was developed for geothermal applications, and consequently considered conditions of elevated temperatures > 100 ˚C, and modest CO_2 partial pressures of order 1-10 bar. The present ECO2N module targets the opposite end of the temperature and pressure range, namely, modest temperatures below 110 ˚C, and high CO_2 pressures up to several hundred bar.

Water properties in TOUGH2/ECO2N are calculated, as in other members of the TOUGH family of codes, from the steam table equations as given by the International Formulation Committee (1967). Properties of pure CO_2 are obtained from correlations developed by Altunin et al. (1975). We began using Altunin's correlations in 1999 when a computer program implementing them was conveniently made available to us by Victor Malkovsky of the Institute of Geology of Ore Deposits, Petrography, Mineralogy and Geochemistry (IGEM) of the Russian Academy of Sciences, Moscow. Altunin's correlations were subsequently extensively cross-checked against experimental data and alternative PVT formulations, such as Span and Wagner (1996). They were found to be very accurate (García, 2003), so there is no need to change to a different formulation.

Altunin's correlations are not used directly in the code, but are used ahead of a TOUGH2/ECO2N simulation to tabulate density, viscosity, and specific enthalpy of pure CO_2 on a regular grid of (T, P)-values. These tabular data are provided to the ECO2N module in a file called "CO2TAB," and property values are obtained during the simulation by means of bivariate interpolation. Fig. 7 shows the manner in which CO_2 properties are tabulated, intentionally showing a coarse (T, P)-grid so that pertinent features of the tabulation may be better seen. (For actual calculations, we use finer grid spacings; the CO2TAB data file distributed with ECO2N covers the range 3.04 ˚C ≤ T ≤ 103.04 ˚C with ΔT = 2 ˚C and 1 bar ≤ P ≤ 600 bar with $\Delta P \leq 4$ bar in most cases. The ECO2N distribution includes a utility program for generating CO2TAB files if users desire a different T,P-range or different increments.) As shown in Fig. 7, the tabulation is made in such a way that for sub-critical conditions the saturation line is given by diagonals of the interpolation quadrangles. On the saturation line, two sets of data are provided, for liquid and gaseous CO_2, respectively, and in quadrangles that include points on both sides of the saturation line, points on the "wrong" side are excluded from the interpolation. This scheme provides for an efficient and accurate determination of thermophysical properties of CO_2.

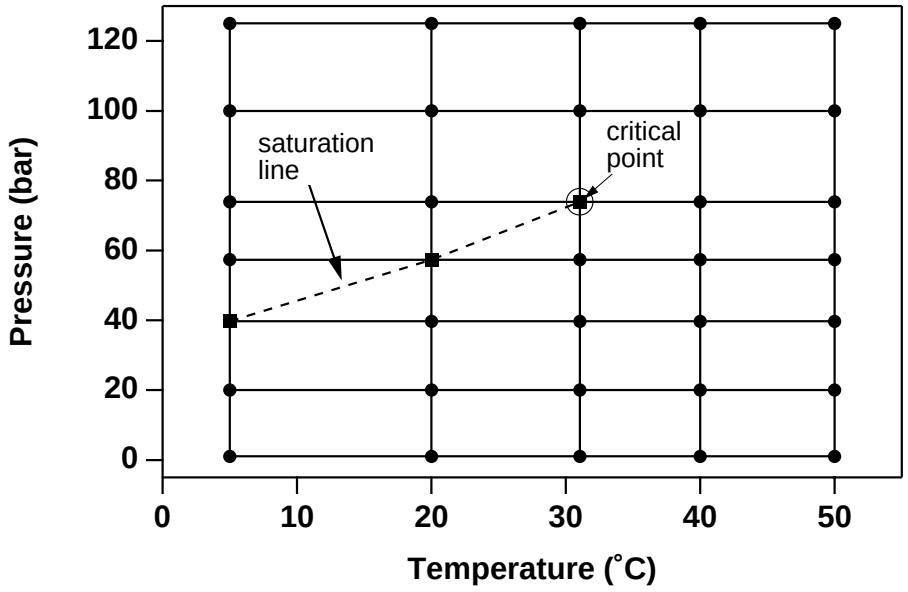

Figure 7. Schematic of the temperature-pressure tabulation of CO_2 properties. The saturation line (dashed) is given by the diagonals of interpolation rectangles.

An earlier version of ECO2N explicitly associated partial pressures of water (vapor) and CO_2 with the gas phase, and calculated CO_2 dissolution in the aqueous phase from the CO_2 partial pressure, using an extended version of Henry's law (Pruess and García, 2002). The present version uses a methodology for calculating mutual solubilities of water and CO_2 (Spycher and Pruess, 2005) that is much more accurate, but has a drawback insofar as no partial pressures are associated with the individual fluid components. This makes it less straightforward to calculate thermophysical properties of the gas phase in terms of individual fluid components. We are primarily interested in the behavior of water-salt-CO_2 mixtures at moderate temperatures, $T < 100$ ˚C, say, where water vapor pressure is a negligibly small fraction of total pressure. Under these conditions the amount of water present in the CO_2-rich phase, henceforth referred to as "gas," is small. Accordingly, we approximate density, viscosity, and specific enthalpy of the gas phase by the corresponding properties of pure CO_2, without water present.

3.1 Density

Brine density ρ_b for the binary system water-salt is calculated as in Battistelli et al. (1997) from the correlations of Haas (1976) and Andersen et al. (1992). The calculation starts from aqueous phase density without salinity at vapor-saturated conditions, which is obtained from the correlations given by the International Formulation Committee (1967). Corrections are then applied

to account for effects of salinity and pressure. The density of aqueous phase with dissolved CO_2 is calculated assuming additivity of the volumes of brine and dissolved CO_2.

$$\frac{1}{\rho_{aq}} = \frac{1-X_2}{\rho_b} + \frac{X_2}{\rho_{CO2}} \tag{8}$$

where X_2 is the mass fraction of CO_2 in the aqueous phase. Partial density of dissolved CO_2, ρ_{CO2}, is calculated as a function of temperature from the correlation for molar volume of dissolved CO_2 at infinite dilution developed by García (2001).

$$V_\phi = a + bT + cT^2 + dT^3 \tag{9}$$

In Eq. (9), molar volume of CO_2 is in units of cm^3 per gram-mole, temperature T is in ˚C, and a–d are fit parameters given in Table 3.

Table 3. Parameters for molar volume of dissolved CO_2 (Eq. 9)

a	37.51
b	-9.585e-2
c	8.740e-4
d	-5.044e-7

Partial density of dissolved CO_2 in units of kg/m^3 is then

$$\rho_{CO2} = \frac{M_{CO2}}{V_\phi} * 10^3 \tag{10}$$

where $M_{CO2} = 44.0$ is the molecular weight of CO_2.

Dissolved CO_2 amounts at most to a few percent of total aqueous density. Accordingly, dissolved CO_2 is always dilute, regardless of total fluid pressure. It is then permissible to neglect the pressure dependence of partial density of dissolved CO_2, and to use the density corresponding to infinite dilution.

As had been mentioned above, the density of the CO_2-rich (gas) phase is obtained by neglecting effects of water, and approximating the density by that of pure CO_2 at the same temperature and pressure conditions. Density is obtained through bivariate interpolation from a tabulation of CO_2 densities as function of temperature and pressure, that is based on the correlations developed by Altunin (1975).

3.2 Viscosity

Brine viscosity is obtained as in EWASG from a correlation presented by Phillips et al. (1981), that reproduces experimental data in the temperature range from 10–350 ˚C for salinities up to 5 molal and pressures up to 500 bar within 2 %. No allowance is made for dependence of brine viscosity on the concentration of dissolved CO_2. Viscosity of the CO_2-rich phase is approximated as being equal to pure CO_2, and is obtained through tabular interpolation from the correlations of Altunin (1975).

3.3 Specific Enthalpy

Specific enthalpy of brine is calculated from the correlations developed by Lorenz et al. (2000), which are valid for all salt concentrations in the temperature range from 25 ˚C ≤ T ≤ 300 ˚C. The enthalpy of aqueous phase with dissolved CO_2 is obtained by adding the enthalpies of the CO_2 and brine (pseudo-) components, and accounting for the enthalpy of dissolution of CO_2.

$$h_{aq} = (1 - X_2)h_b + X_2 h_{CO2,aq} \tag{11}$$

$h_{CO2,aq} = h_{CO2} + h_{dis}$ is the specific enthalpy of aqueous (dissolved) CO_2, which includes heat of dissolution effects that are a function of temperature and salinity. For gas-like (low pressure) CO_2, the specific enthalpy of dissolved CO_2 is

$$h_{CO2,aq}(T, P, X_s) = h_{CO2,g}(T, P) + h_{dis,g}(T, X_s) \tag{12}$$

where $h_{dis,g}$ is obtained as in Battistelli et al. (1997) from an equation due to Himmelblau (1959). For geologic sequestration we are primarily interested in liquid-like (high-pressure) CO_2, for which the specific enthalpy of dissolved CO_2 may be written

$$h_{CO2,aq}(T, P, X_s) = h_{CO2,l}(T, P) + h_{dis,l}(T, X_s) \tag{13}$$

Here $h_{dis,l}$ is the specific heat of dissolution for liquid-like CO_2. Along the CO_2 saturation line, liquid and gaseous CO_2 phases may co-exist, and the expressions Eqs. (12, 13) must be equal there. We obtain

$$h_{dis,l}(T, X_s) = h_{dis,g}(T, X_s) + h_{CO2,gl}(T) \quad (14)$$

where $h_{CO2,gl}(T) = h_{CO2,g}(T, P_s) - h_{CO2,l}(T, P_s)$ is the specific enthalpy of vaporization of CO_2, and $P_s = P_s(T)$ is the saturated vapor pressure of CO_2 at temperature T. Depending upon whether CO_2 is in gas or liquid conditions, we use Eq.(12) or (13) in Eq. (11) to calculate the specific enthalpy of dissolved CO_2. At the temperatures of interest here, $h_{dis,g}$ is a negative quantity, so that dissolution of low-pressure CO_2 is accompanied by an increase in temperature. $h_{CO2,gl}$ is a positive quantity, which will reduce or cancel out the heat-of-dissolution effects. This indicates that dissolution of liquid CO_2 will produce less temperature increase than dissolution of gaseous CO_2, and may even cause a temperature decline if $h_{CO2,gl}$ is sufficiently large.

Application of Eq. (11) is straightforward for single-phase gas and two-phase conditions, where h_{CO2} is obtained as a function of temperature and pressure through bivariate interpolation from a tabulation of Altunin's correlation (1975). A complication arises in evaluating h_{CO2} for single-phase aqueous conditions. We make the assumption that $h_{CO2}(P, X_s, X_2, T)$ for single-phase liquid is identical to the value in a two-phase system with the same composition of the aqueous phase. To determine h_{CO2}, it is then necessary to invert the Spycher and Pruess (2005) phase partitioning relation $X_2 = X_2(P; T, X_s)$, in order to obtain the pressure P in a two-phase aqueous-gas system that would correspond to a dissolved CO_2 mass fraction X_2 in the aqueous phase, $P = P(X_2; X_s, T)$. The inversion is accomplished by Newtonian iteration, using a starting guess P_0 for P that is obtained from Henry's law. Specific enthalpy of gaseous CO_2 in the two-phase system is then calculated as $h_{CO2} = h_{CO2}(T, P)$, and specific enthalpy of dissolved CO_2 is $h_{CO2} + h_{dis}$.

4. Preparation of Input Data

Most of TOUGH2/ECO2N input specifications correspond to the general TOUGH2 input formats as given in the TOUGH2 user's guide (Pruess et al., 1999). This information is not duplicated in the present report; here we discuss only parameter choices specific to ECO2N.

4.1 Initialization Choices

Flow problems in TOUGH2/ECO2N will generally be initialized with the primary thermodynamic variables as used in the code, but some additional choices are available for the convenience of users. The internally used variables are (P, X_{sm}, X3, T) for grid blocks in single-phase (liquid or gas) conditions and (P, X_{sm}, S_g+10, T) for two-phase (liquid and gas) grid blocks (see Table 1). Here X3 is the mass fraction of CO_2 in the fluid. As had been discussed above, for conditions of interest to geologic sequestration of CO_2, X3 is restricted to small values $0 \le X3 \le X_{2,eq}$ (a few percent) for single-phase liquid conditions, or to values near 1 ($Y_{2,eq} \le X3 \le 1$, with $Y_{2,eq} > 0.99$ typically) for single-phase gas (Fig. 6). Intermediate values $X_{2,eq} < X3 < Y_{2,eq}$ correspond to two-phase conditions, and thus should be initialized by specifying S_g+10 as third primary variable. As a convenience to users, ECO2N allows initial conditions to be specified in the full range $0 \le X3 \le 1$. During the initialization phase of a simulation, a check is made whether X3 is in fact within the range of mass fractions that correspond to single-phase (liquid or gas) conditions. If this is found not to be the case, the conditions are recognized as being two-phase, and the corresponding gas saturation is calculated from the phase equilibrium constraint.

$$X3\left(S_l\rho_l + S_g\rho_g\right) = S_l\rho_l X_{2,eq} + S_g\rho_g Y_{2,eq} \tag{15}$$

Using $S_l = 1 - S_g - S_s$, with S_s the "solid saturation" (fraction of pore space occupied by solid salt), we obtain

$$S_g = A \times \left(1 - S_s\right) \tag{16}$$

and the third primary variable is reset internally to X3 = S_g+10. Here the parameter A is given by

$$A = \frac{\left(X3 - X_{2,eq}\right)\rho_l}{\left(X3 - X_{2,eq}\right)\rho_l + \left(Y_{2,eq} - X3\right)\rho_g} \tag{17}$$

Users may think of specifying single-phase liquid (aqueous) conditions by setting X3 = 10 (corresponding to $S_g = 0$), and single-phase gas conditions by setting X3 = 11 - S_s (corresponding

to $S_l = 0$). Strictly speaking this is not permissible, because two-phase initialization requires that both $S_g > 0$ and $S_l > 0$. Single-phase states should instead be initialized by specifying primary variable X3 as CO_2 mass fraction. However, as a user convenience, ECO2N accepts initialization of single-phase liquid conditions by specifying X3 = 10 ($S_g = 0$). Such specification will be converted internally to two-phase in the initialization phase by adding a small number (10^{-11}) to the third primary variable, changing conditions to two-phase with a small gas saturation $S_g = 10^{-11}$.

Salt concentration or saturation of solid salt, if present, is characterized in ECO2N by means of the second primary variable X_{sm}. When no solid phase is present, X_{sm} denotes X_s, the mass fraction of NaCl referred to the two-component system water-NaCl. This is restricted to the range $0 \le X_{sm} \le XEQ$, where XEQ = XEQ(T) is the solubility of salt. For $X_{sm} > 10$ this variable means $S_s + 10$, solid saturation plus 10. Users also have the option to specify salt concentration by means of molality m by assigning $X_{sm} = -m$. Such specification will in the initialization phase be internally converted to X_s by using Eq. (1). When salt concentration (as a fraction of total H_2O + NaCl mass) exceeds XEQ, this corresponds to conditions in which solid salt will be present in addition to dissolved salt in the aqueous phase. Such states should be initialized with a second primary variable $X_{sm} = S_s+10$. However, ECO2N accepts initialization with $X_{sm} > XEQ$, recognizes this as corresponding to presence of solid salt, and converts the second primary variable internally to the appropriate solid saturation that will result in total salt mass fraction in the binary system water-salt being equal to X_{sm}. The conversion starts from the following equation.

$$X_{sm} = \frac{XEQ \times S_l \rho_l (1 - X_2) + S_s \rho_s}{S_l \rho_l (1 - X_2) + S_s \rho_s} \tag{18}$$

where the numerator gives the total salt mass per unit volume, in liquid and solid phases, while the denominator gives the total mass of salt plus water. Substituting $S_l = 1 - S_g - S_s$, this can be solved for S_s to yield

$$S_s = \frac{B \times (1 - S_g)}{1 + B} \tag{19}$$

where the parameter B is given by

$$B = \frac{(X_{sm} - XEQ)\rho_l (1 - X_2)}{\rho_s (1 - X_{sm})} \tag{20}$$

The most general conditions arise when both the second and third primary variables are initialized as mass fractions, nominally corresponding to single-phase fluid conditions with no solid phase present, but both mass fractions being in the range corresponding to two-phase fluid conditions with precipitated salt. Under these conditions, Eqs. (16) and (19) are solved simultaneously in ECO2N for S_s and S_g, yielding

$$S_g = \frac{A}{1 + B - A \times B} \tag{21}$$

and

$$S_s = \frac{B \times (1 - A)}{1 + B - A \times B} \tag{22}$$

Then both second and third primary variables are converted to phase saturations, S_s + 10 and S_g + 10, respectively. Examples of different initialization choices are given in sample problem 1, below.

4.2 Permeability Change from Precipitation and Dissolution of Salt

ECO2N offers several choices for the functional dependence of relative change in permeability, k/k_0, on relative change in active flow porosity.

$$\frac{k}{k_0} = f\left(\frac{\phi_f}{\phi_0}\right) \equiv f(1 - S_s) \tag{23}$$

The simplest model that can capture the converging-diverging nature of natural pore channels consists of alternating segments of capillary tubes with larger and smaller radii, respectively; see Fig. 8. While in straight capillary tube models permeability remains finite as long

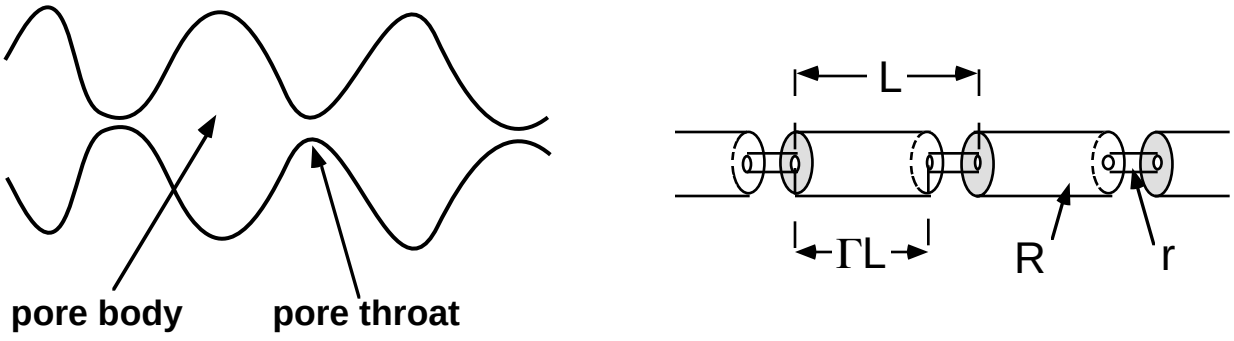

(a) conceptual model (b) tubes-in-series

Figure 8. Model for converging-diverging pore channels.

as porosity is non-zero, in models of tubes with different radii in series, permeability is reduced to zero at a finite porosity. From the tubes-in-series model shown in Fig. 8, the following relationship can be derived (Verma and Pruess, 1988)

$$\frac{k}{k_0} = \theta^2 \frac{1-\Gamma+\Gamma/\omega^2}{1-\Gamma+\Gamma\left[\theta/(\theta+\omega-1)\right]^2} \tag{24}$$

Here

$$\theta = \frac{1-S_s-\phi_r}{1-\phi_r} \tag{25}$$

depends on the fraction $1\text{-}S_s$ of original pore space that remains available to fluids, and on a parameter ϕ_r, which denotes the fraction of original porosity at which permeability is reduced to zero. Γ is the fractional length of the pore bodies, and the parameter ω is given by

$$\omega = 1+\frac{1/\Gamma}{1/\phi_r-1} \tag{26}$$

Therefore, Eq. (24) has only two independent geometric parameters that need to be specified, ϕ_r and Γ. As an example, Fig. 9 shows the permeability reduction factor from Eq. (24), plotted against $\phi/\phi_0 \equiv (1-S_s)$, for parameters of $\phi_r = \Gamma = 0.8$.

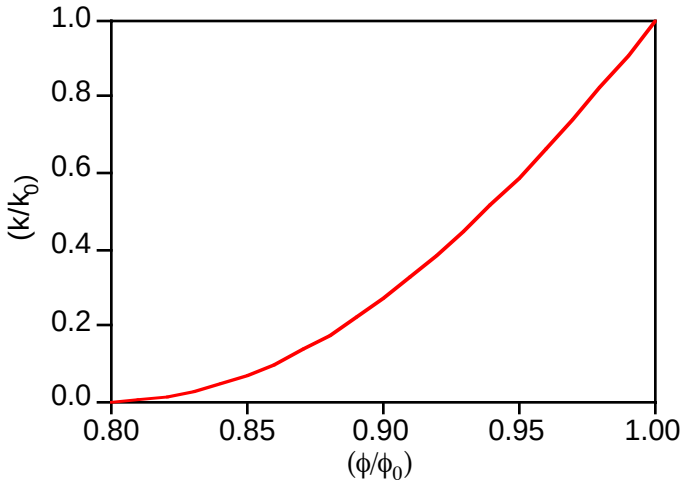

Figure 9. Porosity-permeability relationship for tubes-in-series model, after Verma and Pruess (1988).

For parallel-plate fracture segments of different aperture in series, a relationship similar to Eq. (24) is obtained, the only difference being that the exponent 2 is replaced everywhere by 3 (Verma and Pruess, 1988). If only straight capillary tubes of uniform radius are considered, we have $\phi_r = 0$, $\Gamma = 0$, and Eq. (24) simplifies to

$$k/k_0 = \left(1-S_s\right)^2 \tag{27}$$

4.3 Choice of Program Options

Various options for ECO2N can be selected through parameter specifications in data block SELEC. Default choices corresponding to various selection parameters set equal to zero provide the most comprehensive thermophysical property model. Certain functional dependencies can be turned off or replaced by simpler and less accurate models, see below. These options are offered to enable users to identify the role of different effects in a flow problem, and to facilitate comparison with other simulation programs that may not include full dependencies of thermophysical properties.

SELECTION keyword to introduce a data block with parameters for ECO2N.

Record SELEC.1

Format(16I5)
IE(I), I=1,16

IE(1) set equal to 1, to read one additional data record (a larger value with more data records is acceptable, but only one additional record will be used by ECO2N).

IE(11) selects dependence of permeability on the fraction $\phi_f/\phi_0 = \left(1-S_s\right)$ of original pore space that remains available to fluids.

0: permeability does not vary with ϕ_f.

1: $k/k_0 = \left(1-S_s\right)^\gamma$, with γ = FE(1) (record SELEC.2).

2: fractures in series, i.e., Eq. (24) with exponent 2 everywhere replaced by 3.

3: tubes-in-series, i.e., Eq. (24).

IE(12) allows choice of model for water solubility in CO_2

0: after Spycher and Pruess (2005).

1: evaporation model; i.e., water density in the CO_2-rich phase is calculated as density of saturated water vapor at prevailing temperature and salinity.

IE(13) allows choice of dependence of brine density on dissolved CO_2

0: brine density varies with dissolved CO_2 concentration, according to García's (2001) correlation for temperature dependence of molar volume of dissolved CO_2.

1: brine density is independent of CO_2 concentration.

IE(14) allows choice of treatment of thermophysical properties as a function of salinity

0: full dependence.

1: no salinity dependence of thermophysical properties (except for brine enthalpy; salt solubility constraints are maintained).

IE(15) allows choice of correlation for brine enthalpy at saturated vapor pressure

0: after Lorenz et al. (2000).

1: after Michaelides (1981).

2: after Miller (1978).

Record SELEC.2 introduces parameters for functional dependence of permeability on solid saturation

Format(8E10.4)
FE(1), FE(2)

FE(1) parameter γ (for IE(11)=1); parameter ϕ_r (for IE(11) = 2, 3)

FE(2) parameter Γ (for IE(11) = 2, 3)

The ECO2N module includes a customized version of a subroutine FGTAB that can write data files FOFT, COFT, and GOFT with time series of conditions at user-selected grid blocks and connections for plotting. The parameters written out in comma-delimited format at each time step are as follows.

FOFT: (gas) pressure, dissolved CO_2 mass fraction in liquid, gas saturation, dissolved salt mass fraction and solid saturation (fraction of void space taken up by solid precipitate);

COFT: flow rates of gas, liquid, and total CO_2 (as free phase and dissolved in aqueous phase);

GOFT: well flow rate, flowing enthalpy, flowing CO_2 mass fraction, gas mass fraction of well flow, flowing wellbore pressure (production wells only).

5. Sample Problems

This section presents a number of sample problems for TOUGH2/ECO2N. The problems were chosen to demonstrate the preparation of input data, to illustrate code capabilities, and to provide benchmarks for proper code installation. Three of the problems were taken from a recent code intercomparison study, in which ten groups from six countries exercised different simulation codes to generate results for a suite of test problems (Pruess et al., 2002, 2004). These problems include a basic injection problem (Section 5.2), a basic fault leakage problem (Section 5.3), and a CO_2 storage problem with 2-D geometry loosely patterned after the Sleipner Vest CO_2 injection project (Kongsjorden et al., 1997; Lindeberg et al., 2002) in the Norwegian sector of the North Sea (Section 5.4). In order to provide some context and perspective the current TOUGH2/ECO2N results are compared with results previously obtained in the CO_2 code intercomparison project.

5.1 Problem No. 1 (*rtab*) - Demonstration of Initialization Options

The input file as given in Fig. 10 performs just a single infinitesimal time step ($\Delta t = 10^{-9}$ s) and includes neither flow connections between grid blocks nor sinks or sources. Therefore, there is no flow and no changes in the initially specified thermodynamic conditions. The purpose of this problem is simply to demonstrate different options for initializing thermodynamic conditions.

```
*rtab* ... initialization test for ECO2N
ROCKS----1----*----2----*----3----*----4----*----5----*----6----*----7----*----8
SANDS    2  2600.e00       .35  100.e-15  100.e-15  100.e-15      2.51      920.
   4.5e-10
    7           .457       .30        1.       .05
    7           .457       .00    5.1e-5      1.e7      .999

MULTI----1----*----2----*----3----*----4----*----5----*----6----*----7----*----8
    3    4    3    6
START----1----*----2----*----3----*----4----*----5----*----6----*----7----*----8
----*----1 MOP: 123456789*123456789*1234 ---*----5----*----6----*----7----*----8
PARAM----1----*----2----*----3----*----4----*----5----*----6----*----7----*----8
   1   1       110 0900000000  4    3
                          -1.
     1.e-9
     1.E-5     1.E00
               60.e5                  0.0                0.01                20.0
SELEC....2....3....4....5....6....7....8....9...10...11...12...13...14...15...16
    1                                              0    0    0    0    0    0    0
        .8        .8
ELEME----1----*----2----*----3----*----4----*----5----*----6----*----7----*----8
a   1   10    1SANDS        1.
A  14    7    1SANDS        1.

CONNE----1----*----2----*----3----*----4----*----5----*----6----*----7----*----8
```

Figure 10. TOUGH2/ECO2N input file (first part) for sample problem 1 - demonstration of initialization options.

```
INCON----1----*----2----*----3----*----4----*----5----*----6----*----7----*----8
a   1
              40.0e5                0.0             3.9e-2                30.
a   2
              40.0e5                0.0             3.9e-1                30.
a   3
             340.0e5                0.0             6.6e-2                30.
a   4
             340.0e5                0.3             6.6e-1                30.
a   5
             140.0e5            0.10466             3.6e-2                30.
a   6
             140.0e5            0.10466             3.6e-1                30.
a   7
             140.0e5               0.50             3.6e-2                30.
a   8
             140.0e5               0.50             3.6e-1                30.
a   9
             140.0e5              10.50               0.99                30.
a  10
             140.0e5              10.50              0.999                30.
a  11
             140.0e5               0.50               0.99                30.
A  14
            216.18e5               0.05              10.50               45.0
A  15
            216.18e5              10.05              10.50               45.0
A  16
            216.18e5            0.50000              10.50               45.0
A  17
            216.18e5            0.50000               0.50               45.0
A  18
            216.18e5               10.2               0.50               45.0
A  19
            216.18e5               10.2              10.50               45.0
A  20
            216.18e5               -2.0              10.50               45.0
A  21
            216.18e5               -6.0              10.50               45.0

GENER----1----*----2----*----3----*----4----*----5----*----6----*----7----*----8

ENDCY----1----*----2----*----3----*----4----*----5----*----6----*----7----*----8
```

Figure 10. (continued)

Standard initialization with internally used primary variables (Table 1) is made for a number of grid blocks in single-phase liquid conditions (*a 1*, *a 3*, *a 5*), single-phase gas (*a 10*), and two-phase fluid (*A 14*, *A 15*, *A 19*). Several grid blocks are initialized with single-phase type primary variables, but with a CO_2 mass fraction (primary variable #3) that is larger than can be dissolved in the aqueous phase, and smaller than required for single-phase gas conditions (*a 2*, *a 6*, *a 9*, *A 18*). The CO_2 mass fractions for these blocks correspond to two-phase (liquid-gas) fluid conditions (see Fig. 6 and Section 4.1), and are

internally converted to the appropriate gas saturation in the initialization phase. Primary variable #3 is then re-set to S_g + 10, as can be seen from the list of internally used primary variables that is generated by this problem (Fig. 11). Grid block *A 16* is initialized with primary variable #3 corresponding to internal ECO2N useage, but primary variable #2 is larger than saturated salt mass fraction in the binary system water-salt. This specification corresponds to presence of solid salt, and is internally converted to S_s + 10. In some grid blocks both primary variables #2 and #3 are specified with conventions applicable for single-phase liquid conditions, but with salt mass fraction exceeding the solubility limit, and CO_2 mass fraction being in the intermediate range between the liquid and gas phase limits (*a 4*, *a 7*, *a 8*, *a 11*, *A 17*). Salt as well as CO_2 mass fractions for these blocks are converted to the appropriate internally used saturation variables. Finally, there are grid blocks (*A 20*, *A 21*) in which primary variable #2 is specified as salt molality (counted by convention as undissociated) in the binary water-salt system, which is internally converted to salt mass fraction. The internally used primary variables generated from the INCON data given in Fig. 10 are shown in Fig. 11. Fig. 12 shows part of the printed output for this problem.

We emphasize that the preferred and recommended option is to initialize flow problems by means of the internally used primary variables (Table 1). The options of allowing salt and CO_2 mass fractions that are out of range were created as a convenience to users, to avoid "erroneous initialization" errors when running TOUGH2/ECO2N.

```
PRIMARY VARIABLES

AT ELEMENT *a   1* ---    .400000E+07   .000000E+00   .390000E-01   .300000E+02
AT ELEMENT *a   2* ---    .400000E+07   .000000E+00   .108654E+02   .300000E+02
AT ELEMENT *a   3* ---    .340000E+08   .000000E+00   .660000E-01   .300000E+02
AT ELEMENT *a   4* ---    .340000E+08   .100080E+02   .106980E+02   .300000E+02
AT ELEMENT *a   5* ---    .140000E+08   .104660E+00   .360000E-01   .300000E+02
AT ELEMENT *a   6* ---    .140000E+08   .104660E+00   .103947E+02   .300000E+02
AT ELEMENT *a   7* ---    .140000E+08   .101996E+02   .100239E+02   .300000E+02
AT ELEMENT *a   8* ---    .140000E+08   .101265E+02   .103812E+02   .300000E+02
AT ELEMENT *a   9* ---    .140000E+08   .105000E+02   .104969E+02   .300000E+02
AT ELEMENT *a  10* ---    .140000E+08   .105000E+02   .999000E+00   .300000E+02
AT ELEMENT *a  11* ---    .140000E+08   .100016E+02   .109923E+02   .300000E+02
AT ELEMENT *A  14* ---    .216180E+08   .500000E-01   .105000E+02   .450000E+02
AT ELEMENT *A  15* ---    .216180E+08   .100500E+02   .105000E+02   .450000E+02
AT ELEMENT *A  16* ---    .216180E+08   .101016E+02   .105000E+02   .450000E+02
AT ELEMENT *A  17* ---    .216180E+08   .100957E+02   .105287E+02   .450000E+02
AT ELEMENT *A  18* ---    .216180E+08   .102000E+02   .104677E+02   .450000E+02
AT ELEMENT *A  19* ---    .216180E+08   .102000E+02   .105000E+02   .450000E+02
AT ELEMENT *A  20* ---    .216180E+08   .104661E+00   .105000E+02   .450000E+02
AT ELEMENT *A  21* ---    .216180E+08   .259637E+00   .105000E+02   .450000E+02
```

Figure 11. Primary variables internally used in ECO2N for the INCON data given in Fig. 10.

```
 *rtab* ... initialization test for ECO2N

          OUTPUT DATA AFTER (    1,  1)-2-TIME STEPS                                                       THE TIME IS  .115741E-13 DAYS

@@@@@@@@@@@@@@@@@@@@@@@@@@@@@@@@@@@@@@@@@@@@@@@@@@@@@@@@@@@@@@@@@@@@@@@@@@@@@@@@@@@@@@@@@@@@@@@@@@@@@@@@@@@@@@@@@@@@@@@@@@@@@@@@@@@@@

  TOTAL TIME     KCYC   ITER  ITERC   KON         DX1M          DX2M          DX3M          MAX. RES.      NER    KER        DELTEX
  .100000E-08       1      1      1     2         .00000E+00    .00000E+00    .00000E+00     .00000E+00      0      0       .10000E-08

@@@@@@@@@@@@@@@@@@@@@@@@@@@@@@@@@@@@@@@@@@@@@@@@@@@@@@@@@@@@@@@@@@@@@@@@@@@@@@@@@@@@@@@@@@@@@@@@@@@@@@@@@@@@@@@@@@@@@@@@@@@@@@@@@@@@@

 ELEM. INDEX   P          T        SG           SS          XNACL        YH2OG        XCO2aq        PCAP        k-red.      DG         DL
              (Pa)     (deg-C)                                                                        (Pa)                  (kg/m3)    (kg/m3)

 a    1   1  .40000E+07  30.00  .00000E+00  .00000E+00  .00000E+00  .63683E-03  .39000E-01  .00000E+00  .10000E+01     .00    1004.89
 a    2   2  .40000E+07  30.00  .86541E+00  .00000E+00  .00000E+00  .62838E-03  .39686E-01 -.21079E+06  .10000E+01   89.85    1005.03
 a    3   3  .34000E+08  30.00  .00000E+00  .00000E+00  .00000E+00  .18514E-02  .66000E-01  .00000E+00  .10000E+01     .00    1020.77
 a    4   4  .34000E+08  30.00  .69799E+00  .80128E-02  .26047E+00  .15535E-02  .18190E-01 -.79865E+05  .10000E+01  966.06    1209.49
 a    5   5  .14000E+08  30.00  .00000E+00  .00000E+00  .10089E+00  .14899E-02  .36000E-01  .00000E+00  .10000E+01     .00    1077.59
 a    6   6  .14000E+08  30.00  .39468E+00  .00000E+00  .10080E+00  .15458E-02  .36916E-01 -.28514E+05  .10000E+01  836.45    1077.72
 a    7   7  .14000E+08  30.00  .23863E-01  .19963E+00  .26121E+00  .13675E-02  .15390E-01 -.44869E+04  .10000E+01  836.45    1200.62
 a    8   8  .14000E+08  30.00  .38124E+00  .12654E+00  .26121E+00  .13675E-02  .15390E-01 -.32250E+05  .10000E+01  836.45    1200.62
 a    9   9  .14000E+08  30.00  .49693E+00  .50000E+00  .26121E+00  .13675E-02  .15390E-01 -.83286E+07  .10000E+01  836.45    1200.62
 a   10  10  .14000E+08  30.00  .50000E+00  .50000E+00  .00000E+00  .10000E-02  .15390E-01 -.10000E+08  .10000E+01  836.45        .00
 a   11  11  .14000E+08  30.00  .99230E+00  .15742E-02  .26121E+00  .13675E-02  .15390E-01 -.83286E+07  .10000E+01  836.45    1200.62
 A   14  12  .21618E+08  45.00  .50000E+00  .00000E+00  .47676E-01  .25132E-02  .46477E-01 -.38997E+05  .10000E+01  829.68    1040.48
 A   15  13  .21618E+08  45.00  .50000E+00  .50000E-01  .26332E+00  .21440E-02  .15854E-01 -.42289E+05  .10000E+01  829.68    1200.86
 A   16  14  .21618E+08  45.00  .50000E+00  .10157E+00  .26332E+00  .21440E-02  .15854E-01 -.46537E+05  .10000E+01  829.68    1200.86
 A   17  15  .21618E+08  45.00  .52866E+00  .95745E-01  .26332E+00  .21440E-02  .15854E-01 -.51041E+05  .10000E+01  829.68    1200.86
 A   18  16  .21618E+08  45.00  .46771E+00  .20000E+00  .26332E+00  .21440E-02  .15854E-01 -.51041E+05  .10000E+01  829.68    1200.86
 A   19  17  .21618E+08  45.00  .50000E+00  .20000E+00  .26332E+00  .21440E-02  .15854E-01 -.58702E+05  .10000E+01  829.68    1200.86
 A   20  18  .21618E+08  45.00  .50000E+00  .00000E+00  .10091E+00  .24308E-02  .35822E-01 -.38997E+05  .10000E+01  829.68    1075.88
 A   21  19  .21618E+08  45.00  .50000E+00  .00000E+00  .25536E+00  .21594E-02  .16490E-01 -.38997E+05  .10000E+01  829.68    1194.04

@@@@@@@@@@@@@@@@@@@@@@@@@@@@@@@@@@@@@@@@@@@@@@@@@@@@@@@@@@@@@@@@@@@@@@@@@@@@@@@@@@@@@@@@@@@@@@@@@@@@@@@@@@@@@@@@@@@@@@@@@@@@@@@@@@@@@
```

Figure 12. Output data for sample problem 1.

5.2 Problem No. 2 (*rcc3*) - Radial Flow from a CO_2 Injection Well

This is a basic problem of CO_2 injection into a saline aquifer, examining two-phase flow with CO_2 displacing (saline) water under conditions that may be encountered in brine aquifers at a depth of the order of 1.2 km. A CO_2 injection well fully penetrates a homogeneous, isotropic, infinite-acting aquifer of 100 m thickness (Fig. 13), at conditions of 120 bar pressure, 45 ˚C temperature, and a salinity of 15 % by weight. CO_2 is injected uniformly at a constant rate of 100 kg/s. This problem had been included as test problem #3 in a recent code intercomparison project (Pruess et al., 2002, 2004); full specifications are given in Appendix A.

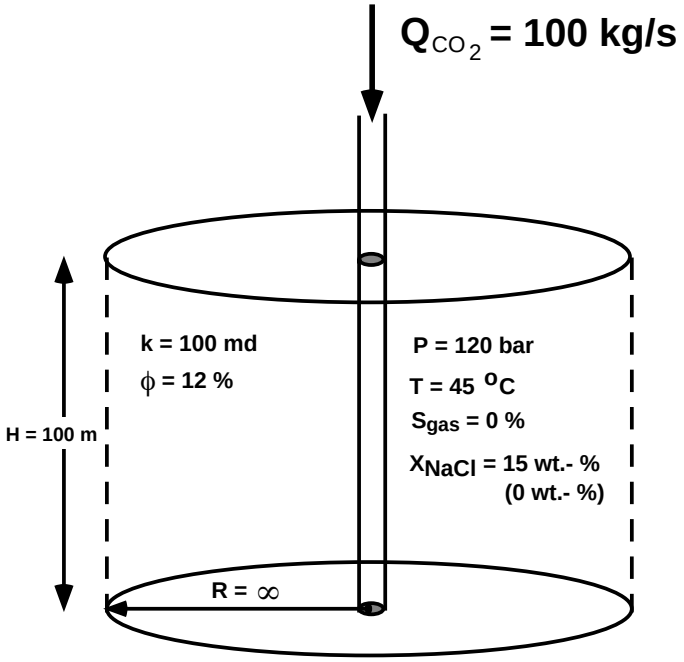

Figure 13. Schematic of sample problem 2.

The TOUGH2 input file used for grid generation is shown in Fig. 14. The well is modeled as a circular grid element of R = 0.3 m (≈ 12"). The numerical grid is extended to a large distance of 100 km, so that the system would be infinite-acting for the time period simulated (10,000 days, 27.38 years). Prior to the flow simulation, a minor amount of editing is performed on the MESH file. The well block is assigned to a domain #2, with a view on facilitating running of a non-isothermal variation of the problem. Further, the nodal distance corresponding to the well block was changed to an infinitesimal value. A fragment of the modified MESH file is shown in Fig. 15, and the TOUGH2 input file used for the simulation is shown in Fig. 16. The simulation is performed in isothermal mode (NEQ = 3 in data block MULTI). A separate ROCKS domain 'well ' with "infinite" rock grain density was included in the input file to enable running of a non-isothermal

```
*rcc3* ... Code Intercomparison problem3: Radial flow from a CO2 Injection Well
MESHMAKER1----*----2----*----3----*----4----*----5----*----6----*----7----*----8
RZ2D
RADII
    1
        0.
EQUID
    1             .3
LOGAR
  200           1.E3
LOGAR
  100           3.E3
LOGAR
  100           1.E4
LOGAR
   34           1.E5
LAYER----1----*----2----*----3----*----4----*----5----*----6----*----7----*----8
    1
      100.

ENDFI----1----*----2----*----3----*----4----*----5----*----6----*----7----*----8
```

Figure 14. TOUGH2 input file for grid generation for radial injection problem.

```
ELEME ---   435    1    1  434    .00000100000.000
A1  1              2 .2827E+02 .5655E+00           .3000E+00          -.5000E+02
A1  2              1 .8728E+02 .1746E+01           .4532E+00          -.5000E+02
A1  3              1 .1501E+03 .3002E+01           .7630E+00          -.5000E+02
A1  4              1 .2169E+03 .4339E+01           .1079E+01          -.5000E+02
...
...

CONNE
A1  1A1  2                   1 .1500E-05 .1532E+00 .1885E+03
A1  2A1  3                   1 .1532E+00 .1565E+00 .3811E+03
A1  3A1  4                   1 .1565E+00 .1599E+00 .5778E+03
...
```

Figure 15. Modified MESH file for radial injection problem.

variation simply by setting NEQ = 4; the well block "A1 1" is assigned to domain 'well ' with "infinite" rock grain density, so that CO_2 injection would effectively occur at initial temperature of 45 ˚C, obviating the need for specifying an injection enthalpy. Part of the output generated from this problem is shown in Fig. 17. As can be seen salt is precipitating around the injection well, but associated permeability reduction is turned off (IE(11) = 0).

An important advantage of the radial flow problem considered here is that it admits a similarity solution. Specifically, the solution depends on radial distance R and time t only through the similarity variable $\xi = R^2/t$, even when taking into account all the non-linearities due to PVT

```
*rcc3* ... Code Intercomparison problem3: Radial flow from a CO2 Injection Well
ROCKS----1----*----2----*----3----*----4----*----5----*----6----*----7----*----8
SAND     2  2600.e00       .12  100.e-15  100.e-15  100.e-15      2.51      920.
   4.5e-10
    7           .457       .30        1.       .05
    7           .457       .00    5.1e-5      1.e7      .999
well     2  2600.e40       .12  100.e-15  100.e-15  100.e-15      2.51      920.
   4.5e-10
    7           .457       .30        1.       .05
    7           .457       .00    5.1e-5      1.e7      .999

MULTI----1----*----2----*----3----*----4----*----5----*----6----*----7----*----8
    3    3    3    6
SELEC....2....3....4....5....6....7....8....9...10...11...12...13...14...15...16
    1                                        0    0    0    0    0    0    0    0
        .8   .8
SOLVR----1----*----2----*----3----*----4----*----5----*----6----*----7----*----8
5  Z1   O0    8.0e-1    1.0e-7
START----1----*----2----*----3----*----4----*----5----*----6----*----7----*----8
----*----1 MOP: 123456789*123456789*1234 ---*----5----*----6----*----7----*----8
PARAM----1----*----2----*----3----*----4----*----5----*----6----*----7----*----8
   1 999     99910003000000000  4    3
             8.64e8       -1.
       1.
     1.E-5     1.E00
             120.e5                 .15                 0.0                45.
FOFT ----1----*----2----*----3----*----4----*----5----*----6----*----7----*----8
A1 49             1 .1745E+04 .2685E+03           .2570E+02          -.6500E+01
A12 2             1 .3080E+08 .4738E+07           .1080E+04          -.6500E+01

GENER----1----*----2----*----3----*----4----*----5----*----6----*----7----*----8
A1  1inj 1                         COM3       100.

INCON----1----*----2----*----3----*----4----*----5----*----6----*----7----*----8

TIMES----1----*----2----*----3----*----4----*----5----*----6----*----7----*----8
    4
 2.592E+06  8.64E+06  8.64E+07  8.64E+08
ENDCY----1----*----2----*----3----*----4----*----5----*----6----*----7----*----8
```

Figure 16. TOUGH2 input file for radial injection problem.

properties and two-phase flow (O'Sullivan, 1981; Doughty and Pruess, 1992). The space and time discretization employed for finite difference simulation will violate the rigorous R^2/t invariance, so that the similarity property will be maintained only approximately. The accuracy of the numerical simulation can be checked by plotting the results as a function of the similarity variable R^2/t (Figs. 18 - 23). Fig. 18 shows the results for pressure as a function of the similarity variable. Data were plotted from the pressure profile obtained at a simulation time of $t = 8.64 \times 10^7$ s, and from the time series data for grid block A1 49, at a radial distance of R = 25.25 m, that were generated by means of FOFT specifications in the input file (Fig. 16). The agreement between the profile data (shown as thick solid lines) and the time series data (shown as thick dashed lines) is excellent,

```
 ...ITERATING...  AT [   1,  1] --- DELTEX =  .100000E+01   MAX. RES. =  .353732E+01  AT ELEMENT A1  1  EQUATION   3
 $$$$$$$$$$$$ GAS PHASE EVOLVES AT ELEMENT *A1  1*  $$$$$    X3 =  .267978E-01   XCO2aq =  .262042E-01 PX =  .136627E+08 PA
 ...ITERATING...  AT [   1,  2] --- DELTEX =  .100000E+01   MAX. RES. =  .246611E-01  AT ELEMENT A1  2  EQUATION   3
 $$$$$$$$ GAS PHASE DISAPPEARS AT ELEMENT *A1  1*  $$$$$    SG = -.892323E-04
 $$$$$$$$$$$$ GAS PHASE EVOLVES AT ELEMENT *A1  1*  $$$$$    X3 =  .262042E-01   XCO2aq =  .261503E-01 PX =  .135439E+08 PA
 ...ITERATING...  AT [   1,  3] --- DELTEX =  .100000E+01   MAX. RES. =  .121096E-01  AT ELEMENT A1  1  EQUATION   3
 $$$$$$$$ GAS PHASE DISAPPEARS AT ELEMENT *A1  1*  $$$$$    SG = -.993540E-04
 ...ITERATING...  AT [   1,  4] --- DELTEX =  .100000E+01   MAX. RES. =  .882447E-02  AT ELEMENT A1  1  EQUATION   3
 ...ITERATING...  AT [   1,  5] --- DELTEX =  .100000E+01   MAX. RES. =  .315412E-04  AT ELEMENT A1  1  EQUATION   3
 A1  1(   1,  6) ST =  .100000E+01 DT =  .100000E+01 DX1=  .166338E+07 DX2= -.303162E-15 T =  45.000 P = 13663377. S =  .000000E+00
 ...ITERATING...  AT [   2,  1] --- DELTEX =  .100000E+01   MAX. RES. =  .100000E+01  AT ELEMENT A1  1  EQUATION   3
 $$$$$$$$$$$$ GAS PHASE EVOLVES AT ELEMENT *A1  1*  $$$$$    X3 =  .515157E-01   XCO2aq =  .264071E-01 PX =  .141315E+08 PA
 ...ITERATING...  AT [   2,  2] --- DELTEX =  .100000E+01   MAX. RES. =  .986648E+00  AT ELEMENT A1  1  EQUATION   3
 ...ITERATING...  AT [   2,  3] --- DELTEX =  .100000E+01   MAX. RES. =  .913019E+00  AT ELEMENT A1  2  EQUATION   3
 ...ITERATING...  AT [   2,  4] --- DELTEX =  .100000E+01   MAX. RES. =  .154995E+00  AT ELEMENT A1  2  EQUATION   3
 ...ITERATING...  AT [   2,  5] --- DELTEX =  .100000E+01   MAX. RES. =  .106964E-01  AT ELEMENT A1  2  EQUATION   3
 ...ITERATING...  AT [   2,  6] --- DELTEX =  .100000E+01   MAX. RES. =  .117013E-03  AT ELEMENT A1  2  EQUATION   3
 A1  2(   2,  7) ST =  .200000E+01 DT =  .100000E+01 DX1=  .111163E+07 DX2=  .974739E-07 T =  45.000 P = 14270694. S =  .000000E+00
 ...ITERATING...  AT [   3,  1] --- DELTEX =  .100000E+01   MAX. RES. =  .496177E+00  AT ELEMENT A1  1  EQUATION   3
 ...ITERATING...  AT [   3,  2] --- DELTEX =  .100000E+01   MAX. RES. =  .121128E-01  AT ELEMENT A1  1  EQUATION   3
 ...ITERATING...  AT [   3,  3] --- DELTEX =  .100000E+01   MAX. RES. =  .242397E-04  AT ELEMENT A1  2  EQUATION   3
 A1  1(   3,  4) ST =  .300000E+01 DT =  .100000E+01 DX1=  .158378E+07 DX2=  .972620E-05 T =  45.000 P = 17949134. S =  .722202E-01
 ...ITERATING...  AT [   4,  1] --- DELTEX =  .200000E+01   MAX. RES. =  .661797E+00  AT ELEMENT A1  1  EQUATION   3
 ...ITERATING...  AT [   4,  2] --- DELTEX =  .200000E+01   MAX. RES. =  .745003E+00  AT ELEMENT A1  2  EQUATION   3
 ...ITERATING...  AT [   4,  3] --- DELTEX =  .200000E+01   MAX. RES. =  .671985E-01  AT ELEMENT A1  2  EQUATION   3
 ...ITERATING...  AT [   4,  4] --- DELTEX =  .200000E+01   MAX. RES. =  .616227E-03  AT ELEMENT A1  2  EQUATION   3
 A1  2(   4,  5) ST =  .500000E+01 DT =  .200000E+01 DX1=  .259506E+06 DX2= -.564015E-06 T =  45.000 P = 14951326. S =  .000000E+00
...
...

          OUTPUT DATA AFTER ( 362,  4)-2-TIME STEPS                                                 THE TIME IS  .100000E+04 DAYS

@@@@@@@@@@@@@@@@@@@@@@@@@@@@@@@@@@@@@@@@@@@@@@@@@@@@@@@@@@@@@@@@@@@@@@@@@@@@@@@@@@@@@@@@@@@@@@@@@@@@@@@@@@@@@@@@@@@@@@@@@@@@@@@@@@@

  TOTAL TIME     KCYC   ITER  ITERC    KON        DX1M         DX2M         DX3M         MAX. RES.      NER    KER        DELTEX
  .864000E+08    362      4   2489      2       .12191E+06   .60620E-01   .91553E-01     .29116E-07       4      3        .12097E+07

@@@@@@@@@@@@@@@@@@@@@@@@@@@@@@@@@@@@@@@@@@@@@@@@@@@@@@@@@@@@@@@@@@@@@@@@@@@@@@@@@@@@@@@@@@@@@@@@@@@@@@@@@@@@@@@@@@@@@@@@@@@@@@@@@@@@

 ELEM. INDEX    P          T         SG          SS         XNACL        YH2OG        XCO2aq        PCAP        k-red.      DG       DL
               (Pa)     (deg-C)                                                                    (Pa)                  (kg/m3)  (kg/m3)

 A1  1    1  .22320E+08  45.00  .93208E+00  .67918E-01  .00000E+00  .00000E+00  .15973E-01 -.10000E+08  .10000E+01  836.08      .00
 A1  2    2  .22243E+08  45.00  .95619E+00  .43809E-01  .00000E+00  .00000E+00  .15960E-01 -.10000E+08  .10000E+01  835.38      .00
 A1  3    3  .22167E+08  45.00  .95895E+00  .41047E-01  .00000E+00  .00000E+00  .15947E-01 -.10000E+08  .10000E+01  834.69      .00
 A1  4    4  .22115E+08  45.00  .95915E+00  .40850E-01  .00000E+00  .00000E+00  .15938E-01 -.10000E+08  .10000E+01  834.22      .00
 A1  5    5  .22076E+08  45.00  .96048E+00  .39518E-01  .00000E+00  .00000E+00  .15931E-01 -.10000E+08  .10000E+01  833.86      .00
 A1  6    6  .22045E+08  45.00  .96105E+00  .38948E-01  .00000E+00  .00000E+00  .15926E-01 -.10000E+08  .10000E+01  833.57      .00
 A1  7    7  .22018E+08  45.00  .96230E+00  .37702E-01  .00000E+00  .00000E+00  .15921E-01 -.10000E+08  .10000E+01  833.33      .00
 A1  8    8  .21995E+08  45.00  .96157E+00  .38430E-01  .00000E+00  .00000E+00  .15917E-01 -.10000E+08  .10000E+01  833.12      .00
 A1  9    9  .21975E+08  45.00  .96257E+00  .37432E-01  .00000E+00  .00000E+00  .15914E-01 -.10000E+08  .10000E+01  832.94      .00
 A1 10   10  .21957E+08  45.00  .96208E+00  .37917E-01  .00000E+00  .00000E+00  .15911E-01 -.10000E+08  .10000E+01  832.77      .00
 A1 11   11  .21940E+08  45.00  .96200E+00  .37999E-01  .00000E+00  .00000E+00  .15908E-01 -.10000E+08  .10000E+01  832.62      .00
 A1 12   12  .21925E+08  45.00  .96088E+00  .39119E-01  .00000E+00  .00000E+00  .15905E-01 -.10000E+08  .10000E+01  832.48      .00
 A1 13   13  .21911E+08  45.00  .96376E+00  .36238E-01  .00000E+00  .00000E+00  .15903E-01 -.10000E+08  .10000E+01  832.35      .00
 A1 14   14  .21898E+08  45.00  .96309E+00  .36913E-01  .00000E+00  .00000E+00  .15901E-01 -.10000E+08  .10000E+01  832.23      .00
 A1 15   15  .21885E+08  45.00  .96087E+00  .39133E-01  .00000E+00  .00000E+00  .15899E-01 -.10000E+08  .10000E+01  832.12      .00
```

Figure 17. Part of printed output for radial flow problem.

confirming the approximate preservation of the similarity property in the numerical solution. Minor deviations in the time series data at values $R^2/t < 10^{-5}$ m^2/s correspond to conditions at very large times, where effects of the finite system size are beginning to be felt. Fig. 19 presents simulated results for gas saturation as a function of the similarity variable, showing three distinct regions emerging from the CO_2 injection process. The first region with $R^2/t \leq 1.3 \times 10^{-5}$ m^2/s corresponds to a zone where complete dry-out of aqueous phase has occurred. Gas saturation in this region is slightly less than 1, however, due to the presence of solid precipitate (Fig. 20). The dry-out zone is followed by an intermediate zone extending to $R^2/t \approx 10^{-2}$ m^2/s where liquid and gas phases coexist. Finally, there is an outer region with $R^2/t > 10^{-2}$ m^2/s in which single-phase liquid conditions prevail.

For comparison Figs. 18 - 22 also include results generated by LBNL for the code intercomparison project with an earlier version of the ECO2N-module. The main difference to the present simulation is that the earlier version used an evaporation model for H_2O partitioning into the CO_2-rich phase. We ran a problem variation using the evaporation model with the present ECO2N module (IE(12)=1), and obtained results that were virtually identical to the previous LBNL results in the code intercomparison project. Fig. 23 shows that the evaporation model strongly underestimates the amount of water dissolving into the CO_2-rich phase. The Spycher and Pruess (2005) model for phase partitioning produces a more vigorous drying process, accelerating the growth of a dry-out zone around the injection well (Fig. 19), and giving rise to increased salt precipitation (Fig. 20). The larger extent of the dry-out zone and increased salt precipitation there are the only significant differences in comparison to the earlier LBNL results. The peculiar behavior of NaCl mass fraction in liquid seen in Fig. 22 is due to dissolution of CO_2. At large $R^2/t > 10^{-2}$ m^2/s, NaCl mass fraction is unchanged from the initial value of 0.15. The modest reduction of NaCl mass fraction to approximately 0.146 in the two-phase zone ($1.3x10^{-5}$ $m^2/s < R^2/t < 10^{-2}$ m^2/s) is due to the volume increase of the aqueous phase upon CO_2 dissolution. The sharp peak in NaCl concentration at the inner boundary of the two-phase zone ($R^2/t \approx 1.3x10^{-5}$ m^2/s) occurs because conditions are approaching dry-out there.

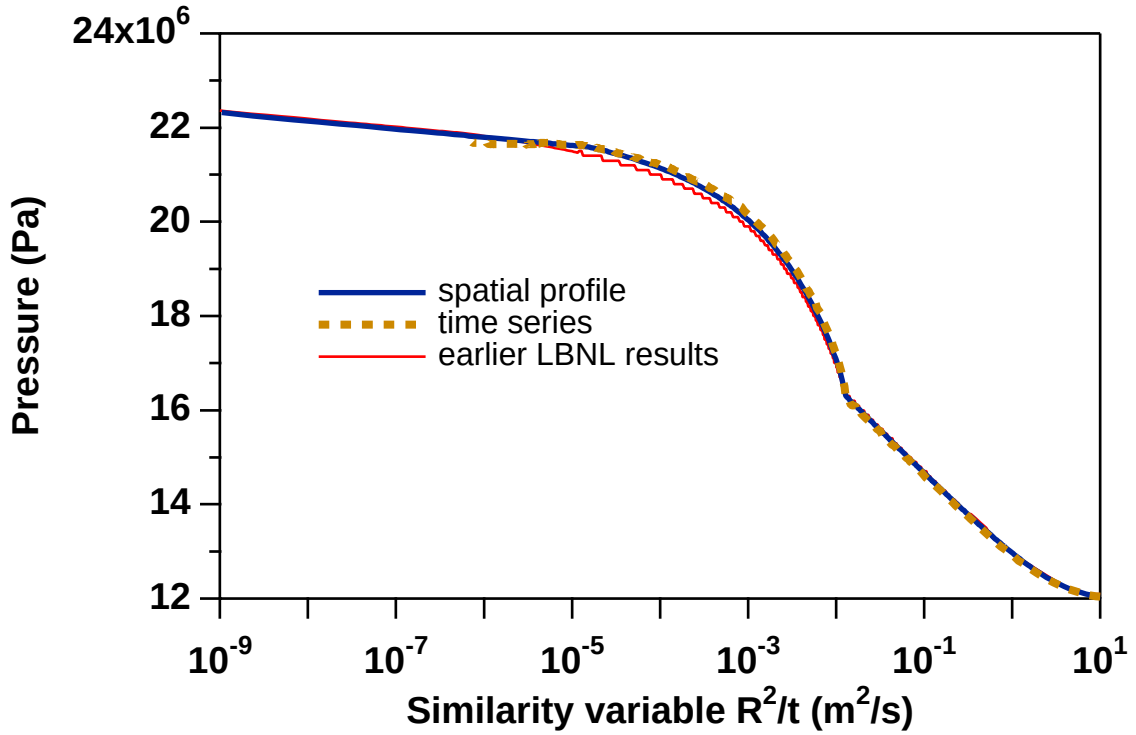

Figure 18. Simulated pressures as a function of the similarity variable. The thick solid line represents a spatial profile at a simulation time of 8.64×10^7 s, while the thick dashed line represents a time series of data for a grid block at a radial distance of R = 25.25 m. The thin line gives the results previously submitted by LBNL to the code intercomparison project, that were obtained with an earlier version of the ECO2N module.

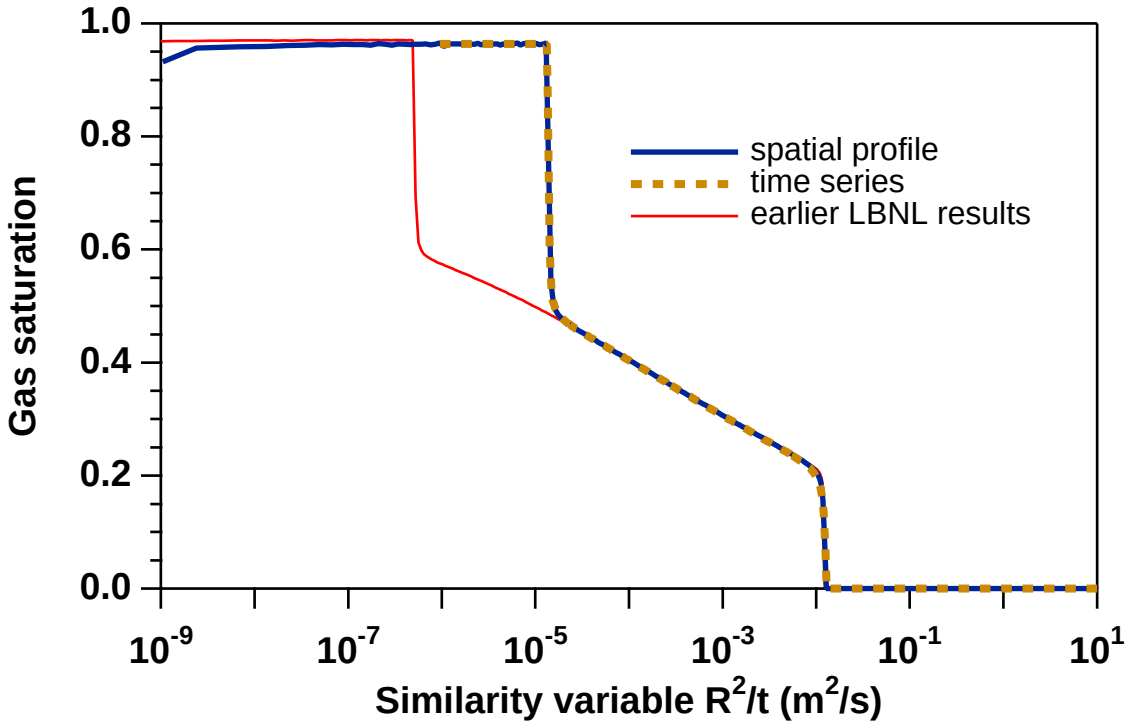

Figure 19. Simulated gas saturations.

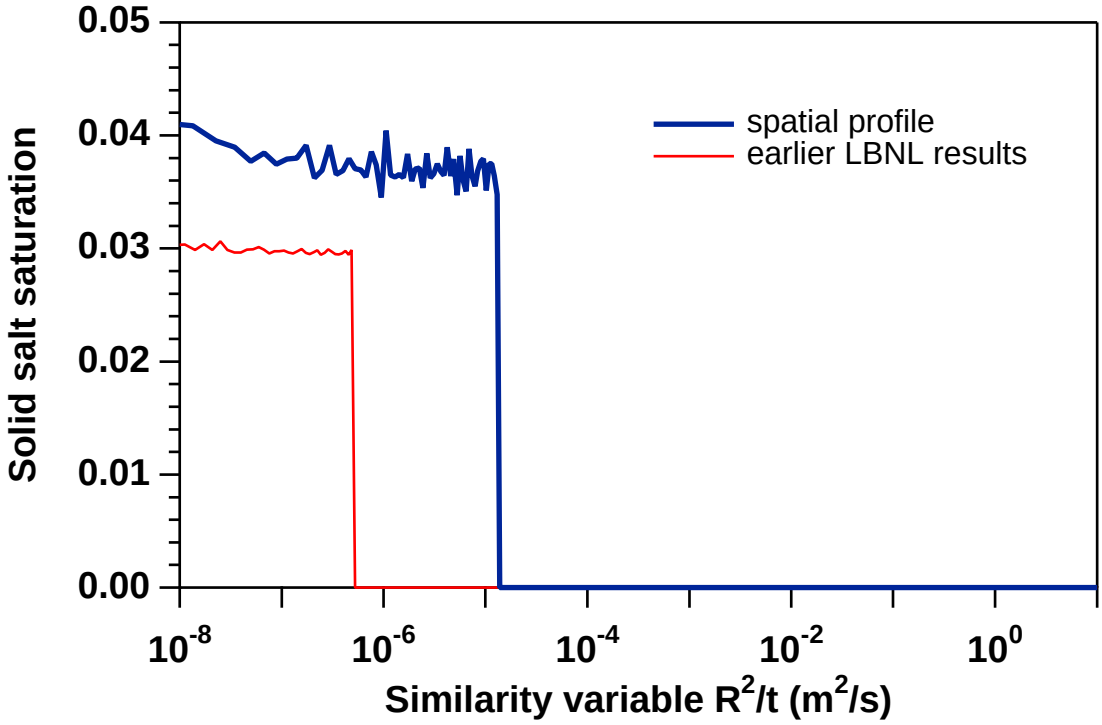

Figure 20. Simulated solid saturations.

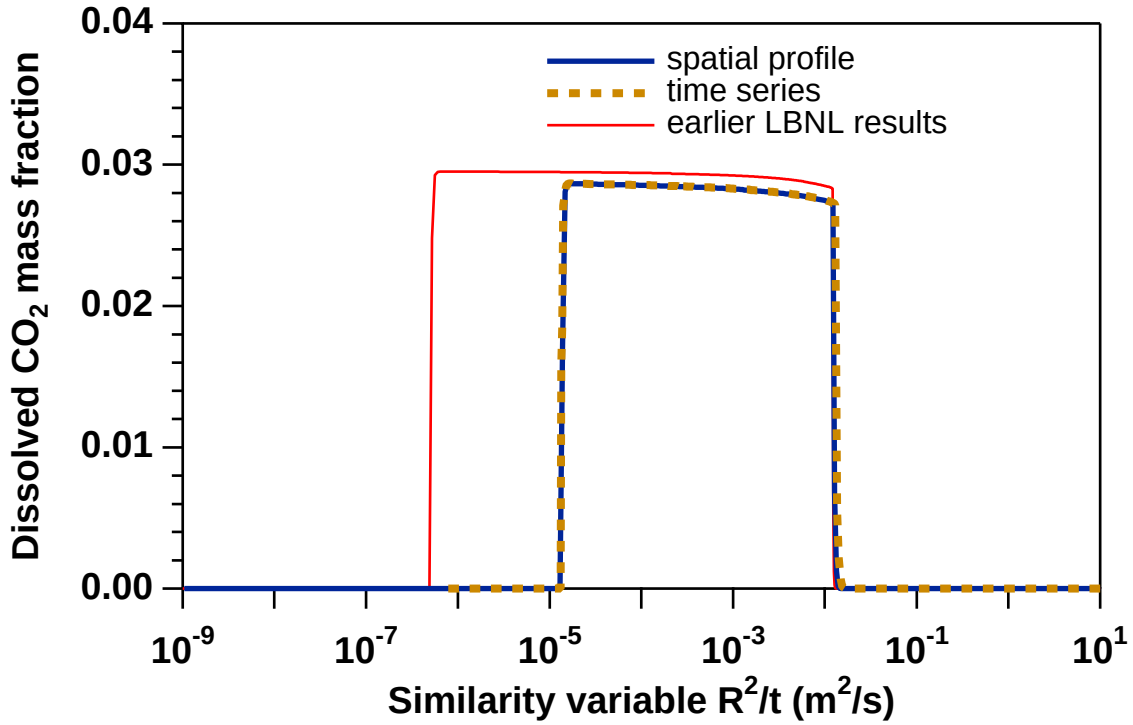

Figure 21. Simulated CO_2 mass fraction in aqueous phase.

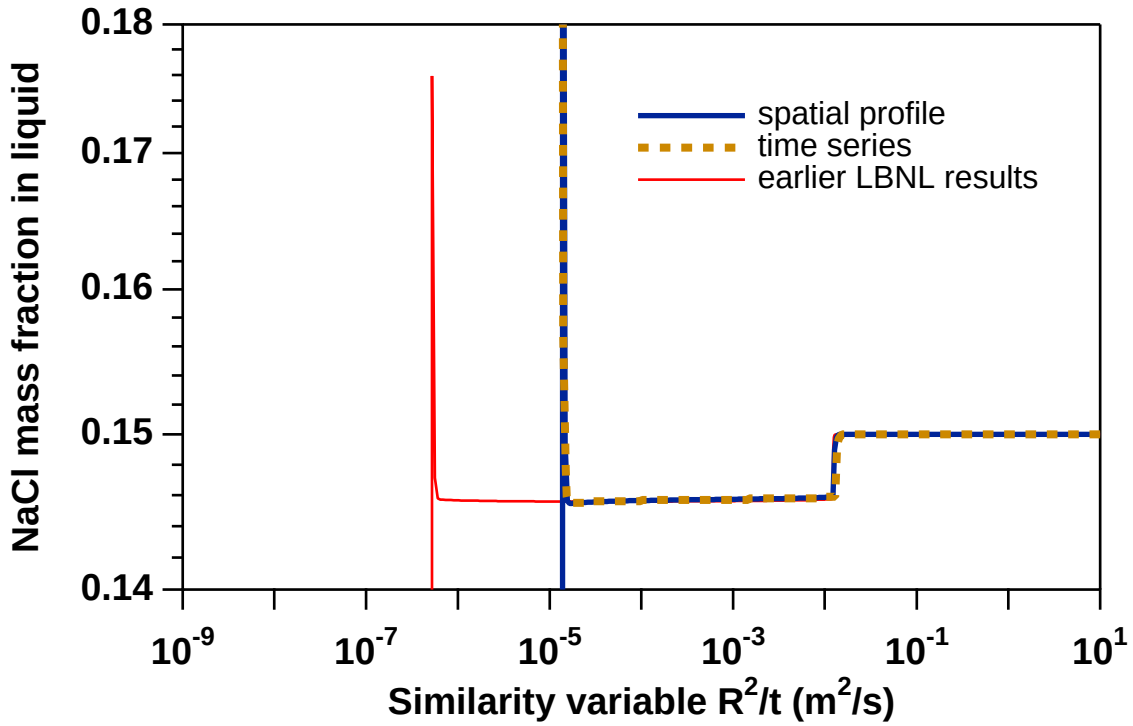

Figure 22. Simulated NaCl mass fraction in aqueous phase.

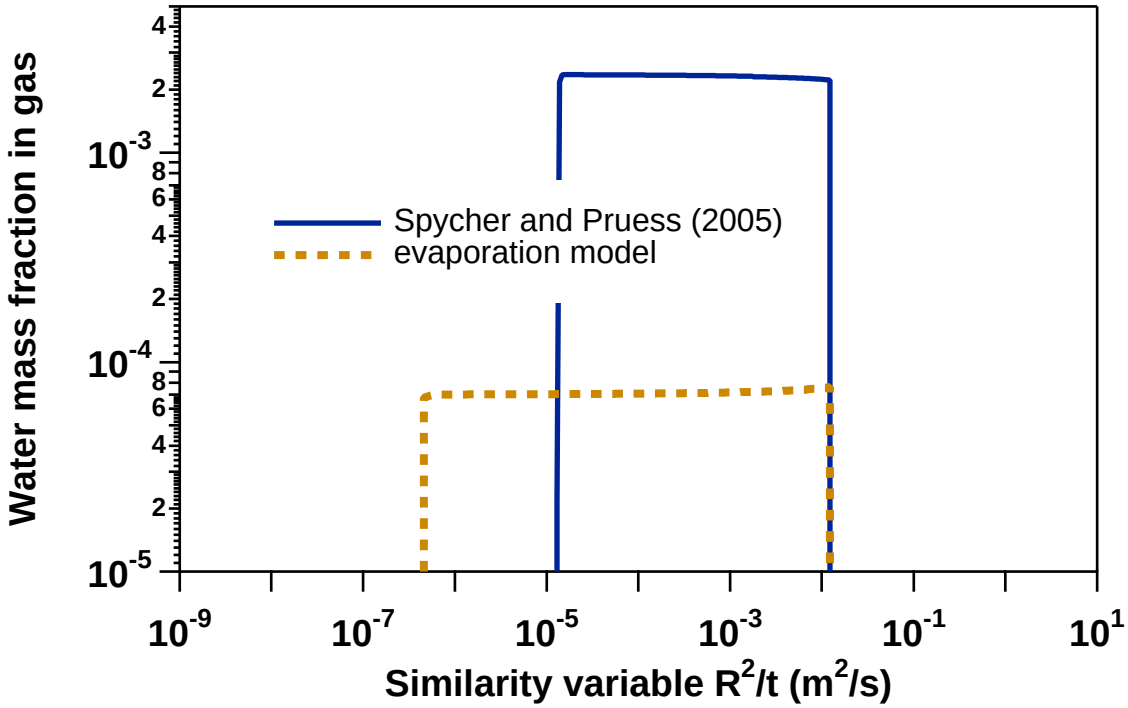

Figure 23. Simulated water mass fraction in CO_2-rich phase.

5.3 Problem No. 3 (*r1dv*) - CO_2 Discharge Along a Fault Zone

The amounts of CO_2 that would need to be disposed of at fossil-fueled power plants are very large. A coal-fired plant with a capacity of 1,000 MWe generates approximately 30,000 tonnes of CO_2 per day (Hitchon 1996). When disposed of into brine formations, CO_2 injection plumes would over time extend to large distances of the order of ten kilometers or more, making it likely that geologic discontinuities such as faults and fractures will be encountered, with an associated potential for CO_2 losses from the primary disposal aquifer. CO_2 leaks through caprock discontinuities have a potential for self-enhancement, because pressures can actually decrease and/or flow rates increase as escaping CO_2 creates a pathway towards shallower strata. It is not known whether or not it may be possible for a runaway process to develop where an initially "small" leak could accelerate and grow over time to the point of an eruptive release.

Migration of CO_2 along a water-saturated fault zone would be subject to gravitational and viscous instabilities, and would likely involve complex two- and three-dimensional flow effects. As a first approximation to this kind of problem, we consider here a highly simplified situation in which a potential CO_2 leakage path is modeled as a 1-D column (Fig. B.1). This problem was also included as #4 in the code intercomparison project (Pruess et al., 2002, 2004); specifications are given in Appendix B.

The problem is run in two segments. A first run segment obtains gravity equilibrium relative to a pressure of 100 bar prescribed at the top boundary. The gravity-equilibrated conditions are then used as initial conditions in a second run segment, where conditions of P = 240 bar and a mass fraction $X_{CO2} = 1$ are maintained at the lower boundary, while upper boundary conditions are unchanged. Note that the CO_2 discharge conditions correspond to a large overpressure, exceeding initial hydrostatic pressure by approximately 60 %. It is unlikely that overpressures this large would be used in practical CO_2 storage systems. All runs are performed for pure water (no salinity) in isothermal mode at T = 45 ˚C. A length of 1 m of fault zone is simulated and a constant vertical grid spacing of 5 m is used. Capillary pressure parameters were chosen so that maximum P_{cap} is 10^7 Pa, and P_{cap} vanishes for small gas saturations of $S_g \leq 0.001$. These and other simulation parameters can be seen from the TOUGH2 input file shown in Fig. 24. For this simple 1-D problem, the calculational mesh is generated simply by directly specifying "repeat" elements and connections in the TOUGH2 input file. The 500 m vertical extent of the fault zone is evenly divided into 100 grid blocks of 5 m height. Additional blocks *top 0* and *bot 0* are used to represent boundary conditions. For the 1 m length of the 25 m wide fault zone modeled, interface areas are 25 m^2. Input data also include COFT and FOFT blocks for generating output data for plotting. For reference we list representative fluid properties used in the simulation in Table 4.

```
*r1dv* ... 1-D vertical column; CO2 migration up a fault zone
ROCKS----1----*----2----*----3----*----4----*----5----*----6----*----7----*----8
fault    2  2600.e00       .35  100.e-15  100.e-15  100.e-15      2.51      920.
   4.5e-10
    7           .457       .30        1.       .05
    7           .457       .00    5.1e-5      1.e7      .999
CO2in    2  2600.e00       .35  100.e-15  100.e-15  100.e-15      2.51      920.
   4.5e-10
    7           .457       .30        1.       .05
    8

MULTI----1----*----2----*----3----*----4----*----5----*----6----*----7----*----8
    3    3    3    6
SELEC....2....3....4....5....6....7....8....9...10...11...12...13...14...15...16
    1                                        0    0    0    0    0    0    0
        .8   .8
SOLVR----1----*----2----*----3----*----4----*----5----*----6----*----7----*----8
5  Z1   O0    8.0e-1    1.0e-7
START----1----*----2----*----3----*----4----*----5----*----6----*----7----*----8
----*----1 MOP: 123456789*123456789*1234 ---*----5----*----6----*----7----*----8
START----1----*----2----*----3----*----4----*----5----*----6----*----7----*----8
PARAM----1----*----2----*----3----*----4----*----5----*----6----*----7----*----8
   11000    9999 000 00000000  4    3
                           -1.                          9.81
        1.        9.      9.e1      9.e2
     1.E-5     1.E00
              100.e5                 .00                 0.0                 45.
INDOM----1----*----2----*----3----*----4----*----5----*----6----*----7----*----8
CO2in
              240.e5                 .00                 1.0                 45.

ELEME----1----*----2----*----3----*----4----*----5----*----6----*----7----*----8
flt 0   99    1fault      125.
ina
top 0
bot 0          CO2in

CONNE----1----*----2----*----3----*----4----*----5----*----6----*----7----*----8
bot 0flt 0                   3     1.e-3       2.5       25.       -1.
flt 0flt 1   98    1    1    3       2.5       2.5       25.       -1.
flt99top 0                   3       2.5     1.e-3       25.       -1.

COFT ----1----*----2----*----3----*----4----*----5----*----6----*----7----*----8
bot 0flt 0                   3     1.e-3       2.5       25.        1.
flt99top 0                   3       2.5     1.e-3       25.        1.

FOFT ----1----*----2----*----3----*----4----*----5----*----6----*----7----*----8
flt74
flt75

GENER----1----*----2----*----3----*----4----*----5----*----6----*----7----*----8

TIMES----1----*----2----*----3----*----4----*----5----*----6----*----7----*----8
    8
      1.E5      1.e6      1.e7      2.e7      1.e8      1.e9     1.e10     1.e11
ENDCY----1----*----2----*----3----*----4----*----5----*----6----*----7----*----8
```

Figure 24. TOUGH2 input file for fault zone problem.

Table 4. PVT properties at a temperature of 45 ˚C at selected pressures, as used in the TOUGH2/ECO2N simulation.

Pressure (bar) fluid phase	120	160	200	240
pure water				
density (kg/m^3)	994.768	996.292	997.821	999.354
viscosity (Pa s)	5.97778e-4	5.98341e-4	5.98929e-4	5.99540e-4
water with CO_2				
density (kg/m^3)	1005.79	1008.00	1009.94	1011.74
viscosity (Pa s)	5.97778e-4	5.98341e-4	5.98929e-4	5.99540e-4
CO_2 mass fraction	5.20592e-2	5.55092e-2	5.76593e-2	5.91875e-2
gas				
density (kg/m^3)	659.261	760.931	813.504	850.176
viscosity (Pa s)	5.17641e-5	6.56503e-5	7.45231e-5	8.15904e-5
water mass fraction	2.14658e-3	2.41648e-3	2.54446e-3	2.62678e-3

5.3.1 Gravity Equilibration

Gravity-equilibrated initial conditions are obtained from a simulation in which the element *bot 0* is removed from the input file. Larger time steps (Δt_1 = 1.e3, Δt_2 = 9.e3 s) are used, along with a tight convergence tolerance of RE1 = 1.e-10. Pore compressibility is set to 0 in this part of the simulation, so that porosity remains a constant 35 % throughout as fluid pressures change. After 22 time steps and a simulation time of t = 4.72×10^9 seconds an accurate hydrostatic equilibrium is obtained, with maximum pore velocities of 2×10^{-19} m/s. Pressure in the lowest grid block, 2.5 m above the lower boundary, is computed as 148.56 bar.

5.3.2 CO_2 Displacement

Migration of CO2 up the fault zone is simulated with the input file as given in Fig. 24, and using the SAVE file from the gravity equilibration as INCON. The main process in this problem is immiscible displacement of water by CO_2. In response to the applied step change in pressure at the bottom of the fault, CO_2 enters the system at the lower boundary and migrates up the fault, displacing some of the water and also partially dissolving in residual water, while some water also dissolves in the CO_2. The problem is run in two variations, (1) using the Spycher and Pruess (2005) phase partitioning model, and (2) using an evaporation model for water partitioning into the gas phase (parameter IE(12)=1).

```
 flt 0(   1,  3) ST =  .100000E+01 DT =  .100000E+01 DX1=  .165690E+07 DX2=  .000000E+00 T =  45.000 P = 16512647. S =  .000000E+00
 flt 0(   2,  3) ST =  .100000E+02 DT =  .900000E+01 DX1=  .464971E+07 DX2=  .000000E+00 T =  45.000 P = 21162352. S =  .000000E+00
 flt 1(   3,  3) ST =  .100000E+03 DT =  .900000E+02 DX1=  .363610E+07 DX2=  .000000E+00 T =  45.000 P = 19411972. S =  .000000E+00
 flt 1(   4,  4) ST =  .100000E+04 DT =  .900000E+03 DX1=  .290174E+07 DX2=  .000000E+00 T =  45.000 P = 22313713. S =  .000000E+00
 flt 1(   5,  7) ST =  .280000E+04 DT =  .180000E+04 DX1=  .277921E+06 DX2=  .000000E+00 T =  45.000 P = 22591635. S =  .000000E+00
 flt 1(   6,  4) ST =  .460000E+04 DT =  .180000E+04 DX1=  .617239E+05 DX2=  .000000E+00 T =  45.000 P = 22653358. S =  .000000E+00
 flt 1(   7,  4) ST =  .820000E+04 DT =  .360000E+04 DX1= -.862272E+04 DX2=  .000000E+00 T =  45.000 P = 22644736. S =  .000000E+00
 flt 2(   8,  4) ST =  .154000E+05 DT =  .720000E+04 DX1=  .301216E+05 DX2=  .000000E+00 T =  45.000 P = 22260427. S =  .000000E+00
 flt 1(   9,  4) ST =  .298000E+05 DT =  .144000E+05 DX1= -.147843E+05 DX2=  .000000E+00 T =  45.000 P = 22553169. S =  .000000E+00
 flt 2(  10,  7) ST =  .586000E+05 DT =  .288000E+05 DX1=  .321292E+06 DX2=  .000000E+00 T =  45.000 P = 22638774. S =  .000000E+00
 flt 1(  11,  4) ST =  .874000E+05 DT =  .288000E+05 DX1=  .429207E+06 DX2=  .000000E+00 T =  45.000 P = 23325094. S =  .544962E-01
 flt 1(  12,  3) ST =  .100000E+06 DT =  .126000E+05 DX1=  .928885E+05 DX2=  .000000E+00 T =  45.000 P = 23417983. S =  .748881E-01

 *r1dv* ... 1-D vertical column; CO2 migration up a fault zone

          OUTPUT DATA AFTER (  12,  3)-2-TIME STEPS                                                   THE TIME IS  .115741E+01 DAYS

@@@@@@@@@@@@@@@@@@@@@@@@@@@@@@@@@@@@@@@@@@@@@@@@@@@@@@@@@@@@@@@@@@@@@@@@@@@@@@@@@@@@@@@@@@@@@@@@@@@@@@@@@@@@@@@@@@@@@@@@@@@@@@@@@@@

  TOTAL TIME     KCYC    ITER  ITERC    KON        DX1M          DX2M          DX3M         MAX. RES.       NER    KER        DELTEX
  .100000E+06     12       3     50      2       .24551E+06    .00000E+00    .20392E-01     .37926E-05       2      3       .12600E+05

@@@@@@@@@@@@@@@@@@@@@@@@@@@@@@@@@@@@@@@@@@@@@@@@@@@@@@@@@@@@@@@@@@@@@@@@@@@@@@@@@@@@@@@@@@@@@@@@@@@@@@@@@@@@@@@@@@@@@@@@@@@@@@@@@@@

 ELEM. INDEX   P          T         SG          SS         XNACL        YH2OG       XCO2aq       PCAP        k-red.       DG         DL
              (Pa)     (deg-C)                                                                   (Pa)                   (kg/m3)    (kg/m3)

 flt 0    1  .23971E+08  45.00  .20235E+00  .00000E+00  .00000E+00  .26293E-02  .59178E-01 -.15342E+05  .10000E+01  849.95    1011.73
 flt 1    2  .23418E+08  45.00  .74888E-01  .00000E+00  .00000E+00  .26189E-02  .58995E-01 -.77996E+04  .10000E+01  845.47    1011.48
 flt 2    3  .22886E+08  45.00  .00000E+00  .00000E+00  .00000E+00  .10000E+01  .10509E-01  .00000E+00  .10000E+01     .00    1001.11
 flt 3    4  .22725E+08  45.00  .00000E+00  .00000E+00  .00000E+00  .10000E+01  .13021E-02  .00000E+00  .10000E+01     .00     999.13
 flt 4    5  .22564E+08  45.00  .00000E+00  .00000E+00  .00000E+00  .10000E+01  .13793E-03  .00000E+00  .10000E+01     .00     998.83
```

Figure 25. Part of printed output for fault leakage problem.

Part of the printed output is shown in Fig. 25. Simulation results are plotted in Figs. 26 - 30, with thick solid lines representing variation (1), thick dashed lines representing variation (2), and thin dotted lines showing results from various groups that participated in the code intercomparison study. Variation (1) is considered the most accurate, while variation (2) strongly underestimates the uptake of water by the CO_2 rich phase. Variation (2) was included here to bring out effects of water dissolution in the gas phase that are missed in the simplistic evaporation model, and to offer a comparison to results submitted in the code intercomparison project, all of which employ an evaporation model. The variation (2) results agree closely with the LBNL submission to the code intercomparison project.

The simulated evolution of the system proceeds through four stages (Figs. 26, 27). In Stage 1, CO_2 enters the first grid block above the lower boundary, evolving a gas phase there and causing rapid pressurization that migrates up the fault. Stage 1 ends at approximately 10^4 seconds when the pressure pulse reaches the top of the fault, causing outflow of water to commence. During the subsequent Stage 2 the CO_2 displacement front migrates up the fault until, after about $3x10^7$ seconds, the front reaches the top. At this time CO_2 discharge from the fault begins, while water discharge is reduced because of relative permeability effects, and also because capillary effects reduce the effective pressure gradient for the aqueous phase at the top of the fault. Stage 3 lasts from approximately $3x10^7$ to $3x10^9$ seconds, and is characterized by two-phase outflow of liquid and gas from the fault. Water continues to be removed from the fault not only by advection, but also by dissolution into the flowing gas phase, causing gas relative permeabilities and flow rates to

increase. As gas saturations increase capillary pressures get stronger, and at 3.1×10^9 seconds the effective pressure gradient for the aqueous phase at the top of the fault reverses, leading to downflow of water from the top boundary. The water dissolves into the flowing CO_2 stream and is carried right back out at the top. Eventually the entire flow system dries out, and in Stage 4 we have a steady single-phase gas flow up the fault. TOUGH2 recognizes a steady state, and the simulation terminates after 395 time steps and a simulation time of 1.0×10^{11} seconds.

Simulation progress and time stepping reflect non-linearities of the flow processes. Many relatively small time steps are required toward the end of Stage 2 as the two-phase front approaches the upper boundary (Fig. 26). Smaller time steps again occur towards the end of Stage 3 when the dryout front approaches the top boundary.

Gas saturations are shown at times of 10^7 and 10^9 seconds in Fig. 28. At earlier time there is little difference between the profiles calculated with the two alternative models for water partitioning into gas, while at later time the more accurate Spycher and Pruess (2005) model gives rise to more vigorous dry-out. The pressure profile at 10^7 seconds has a change in slope at an elevation of 215 m, due to the transition from two-phase conditions below to single-phase conditions above (Fig. 29). The pressure gradient in the two-phase zone is larger than in the single-phase region, indicating that mobility loss from relative permeability effects dominates over mobility gain from the lower viscosity of CO_2 as compared to water. At late time pressure gradients are smaller in the single-phase dry-out region, due to increased fluid mobility there, while gradients are larger in the overlying two-phase zone. Upward movement of the dry-out zone results in increasing pressure gradients at the top of the fault, giving rise to a local maximum in water outflow rate at about 3×10^9 s (Fig. 27). Simulated phase partitioning after 10^7 seconds is shown in Fig. 30.

Results for the simulated CO_2 inventory of the system at $t = 10^7$ and 2×10^7 seconds are given in Table 5.

Table 5. CO_2 inventory.

time	10^7 seconds	2×10^7 seconds
gas phase	401.498 tonnes	692.639 tonnes
liquid phase	85.340 tonnes	147.258 tonnes
total	486.838 tonnes	839.897 tonnes

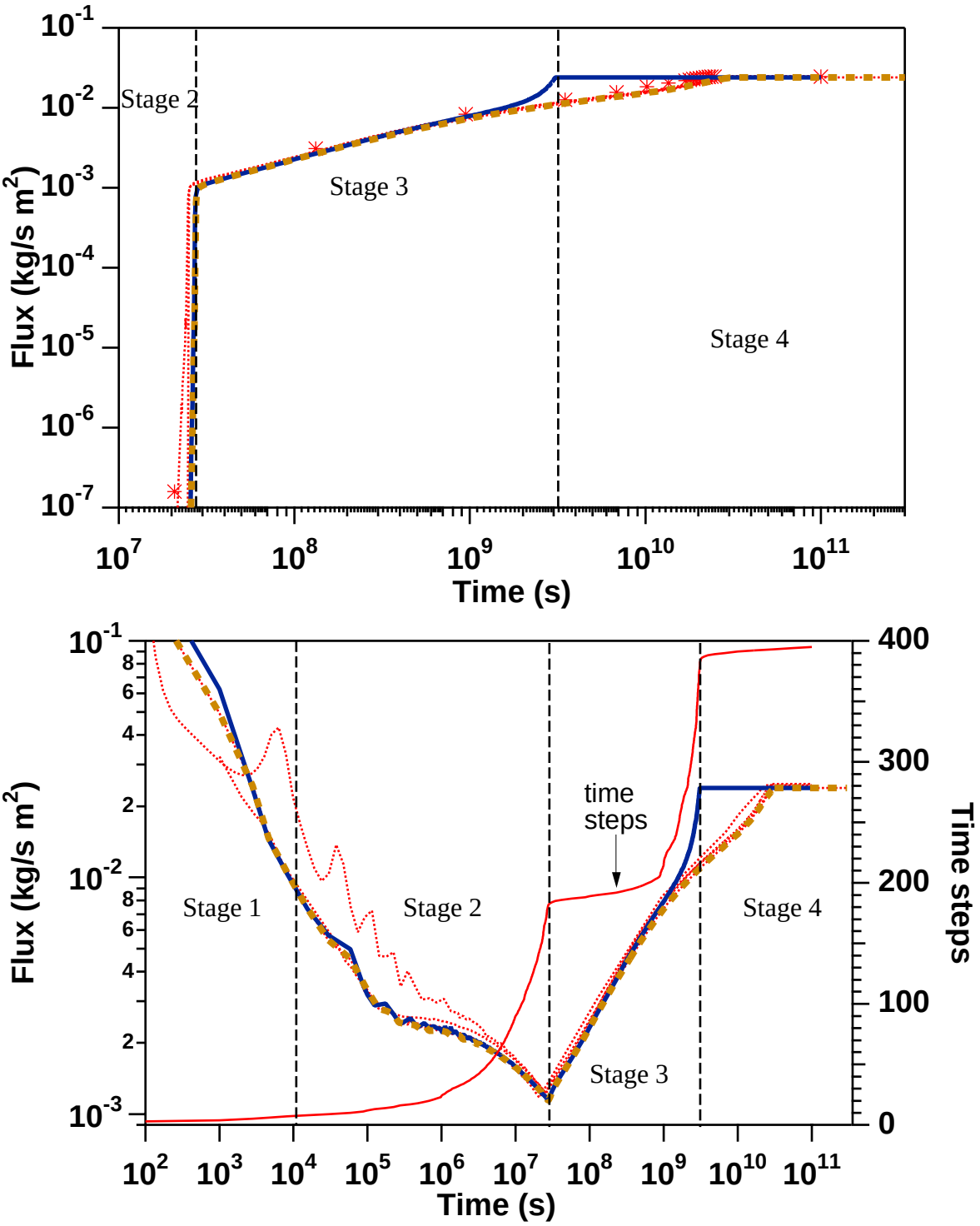

Figure 26. Simulated CO_2 fluxes at bottom (lower frame) and top (upper frame) of fault zone. Thick lines are for variation (1) - rigorous H_2O-CO_2 phase partitioning, while dashed lines are for variation (2) - evaporation model for H_2O partitioning into the CO_2-rich phase. Thin lines and symbols represent results submitted in the code intercomparison project. The dashed vertical lines mark the different stages in the evolution of the system.

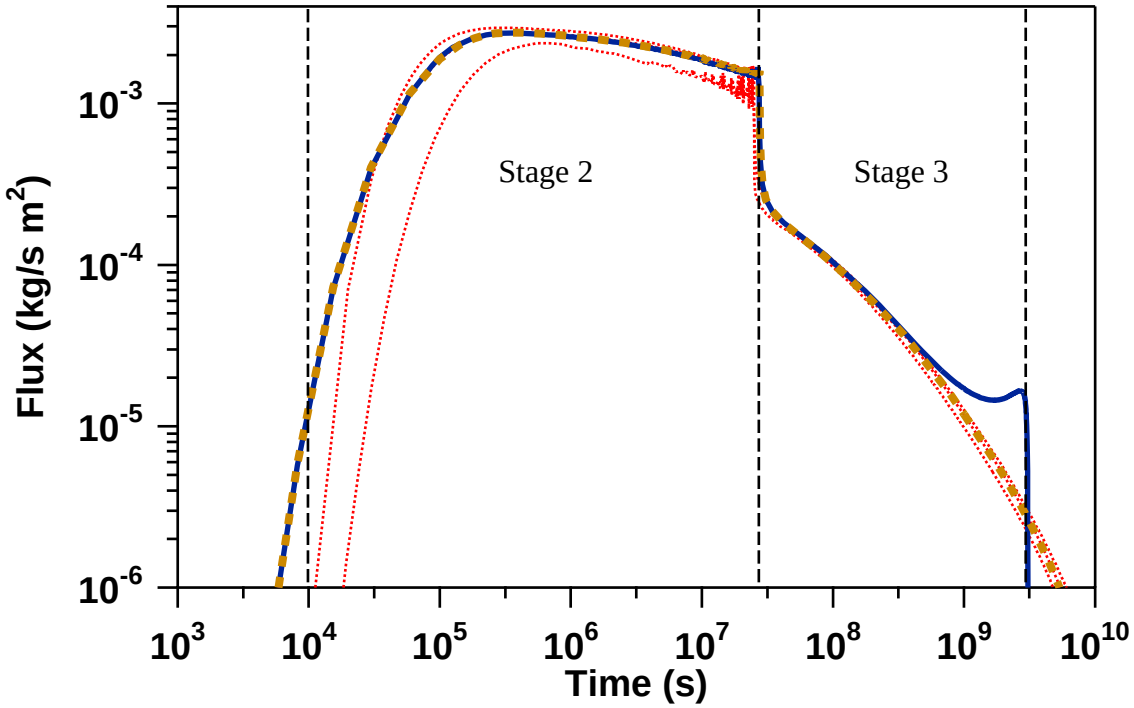

Figure 27. Simulated water flux at top of fault zone. Thick line is for variation (1), dashed line for variation (2), and thin lines represent results submitted in the code intercomparison project.

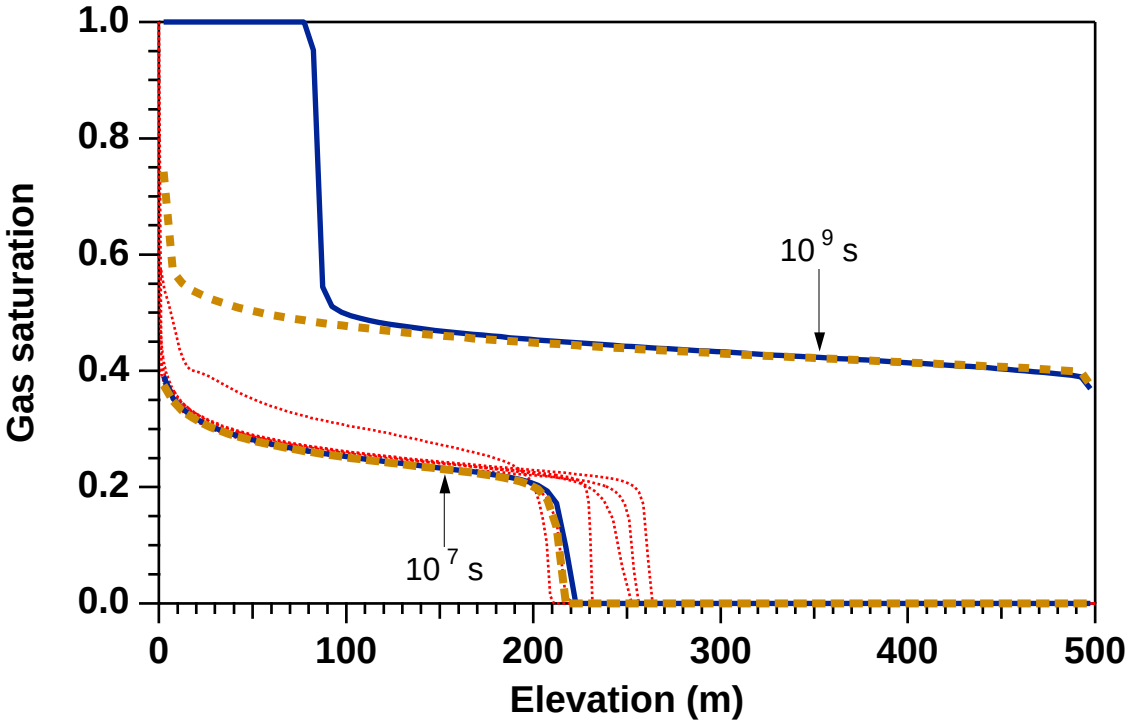

Figure 28. Gas saturation profiles at times of 10^7 and 10^9 seconds. Thick line is for variation (1), dashed line for variation (2), and thin lines represent results from the code intercomparison project.

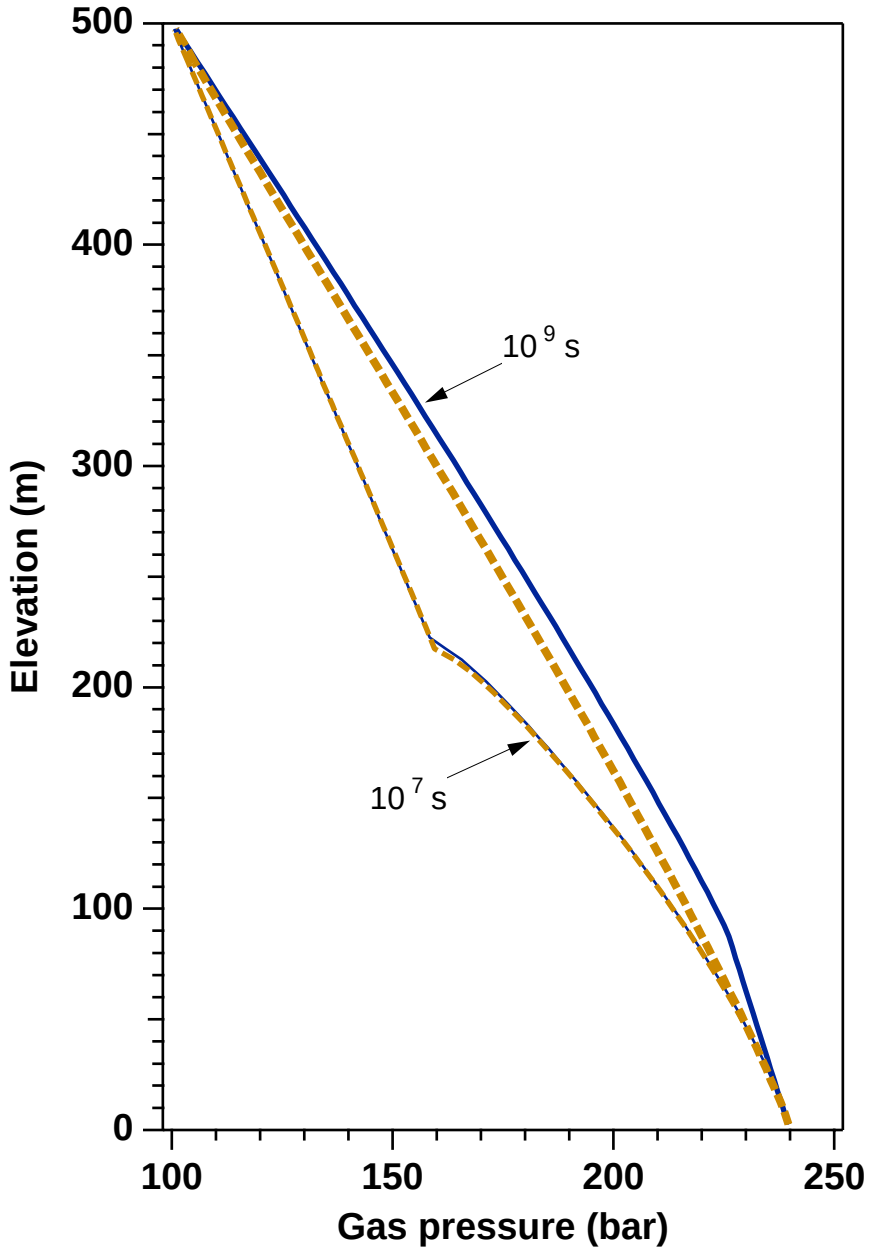

Figure 29. Pressure profiles at times of 10^7 and 10^9 seconds. Solid lines are for variation (1), dashed lines for variation (2).

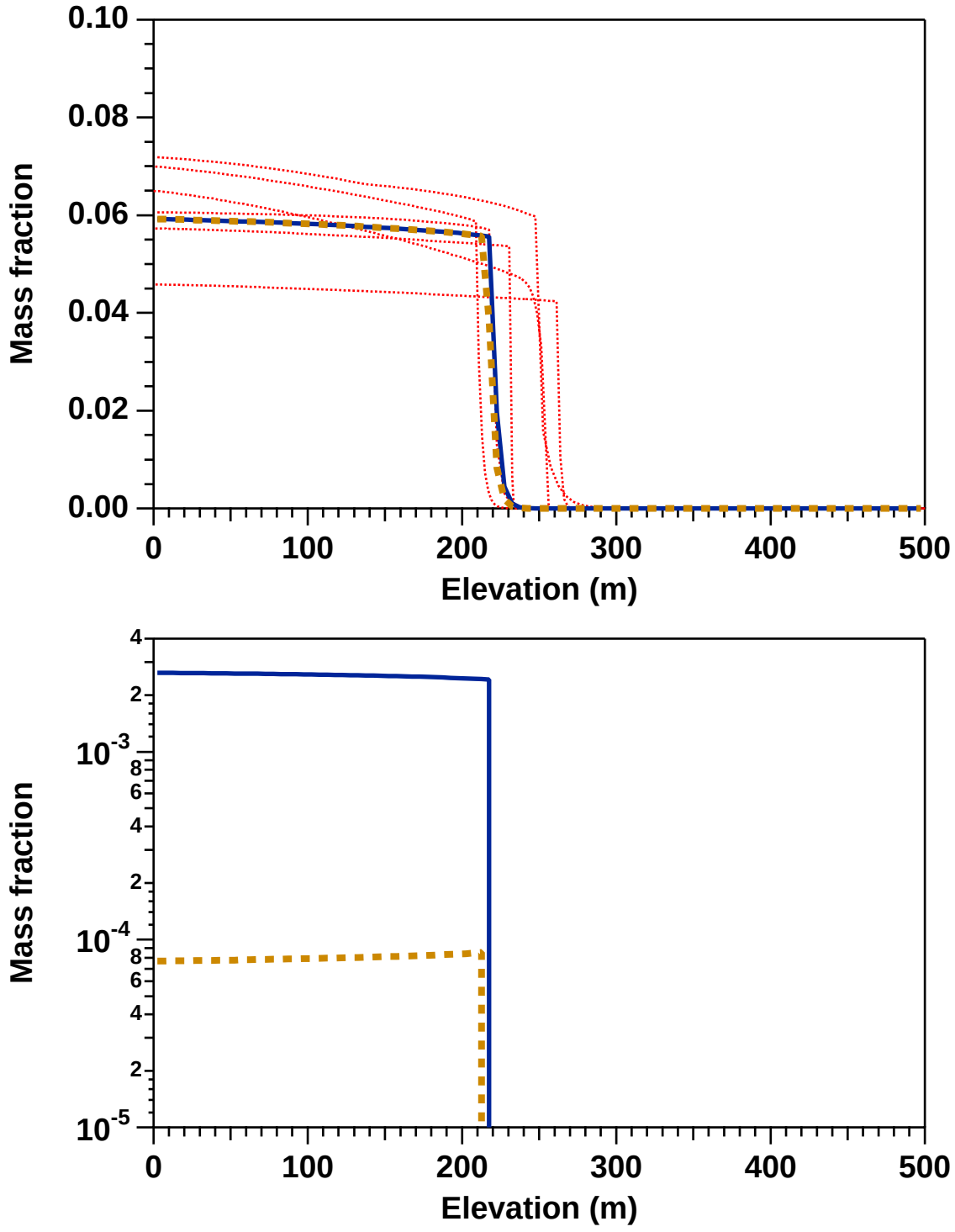

Figure 30. Dissolved CO_2 mass fraction in aqueous phase (top) and dissolved water mass fraction in gas (bottom) after 10^7 s. Thick lines are for variation (1), dashed lines for variation (2), and thin lines represent results submitted in the code intercomparison project.

5.4 Problem No. 4 (*rtp7*) - CO_2 Injection into a 2-D Layered Brine Formation

The first industrial-scale CO_2 disposal project to become operational is at the Sleipner Vest field in the Norwegian sector of the North Sea, where approximately 10^6 tonnes of CO_2 per year have been injected since 1996 through a horizontal well into sands of the Utsira formation. Time-lapse seismic surveys have shown that CO_2 migration at Sleipner is dominated by buoyancy effects and is strongly affected by shale interbeds of low permeability (Lindeberg et al., 2002). The present test problem was patterned after conditions at Sleipner and was designed to investigate CO_2 migration in a heterogeneous sand-shale sequence. It had been included as #7 in the code intercomparison project (Pruess et al., 2002, 2004). A 2-D vertical section was modeled (Fig. C.1, Appendix C), with problem specifications given in Appendix C. The problem was run in several segments to first obtain the initial and boundary conditions, and then inject CO_2 according to specifications. All runs were performed in isothermal mode at a temperature of 37 ˚C and a salinity of 3.2 wt.-% NaCl.

The grid should be designed in such a way as to obtain "adequate" spatial resolution in regions where significant gradients occur, i.e., near the injection well, and near the shale layers (Fig. C.1). The grid is generated with the MESHMAKER facility of TOUGH2 as a horizontal (x-y) grid and is then rotated by 90 degrees around the x-axis to obtain a vertical section. Subroutine GXYZ was modified to automatically assign "sand" and "shale" domain identifiers to grid blocks at the appropriate elevations (Fig. 31). Gridding in the x-direction starts with 1 m increments at the well, and becomes coarser at increasing distance (Table 6). 28 grid blocks are used to get out to a distance of 6,000 m, followed by a small grid increment of 10^{-3} m to serve as boundary blocks to maintain a hydrostatic pressure profile. Gridding in the y-direction also uses a 1 m increment at the well, with coarser gridding below and above. The shale layers are represented as single grid layers of 3 m height, with 3 m gridding also in the sands above and below. The thickness of the grid is 1 m. Overall the gridding is considered rather coarse, meeting minimum requirements for spatial resolution at the well and at the shale layers.

```
      DO1 J=1,NY
      JM=MOD(J-1,35)+1
      NOVJ=(J-1)/35
      IF(J.GT.1) YJ=YJ+DY(J)/2.+DY(J-1)/2.
c
c.....10-12-01: add domain identifiers
      dom='sand '
      yj52=yj-52.
      if(yj52.ge.0..and.mod(yj52,33.).le.3.) dom='shale'
```

Figure 31. Code fragment of subroutine GXYZ (module meshm.f), showing modifications for assigning domain identifiers to the heterogeneous sand-shale medium.

Table 6. MESHMAKER input data for grid generation.

```
MESHMAKER1----*----2----*----3----*----4----*----5----*----6----*----7----*----8
XYZ
       90.
NX      29
        1.        1.        2.        4.        4.        8.       15.       20.
       30.       40.       50.       50.      100.      150.       50.      150.
      300.       50.      475.      500.      500.      500.      500.      500.
      500.      500.      500.      500.     1.e-3
NY      34
        7.        6.        6.       2.5        1.       2.5        6.       12.
        6.        3.        3.        3.        6.       12.        6.        3.
        3.        3.        6.       12.        6.        3.        3.        3.
        6.       12.        6.        3.        3.        3.        6.       12.
        6.        3.
NZ       1       1.0

ENDFI----1----*----2----*----3----*----4----*----5----*----6----*----7----*----8
```

5.4.1 Gravity Equilibration

Initial conditions are generated in stages. A first simulation run uses a slightly modified version of the input file shown in Fig. 32 and involves just the column of boundary grid blocks beyond x = 6,000 m. Thermodynamic properties are specified as P = 110 bars, T = 37 ˚C, salinity X_S = 0.032, CO_2 mass fraction $X_{CO2} = 4.54104 \times 10^{-4}$. The latter value was obtained by trial and error, executing a few single-grid block initializations to obtain the desired P_{CO2} = 0.5 bar. Pressure is held constant at P = 110 bar at the elevation of the injection node (22 m) and the system is run to gravity equilibrium. To facilitate reaching an accurate equilibrium state, the shale layers are given the same absolute permeability as the sand layers for this simulation. Gravity equilibrium using a tight convergence tolerance of 10^{-8} is attained in seven time steps, corresponding to a simulation time of 3.25×10^9 s. Maximum pore velocities in the equilibrium state are below 10^{-17} m/s. A second run with the full two-dimensional grid is then performed, using the same initialization as for the 1-D gravity equilibration just described, and maintaining the 1-D gravity equilibrium as boundary conditions at the right hand side. For this calculation we again specify the same absolute permeability for shale as for sand. Gravity equilibration in the 2-D grid takes 12 time steps and a simulation time of 2.93×10^9 s.

5.4.2 Response to CO_2 Injection

CO_2 injection at a constant prescribed rate of 0.1585 kg/s is simulated with the input file as shown in Fig. 32. This input file specifies a total simulation time of 63.1152×10^6 s (2 years), with additional printout generated at times of 30 days (2.592×10^6 s) and one year (31.5576×10^6 s). A portion of the printed output is shown in Fig. 33, and results are given in Figs. 34-42.

```
*rtp7* ... test problem # 7: CO2 in layered formation
ROCKS----1----*----2----*----3----*----4----*----5----*----6----*----7----*----8
sand     2  2600.e00       .35    3.e-12    3.e-12    3.e-12      2.51      920.
   0.0e-10
    7           0.40      0.20        1.      0.05
    7           0.40      0.20   2.79e-4      1.e7      .999
shale    2  2600.e00     .1025   10.e-15   10.e-15   10.e-15      2.51      920.
   0.0e-10
    7           0.40      0.20        1.      0.05
    7           0.40      0.20   1.61e-5      1.e7      .999

MULTI----1----*----2----*----3----*----4----*----5----*----6----*----7----*----8
    3    3    3    6
SELEC....2....3....4....5....6....7....8....9...10...11...12...13...14...15...16
    1                                          0    0    0    0    0    0    0
        .8   .8
START----1----*----2----*----3----*----4----*----5----*----6----*----7----*----8
----*----1 MOP: 123456789*123456789*1234 ---*----5----*----6----*----7----*----8
PARAM----1----*----2----*----3----*----4----*----5----*----6----*----7----*----8
   1 600    99991000 00000000  4    3
          63.1152e6       -1.                          -9.81
     1.e2
    1.E-5     1.E00
             110.e5              3.2e-2         .454104e-03                 37.
SOLVR----1----*----2----*----3----*----4----*----5----*----6----*----7----*----8
5  Z1   O0    8.0e-1    1.0e-7
GENER----1----*----2----*----3----*----4----*----5----*----6----*----7----*----8
A15 1inj 1                  1     COM3      .1585

TIMES----1----*----2----*----3----*----4----*----5----*----6----*----7----*----8
    3
   2.592e6 31.5576e6 63.1152e6
FOFT ----1----*----2----*----3----*----4----*----5----*----6----*----7----*----8
A14 1          sand  .2500E+01 .5000E+01           .5000E+00 .2025E+02-.5000E+00
A15 1          sand  .1000E+01 .2000E+01           .5000E+00 .2200E+02-.5000E+00
A16 1          sand  .2500E+01 .5000E+01           .5000E+00 .2375E+02-.5000E+00
A1G 1          sand  .3000E+01 .6000E+01           .5000E+00 .8350E+02-.5000E+00
A15 2          sand  .1000E+01 .2000E+01           .1500E+01 .2200E+02-.5000E+00

COFT ----1----*----2----*----3----*----4----*----5----*----6----*----7----*----8
A14 1A15 1                  2 .1250E+01 .5000E+00 .1000E+01 .1000E+01
A15 1A15 2                  1 .5000E+00 .5000E+00 .1000E+01
A15 1A16 1                  2 .5000E+00 .1250E+01 .1000E+01 .1000E+01

GOFT ----1----*----2----*----3----*----4----*----5----*----6----*----7----*----8

ENDCY----1----*----2----*----3----*----4----*----5----*----6----*----7----*----8
```

Figure 32. TOUGH2 input file for CO_2 injection into a 2-D layered brine formation.

```
 ...ITERATING...  AT [   1,  1] --- DELTEX =  .100000E+03   MAX. RES. =  .158500E+02  AT ELEMENT A15 1  EQUATION   3
 ...ITERATING...  AT [   1,  2] --- DELTEX =  .100000E+03   MAX. RES. =  .710270E+00  AT ELEMENT A15 1  EQUATION   3
 ...ITERATING...  AT [   1,  3] --- DELTEX =  .100000E+03   MAX. RES. =  .252555E-03  AT ELEMENT A15 1  EQUATION   3
 A15 1(   1,  4) ST =  .100000E+03 DT =  .100000E+03 DX1=  .652013E+05 DX2=  .305860E-15 T =  37.000 P = 11065201. S =  .000000E+00
 ...ITERATING...  AT [   2,  1] --- DELTEX =  .200000E+03   MAX. RES. =  .197905E+01  AT ELEMENT A15 1  EQUATION   3
 ...ITERATING...  AT [   2,  2] --- DELTEX =  .200000E+03   MAX. RES. =  .185919E+01  AT ELEMENT A15 1  EQUATION   3
 ...ITERATING...  AT [   2,  3] --- DELTEX =  .200000E+03   MAX. RES. =  .367604E+02  AT ELEMENT A15 2  EQUATION   3
 ...ITERATING...  AT [   2,  4] --- DELTEX =  .200000E+03   MAX. RES. =  .577264E+02  AT ELEMENT A15 2  EQUATION   3
 ...ITERATING...  AT [   2,  5] --- DELTEX =  .200000E+03   MAX. RES. =  .124402E+02  AT ELEMENT A15 2  EQUATION   3
 ...ITERATING...  AT [   2,  6] --- DELTEX =  .200000E+03   MAX. RES. =  .527747E+00  AT ELEMENT A15 2  EQUATION   3
 ...ITERATING...  AT [   2,  7] --- DELTEX =  .200000E+03   MAX. RES. =  .222934E-04  AT ELEMENT A14 2  EQUATION   3
 A15 2(   2,  8) ST =  .300000E+03 DT =  .200000E+03 DX1=  .664859E+05 DX2=  .723780E-07 T =  37.000 P = 11119116. S =  .000000E+00
 ...ITERATING...  AT [   3,  1] --- DELTEX =  .200000E+03   MAX. RES. =  .824732E+00  AT ELEMENT A15 2  EQUATION   3
 ...ITERATING...  AT [   3,  2] --- DELTEX =  .200000E+03   MAX. RES. =  .596875E+01  AT ELEMENT A15 2  EQUATION   3
 ...ITERATING...  AT [   3,  3] --- DELTEX =  .200000E+03   MAX. RES. =  .944035E+00  AT ELEMENT A15 2  EQUATION   3
 ...ITERATING...  AT [   3,  4] --- DELTEX =  .200000E+03   MAX. RES. =  .417340E-01  AT ELEMENT A15 2  EQUATION   3
 ...ITERATING...  AT [   3,  5] --- DELTEX =  .200000E+03   MAX. RES. =  .934024E-04  AT ELEMENT A15 2  EQUATION   3
 A15 2(   3,  6) ST =  .500000E+03 DT =  .200000E+03 DX1=  .959641E+04 DX2= -.963424E-06 T =  37.000 P = 11128712. S =  .000000E+00
...
...
 *rtp7* ... test problem # 7: CO2 in layered formation

         OUTPUT DATA AFTER ( 110,  4)-2-TIME STEPS                                                  THE TIME IS  .300000E+02 DAYS

@@@@@@@@@@@@@@@@@@@@@@@@@@@@@@@@@@@@@@@@@@@@@@@@@@@@@@@@@@@@@@@@@@@@@@@@@@@@@@@@@@@@@@@@@@@@@@@@@@@@@@@@@@@@@@@@@@@@@@@@@@@@@@@@@@@@@

  TOTAL TIME     KCYC    ITER  ITERC    KON        DX1M        DX2M         DX3M          MAX. RES.      NER    KER        DELTEX
  .259200E+07     110       4    733      2       .11897E+05   .19575E-02   .10307E-01     .10526E-10     39     3        .22700E+05

@@@@@@@@@@@@@@@@@@@@@@@@@@@@@@@@@@@@@@@@@@@@@@@@@@@@@@@@@@@@@@@@@@@@@@@@@@@@@@@@@@@@@@@@@@@@@@@@@@@@@@@@@@@@@@@@@@@@@@@@@@@@@@@@@@@@@

 ELEM. INDEX    P          T         SG           SS          XNACL        YH2OG        XCO2aq         PCAP        k-red.      DG          DL
               (Pa)     (deg-C)                                                                      (Pa)                 (kg/m3)     (kg/m3)

 A11 1   1  .13059E+08  37.00  .21767E+00  .00000E+00  .30420E-01  .18787E-02  .49306E-01 -.40090E+04  .10000E+01  771.37    1028.74
 A12 1   2  .13011E+08  37.00  .35418E+00  .00000E+00  .30421E-01  .18767E-02  .49275E-01 -.73367E+04  .10000E+01  770.47    1028.72
 A13 1   3  .12969E+08  37.00  .41391E+00  .00000E+00  .30427E-01  .18751E-02  .49246E-01 -.95948E+04  .10000E+01  769.68    1028.70
 A14 1   4  .12942E+08  37.00  .56149E+00  .00000E+00  .31470E-01  .18729E-02  .48980E-01 -.21328E+05  .10000E+01  769.17    1029.35
 A15 1   5  .12931E+08  37.00  .73398E+00  .00000E+00  .24269E+00  .16120E-02  .16309E-01 -.15074E+06  .10000E+01  768.97    1182.21
 A16 1   6  .12915E+08  37.00  .53472E+00  .00000E+00  .31421E-01  .18719E-02  .48974E-01 -.18012E+05  .10000E+01  768.66    1029.30
 A17 1   7  .12875E+08  37.00  .38596E+00  .00000E+00  .30422E-01  .18713E-02  .49188E-01 -.84467E+04  .10000E+01  767.92    1028.66
 A18 1   8  .12791E+08  37.00  .31805E+00  .00000E+00  .30424E-01  .18679E-02  .49134E-01 -.62687E+04  .10000E+01  766.32    1028.62
 A19 1   9  .12710E+08  37.00  .33097E+00  .00000E+00  .30426E-01  .18645E-02  .49076E-01 -.66303E+04  .10000E+01  764.68    1028.58
 A1A 1  10  .12673E+08  37.00  .49130E+00  .00000E+00  .30428E-01  .18629E-02  .49050E-01 -.14078E+05  .10000E+01  763.92    1028.56
 A1B 1  11  .12651E+08  37.00  .18095E+00  .00000E+00  .30428E-01  .18619E-02  .49034E-01 -.58019E+05  .10000E+01  763.46    1028.55
 A1C 1  12  .12238E+08  37.00  .72424E-01  .00000E+00  .30437E-01  .18433E-02  .48740E-01 -.16112E+04  .10000E+01  754.75    1028.34
 A1D 1  13  .12190E+08  37.00  .00000E+00  .00000E+00  .31816E-01  .10000E+01  .57473E-02  .00000E+00  .10000E+01     .00    1020.08
 A1E 1  14  .12099E+08  37.00  .00000E+00  .00000E+00  .31980E-01  .10000E+01  .63478E-03  .00000E+00  .10000E+01     .00    1019.08
 A1F 1  15  .12009E+08  37.00  .00000E+00  .00000E+00  .31985E-01  .10000E+01  .46419E-03  .00000E+00  .10000E+01     .00    1019.01
...
...
```

Figure 33. Part of printed output for problem of CO_2 injection into a layered brine formation.

Startup of CO_2 injection causes pressures to rise initially, most strongly and rapidly in the well block, and less strongly and with some time delay at more distant locations (Fig. 34). The system quickly establishes quasi-steady flow conditions at the well block (Fig. 35), and the sum of the absolute values of the flow rates quickly approaches the total injection rate of 0.1585 kg/s. As gas saturations increase near the injection point, injection pressures actually decline slowly. The plot of time steps vs. time shows decreasing slope over time (Fig. 34), reflecting an overall trend towards increasing time step sizes as the simulation progresses.

Gas saturations at and near the well block (A15 1) show interesting non-monotonic behavior (Fig. 36), due to an interplay of gas-liquid counterflow, relative permeability effects and precipitation of solid salt. After approximately 4.5×10^6 s, gas saturation at the well block reaches a maximum value of 75.1 % and then declines slowly. This decline is caused by increasing salt precipitation (Fig. 37). Liquid saturation declines rapidly initially, but later almost stabilizes near 20 % (note the logarithmic time scale on Fig. 37), due to capillary-driven inflow of liquid from

neighboring grid blocks. At early time liquid flow is away from the well block, but at approximately $5x10^5$ s liquid flow reverses and subsequently is towards the well block, as capillary pressures there become stronger due to increasing gas saturation (Fig. 38). As time goes on, gas saturations in the blocks adjacent to the well block continue a slow increase (Fig. 36). This reduces relative permeability to liquid, but liquid flow rates into the well block remain essentially constant for a while, because increasing strength of capillary pressure in the well block compensates for the reduction in relative permeability. After approximately 10^7 s, capillary pressure in the well block reaches the cutoff value of 10^7 Pa specified in the input file (Fig. 32). Subsequently the flow of aqueous phase towards the well block brings in less water than is carried out by the gas phase, leading to accelerated precipitation and rapid dry-out. This explains the very rapid increase in gas saturation in the well block at approximately $1.1x10^7$ s. Fig. 36 shows similar patterns of gas saturation behavior in grid blocks neighboring the well block that dry out at later times. The evolution of solid saturations in selected blocks is shown in Fig. 39.

The simulation of this problem previously submitted by LBNL for the code intercomparison project did not generate any solid precipitate (Pruess et al., 2002, 2004). The different behavior seen in the present simulation is due to the much more vigorous removal of water into the flowing gas stream, as compared to the evaporation model for water partitioning into the gas phase that had been used in the earlier calculation. The mechanisms contributing to solid precipitation and formation dry-out near the injection well are believed to be represented realistically in the present simulation, but the space discretization near the injection well is rather coarse, and considerably finer gridding would be needed to achieve accurate results.

Figs. 40-42 show contour maps of pressure, gas saturation, and dissolved CO_2 mass fraction after two years of simulation time. These results are all very similar to our earlier calculations using an evaporation model for water in the CO_2 rich phase. Highest gas saturations of approximately 60 % occur beneath the shale layers at elevations of 52, 85, and 118 m. Gas is just beginning to reach the top shale layer at an elevation of 151 m. CO_2 mass fraction dissolved in the aqueous phase after two years is in the range of 4.5 - 4.85 % throughout most of the two-phase zone, with smaller but significant CO_2 concentrations occurring beyond the two-phase region.

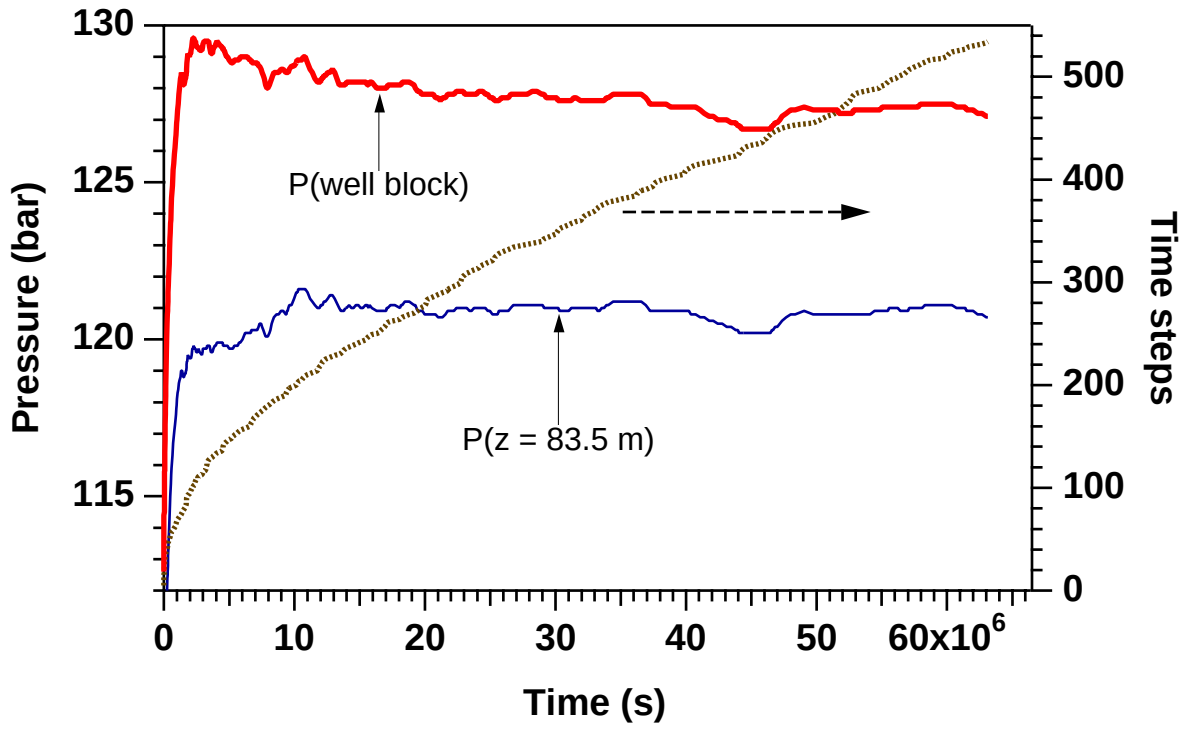

Figure 34. Time evolution of pressures in two grid blocks (A15 1 and A1G 1) and time stepping for CO_2 injection into a layered brine formation.

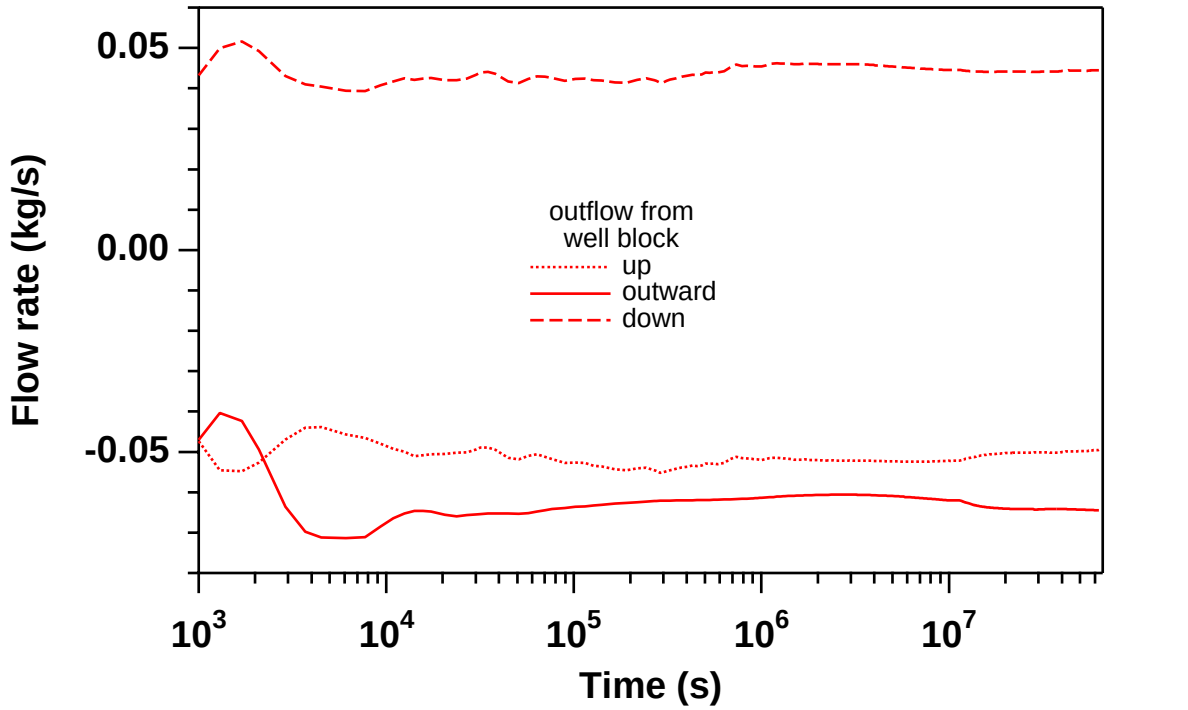

Figure 35. Gas flow rates at the well block. Gas flow is away from the well block, and is plotted as a positive or negative, depending upon whether the well block is the first or second element in a flow connection.

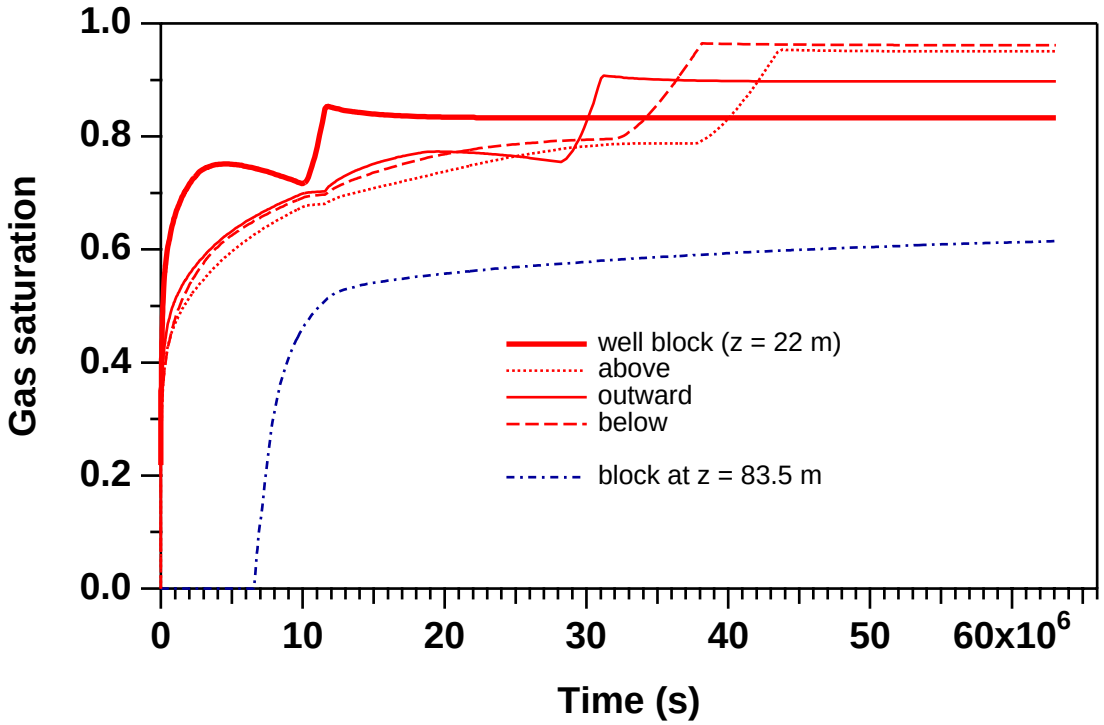

Figure 36. Gas saturations at the well block and its neighbors (above - A16 1; outward - A15 2; below - A14 1). Gas saturations at block A1G 1 at an elevation of 83.5 m (61.5 m above well block) are also shown.

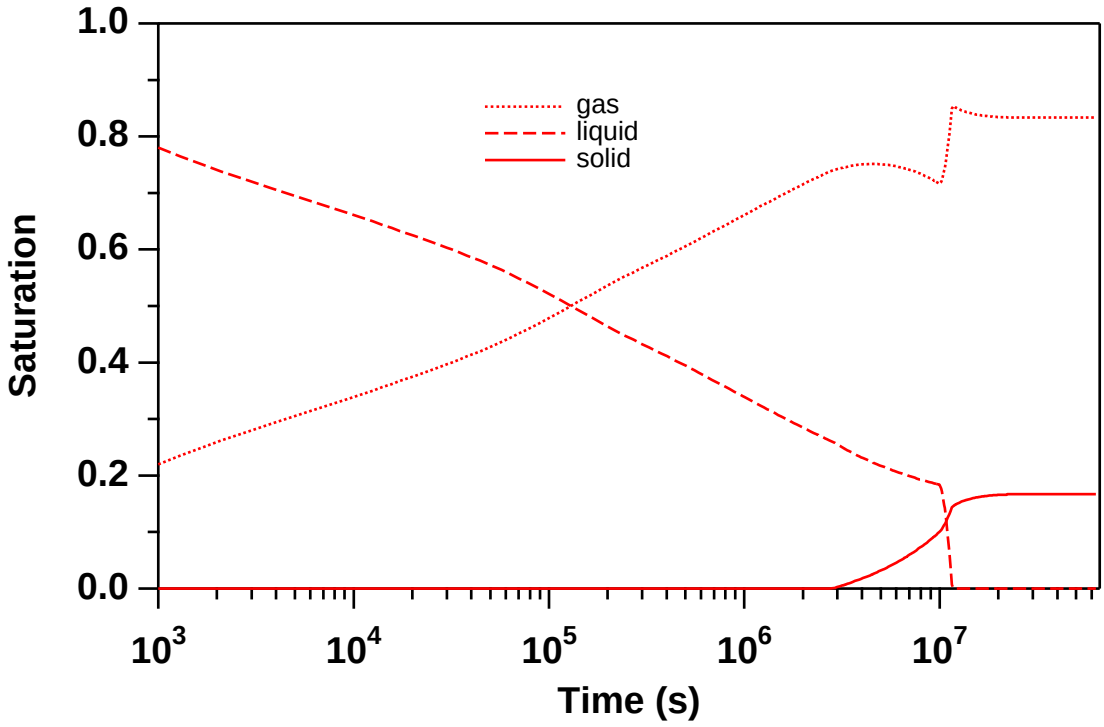

Figure 37. Phase saturations at the well block (A15 1).

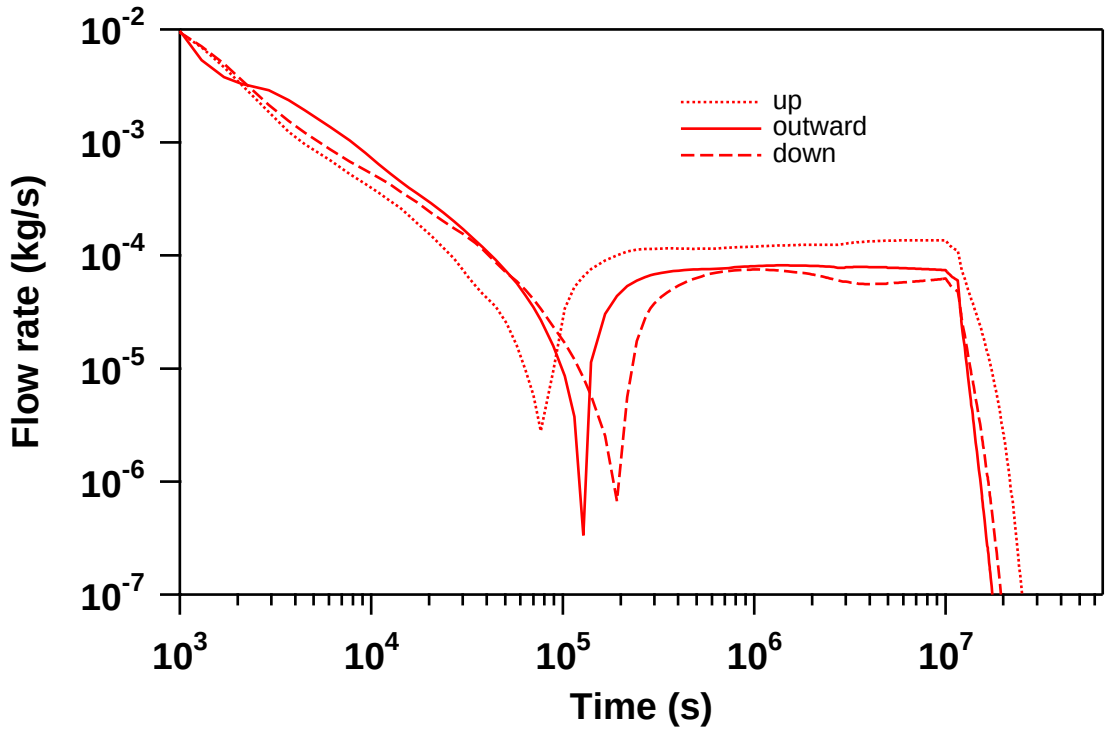

Figure 38. Absolute values of aqueous phase flow rates between the well block and neighboring grid blocks. Up to approximately 10^5 s flow is away from the well block, then reverses.

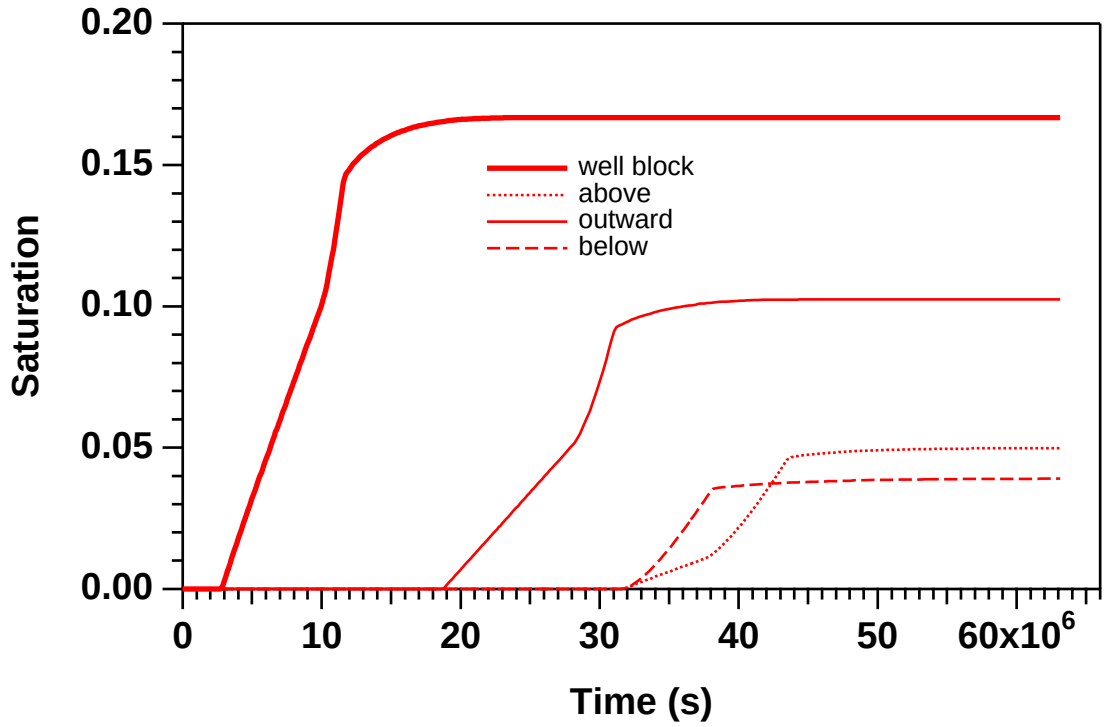

Figure 39. Solid saturations (fraction of void space taken up by solid precipitate) in the well block and its neighbors.

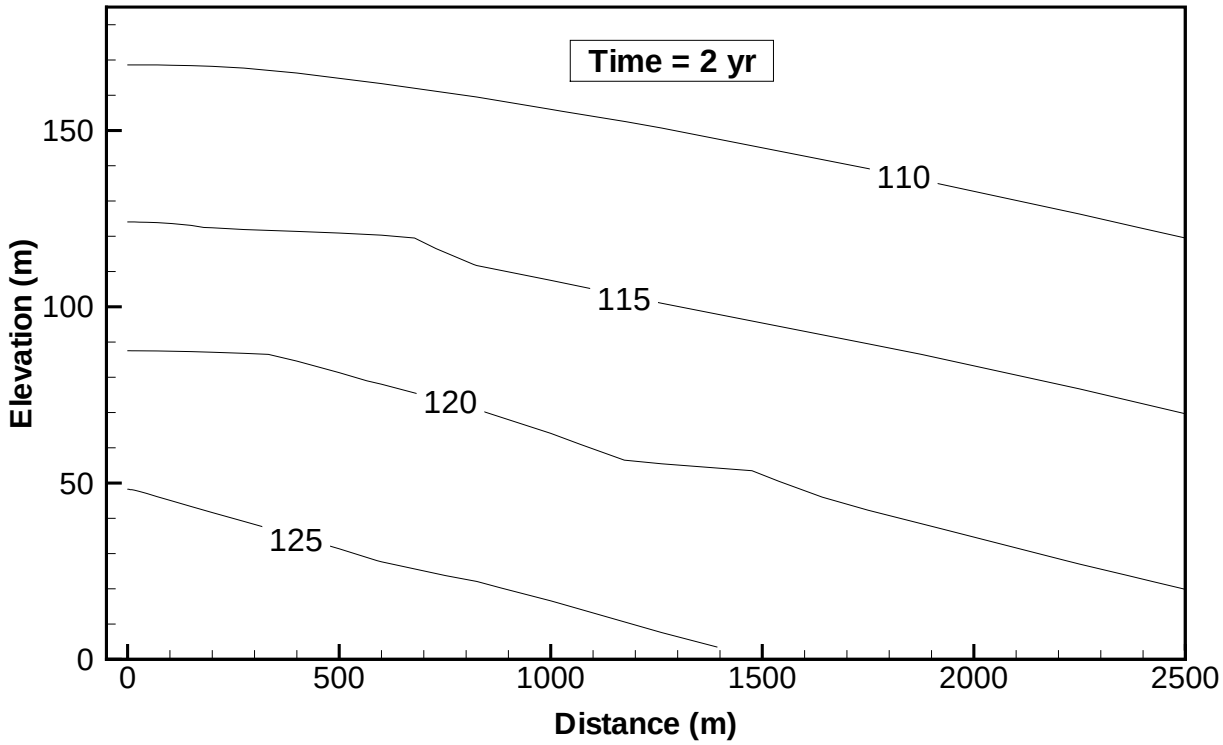

Figure 40. Contour map of fluid pressures after 2 years of CO_2 injection.

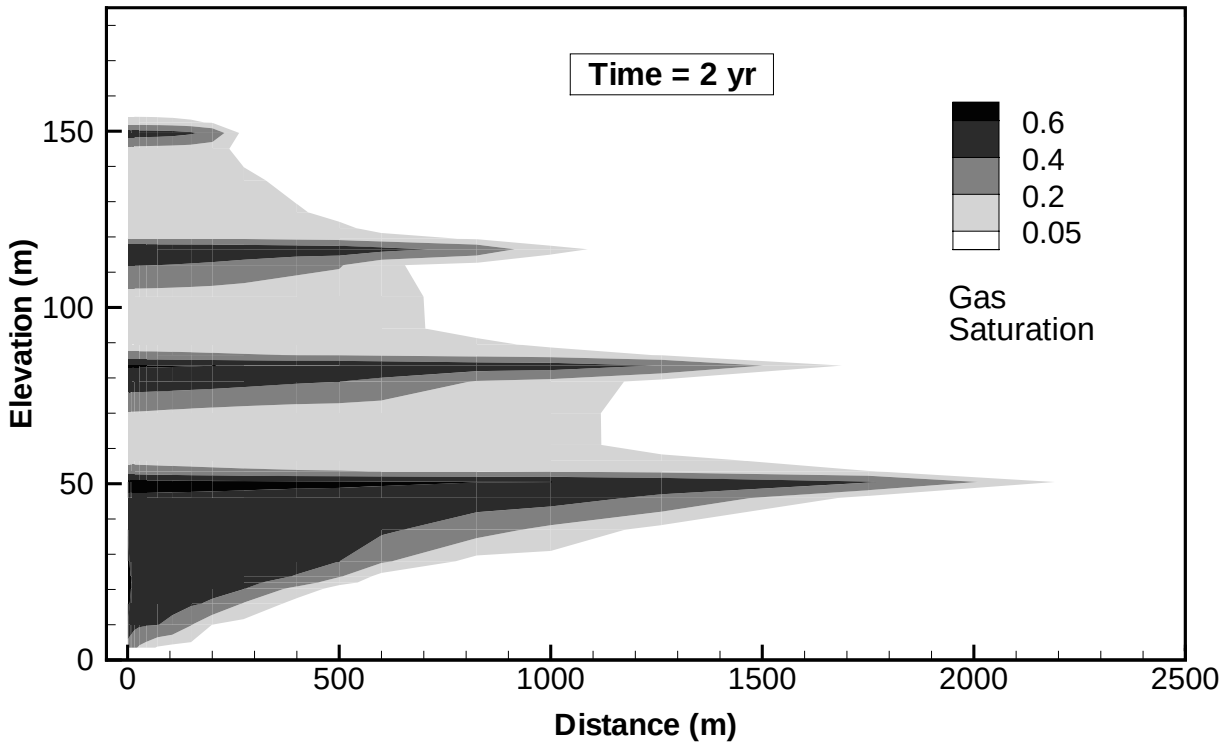

Figure 41. Contour map of gas saturations after 2 years of CO_2 injection.

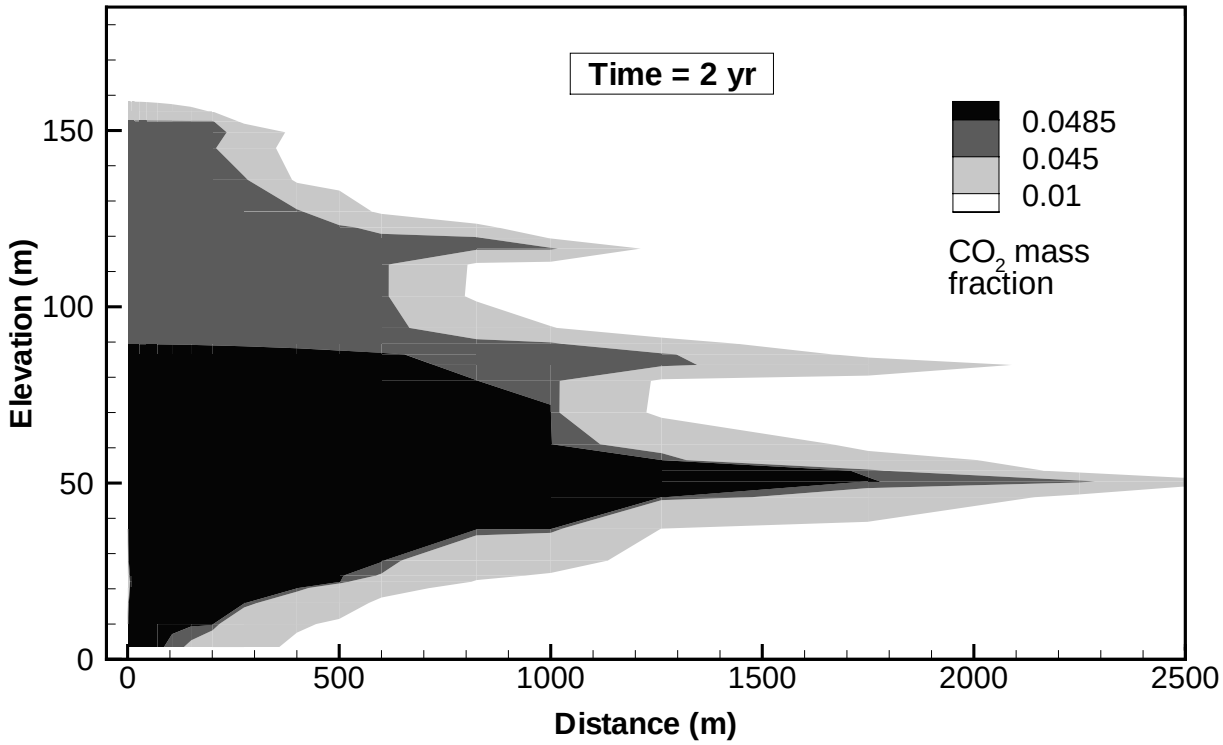

Figure 42. Contour map of dissolved CO_2 mass fractions after 2 years of CO_2 injection.

Table 7. CO_2 inventory (in units of 10^6 kg) for injection into a saline 2-D layered system.

	t = 0	30 days	1 year	2 years
total CO2	0.1787	0.5893	5.178	10.18
CO2 injected	0.0000	0.4108	5.002	10.00
CO2 (aq.)	0.1787	0.2708	1.120	2.037
CO2 (gas)	0.0000	0.3185	4.058	8.140
fraction of CO2 in aq. phase	1.000	0.4596	0.2163	0.2002

6. Concluding Remarks

ECO2N is a new fluid property module for the multiphase, multicomponent simulator TOUGH2, Version 2.0. It provides capabilities for modeling advective and diffusive flow and transport in multidimensional heterogeneous systems containing H_2O - NaCl - CO_2 mixtures. Process capabilities include coupling between fluid and heat flow, partitioning of H_2O and CO_2 among different phases, and precipitation/dissolution of solid salt. The code represents thermophysical properties of brine-CO_2 mixtures generally within experimental accuracy for the range of conditions of interest in geologic disposal of CO_2. A fluid property table provided with ECO2N covers temperatures from ambient to 103 ˚C and pressures from ambient to 600 bar. Software to generate property tables is provided with ECO2N, making possible applications to a more extensive range of conditions. Super- as well as sub-critical conditions may be modeled, but the code currently has no provisions to treat separate liquid and gas CO_2 phases, or transitions between them.

Acknowledgement

Thanks are due to Sally Benson and Jens Birkholzer for a careful review of the manuscript and the suggestion of improvements. This work was supported by the Director, Office of Science, Office of Basic Energy Sciences of the U.S. Department of Energy, and by the Zero Emission Research and Technology project (ZERT) under Contract No. DE-AC03-76SF00098.

References

Altunin, V.V. *Thermophysical Properties of Carbon Dioxide,* Publishing House of Standards, 551 pp., Moscow, 1975 (in Russian).

Andersen, G., A. Probst, L. Murray and S. Butler. An Accurate PVT Model for Geothermal Fluids as Represented by H_2O-NaCl-CO_2 Mixtures, *Proceedings 17th Workshop on Geothermal Reservoir Engineering,* pp. 239 - 248, Stanford, CA, 1992.

Battistelli, A., C. Calore and K. Pruess. The Simulator TOUGH2/EWASG for Modeling Geothermal Reservoirs with Brines and Non-Condensible Gas, *Geothermics*, Vol. 26, No. 4, pp. 437 - 464, 1997.

Chou, I.M. Phase Relations in the System NaCl–KCl–H_2O: III: Solubilities of Halite in Vapor-Saturated Liquids Above 445 ˚C and Redetermination of Phase Equilibrium Properties in the System NaCl–H_2O, *Geochim. Cosmochim. Acta,* Vol. 51, pp. 1965–1975, 1987.

Doughty, C. and K. Pruess. A Similarity Solution for Two-Phase Water, Air and Heat Flow Near a Linear Heat Source in a Porous Medium, *J. of Geophys. Res.,* Vol. 97 (B2), pp. 1821 - 1838, 1992.

Evans, R.D. *The Atomic Nucleus,* Reprint Edition, Robert E. Krieger Publ. Co., Malabar, FL, 1982.

García, J.E. Density of Aqueous Solutions of CO2, Lawrence Berkeley National Laboratory Report LBNL-49023, Berkeley, CA, 2001.

García, J.E. *Fluid Dynamics of Carbon Dioxide Disposal into Saline Aquifers*, PhD Thesis, University of California at Berkeley, December 2003.

Haas, J.L. Jr. Physical Properties of the Coexisting Phases and Thermochemical Properties of the H2O Component in Boiling NaCl solutions, USGS Bulletin 1421-A, Washington, DC, 73 pp., 1976.

Himmelblau, D.M. Partial Molal Heats and Entropies of Solution for Gases Dissolved in Water from the Freezing to the Near Critical Point, *J. of Phys. Chem.,* Vol. 63, pp. 1803–1808, 1959.

Hitchon, B. (ed.). *Aquifer Disposal of Carbon Dioxide,* Geoscience Publishing, Ltd., Sherwood Park, Alberta, Canada, 1996.

International Formulation Committee. *A Formulation of the Thermodynamic Properties of Ordinary Water Substance,* IFC Secretariat, Düsseldorf, Germany, 1967.

Kongsjorden, H., O. Karstad and T.A. Torp. Saline Aquifer Storage of Carbon Dioxide in the Sleipner Project, *Waste Management,* Vol. 17, No. 5/6, pp. 303 - 308, 1997.

Lindeberg, E., P. Bergmo and A. Moen. The Long-Term Fate of CO2 Injected into an Aquifer, paper G1-4, presented at Sixth International Conference on Greenhouse Gas Technologies (GHGT-6), Kyoto, Japan, October 1-4, 2002.

Lorenz, S., D. Maric and C. Rirschl. Eine analytische Funktion zur Bestimmung der Enthalpie wässriger NaCl Lösungen, draft report, Institut für Sicherheitstechnologie, Köln, Germany, April 2000.

Michaelides, E.E. Thermodynamic Properties of Geothermal Fluids, Geothermal Resources Council Transactions, Vol. 5, pp. 361 - 364, 1981.

Miller, A.B. A Brine-Steam Properties Computer Program for Geothermal Energy Calculations, Lawrence Livermore National Laboratory Report UCRL-52495, Livermore, CA, June 1978.

O'Sullivan, M.J. A Similarity Method for Geothermal Well Test Analysis, *Water Resour. Res.*, Vol. 17, No. 2, pp. 390 – 398, 1981.

Phillips, S.L., A. Igbene, J.A. Fair, H. Ozbek and M. Tavana. A Technical Databook for Geothermal Energy Utilization, Lawrence Berkeley National Laboratory Report LBL-12810, Berkeley, CA, 46 pp., 1981.

Prausnitz, J. M., R. N. Lichtenthaler, and E. G. de Azevedo. *Molecular Thermodynamics of Fluid-Phase Equilibria*, Prentice-Hall Inc., Englewood Cliffs, N. J., 1986.

Pruess, K. The TOUGH Codes—A Family of Simulation Tools for Multiphase Flow and Transport Processes in Permeable Media, *Vadose Zone J.*, Vol. 3, pp. 738 - 746, 2004.

Pruess, K., C. Oldenburg and G. Moridis. TOUGH2 User's Guide, Version 2.0, Lawrence Berkeley National Laboratory Report LBNL-43134, Berkeley, CA, November 1999.

Pruess, K. and J. García. Multiphase Flow Dynamics During CO2 Injection into Saline Aquifers, *Environmental Geology*, Vol. 42, pp. 282 - 295, 2002.

Pruess, K., J. García, T. Kovscek, C. Oldenburg, J. Rutqvist, C. Steefel and T. Xu. Intercomparison of Numerical Simulation Codes for Geologic Disposal of CO2, Lawrence Berkeley National Laboratory Report LBNL-51813, Berkeley, CA 94720, December 2002.

Pruess, K., J. García, T. Kovscek, C. Oldenburg, J. Rutqvist, C. Steefel and T. Xu. Code Intercomparison Builds Confidence in Numerical Simulation Models for Geologic Disposal of CO2, *Energy*, Vol. 29, Issues 9-10, pp. 1431-1444, doi:10.1016/j.energy.2004.03.077, July-August 2004.

Span, R. and W. Wagner. A New Equation of State for Carbon Dioxide Covering the Fluid Region from the Triple-Point Temperature to 1100 K at Pressures up to 800 MPa, *J. Phys. Chem. Ref. Data*, Vol. 25, No. 6, pp. 1509 - 1596, 1996.

Spycher, N., K. Pruess and J. Ennis-King. CO_2-H_2O Mixtures in the Geological Sequestration of CO_2. I. Assessment and Calculation of Mutual Solubilities from 12 to 100 °C and up to 600 bar, *Geochim. Cosmochim. Acta*, Vol. 67, No. 16, pp. 3015 - 3031, doi:10.1016/S0016-7037(03)00273-4, 2003.

Spycher, N. and K. Pruess. CO_2-H_2O Mixtures in the Geological Sequestration of CO_2. II. Partitioning in Chloride Brines at 12–100 ˚C and up to 600 bar, *Geochim. Cosmochim. Acta*, Vol. 69, No. 13, pp. 3309–3320, doi:10.1016/j.gca.2005.01.015, 2005.

Vargaftik, N.B. *Tables on the Thermophysical Properties of Liquids and Gases*, 2nd Ed., John Wiley & Sons, New York, NY, 1975.

Verma, A. and K. Pruess. Thermohydrologic Conditions and Silica Redistribution Near High-Level Nuclear Wastes Emplaced in Saturated Geological Formations, *Journal of Geophysical Res.*, Vol. 93 (B2), pp. 1159-1173, 1988.

APPENDIX A

Code Intercomparison Problem 3: Radial Flow from a CO2 Injection Well[&]

1. INTRODUCTION AND GENERAL DESCRIPTION

This problem addresses two-phase flow of CO2 and water for simplified flow geometry and medium properties. The aquifer into which injection is made is assumed infinite-acting, homogenoeus, and isotropic. Gravity and inertial effects are neglected, injection is made at a constant mass rate, and flow is assumed 1-D radial (line source). Under the conditions stated the problem has a similarity solution where dependence on radial distance R and time t occurs only through the similarity variable $\xi = R^2/t$ (O'Sullivan 1981; Doughty and Pruess 1992).

2. LIST OF PROCESSES BEING STUDIED

Two-phase flow of CO2 and water subject to relative permeability and capillary effects.
Change of fluid density, viscosity, and CO2 solubility with pressure and salinity.
Formation dry-out with precipitation of salt.

3. DEFINITION OF THE PROBLEM AND INPUT DATA

Problem parameters are summarized in Tables A.1 and A.2.

4. PROBLEM VARIATIONS

Neglect salinity of the aqueous phase. Include non-isothermal effects. Include permeability changes due to precipitation. Inject gas that is 50 % CO2, 50 % N2.

5. DEFINITION OF RESULTS TO BE CALCULATED

Data on CO2 and brine density and viscosity, and CO2 solubility, for the range of thermodynamic conditions encountered in the problem. Gas saturation, dissolved CO2 mass fraction, fraction of void space containing precipitated salt, and fluid pressure as functions of the similarity variable $\xi = R^2/t$. (Use both profiles at constant time and time-series data at a specific location for plotting.)

6. COMPARISON CRITERIA

Results should match within +/- 5 %.

7. REFERENCES

Corey, A.T. The Interrelation Between Gas and Oil Relative Permeabilities, *Producers Monthly*, pp. 38 - 41, November 1954.

[&] proposed by Karsten Pruess; e-mail: K_Pruess@lbl.gov

Doughty, C. and K. Pruess. A Similarity Solution for Two-Phase Water, Air and Heat Flow Near a Linear Heat Source in a Porous Medium, *J. of Geophys. Res.*, 97 (B2), 1821-1838, 1992.

O'Sullivan, M.J. A Similarity Method for Geothermal Well Test Analysis, *Water Resour. Res.*, Vol. 17, No. 2, pp. 390 – 398, 1981.

van Genuchten, M.Th. A Closed-Form Equation for Predicting the Hydraulic Conductivity of Unsaturated Soils, *Soil Sci. Soc. Am. J.*, Vol. 44, pp. 892 - 898, 1980.

Table A.1 Hydrogeologic parameters.

Permeability	$k = 10^{-13}$ m^2
Porosity	$\phi = 0.12$
Pore compressibility	$c = 4.5 \times 10^{-10}$ Pa^{-1}
Aquifer thickness	100 m
Relative permeability	
liquid: van Genuchten function (1980) $k_{rl} = \sqrt{S^*}\left\{1-\left(1-\left[S^*\right]^{1/\lambda}\right)^{\lambda}\right\}^2$	$S^* = (S_l - S_{lr})/(1 - S_{lr})$
irreducible water saturation exponent	$S_{lr} = 0.30$ $\lambda = 0.457$
gas: Corey curve (1954) $k_{rg} = \left(1-\hat{S}\right)^2\left(1-\hat{S}^2\right)$	$\hat{S} = \dfrac{(S_l - S_{lr})}{(1 - S_{lr} - S_{gr})}$
irreducible gas saturation	$S_{gr} = 0.05$
Capillary pressure	
van Genuchten function (1980) $P_{cap} = -P_0\left(\left[S^*\right]^{-1/\lambda} - 1\right)^{1-\lambda}$	$S^* = (S_l - S_{lr})/(1 - S_{lr})$
irreducible water saturation exponent strength coefficient	$S_{lr} = 0.0$ $\lambda = 0.457$ $P_0 = 19.61$ kPa

Table A.2 Initial conditions and injection specifications

Pressure	120 bar
Temperature	45 ˚C
Salinity	15 wt.-% NaCl
CO2 injection rate	100 kg/s

APPENDIX B

Code Intercomparison Problem 4: CO2 Discharge Along a Fault Zone*

1. INTRODUCTION AND GENERAL DESCRIPTION

This problem explores CO2 loss from storage through a leaky fault, using a highly simplified 1-D linear flow geometry. It is envisioned that an aquifer into which CO2 disposal is made is intersected by a vertical fault, which establishes a connection through an otherwise impermeable caprock to another aquifer 500 m above the storage aquifer (Fig. B.1a). This situation is idealized by assuming 1-D flow geometry and constant pressure boundary conditions as shown in Fig. B.1b (Pruess and García, 2000).

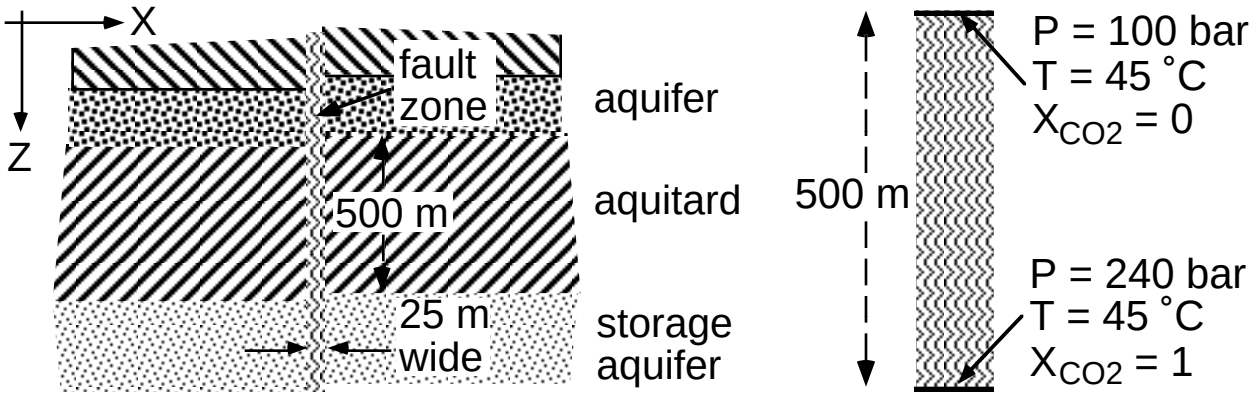

(a) (b)

Figure B.1 Schematic of the fault zone model (a) and applied boundary conditions (b).

2. LIST OF PROCESSES BEING STUDIED

Immiscible displacement of water by CO2 subject to pressure, gravity, and capillary pressure effects.

Change of fluid density, viscosity, and CO2 solubility with pressure.

Formation dry-out.

3. DEFINITION OF THE PROBLEM AND INPUT DATA

Hydrogeologic parameters are identical to those of problem 3 (Table A.1), except that porosity is increased to 35 %. The fault zone is assumed to be 25 m wide and 500 m tall, with boundary conditions as given in Fig. B.1b. The reservoir fluid is assumed to be pure water (no salinity). Initial conditions are pressures in hydrostatic equilibrium relative to P = 100 bar at the top; temperature is held constant at T = 45 ˚C throughout.

---

* proposed by Karsten Pruess; e-mail: K_Pruess@lbl.gov

4. PROBLEM VARIATIONS

Include salinity of the aqueous phase and permeability changes due to precipitation. Include non-isothermal effects. Assume gas composition is 50 % CO2, 50 % N2.

5. DEFINITION OF RESULTS TO BE CALCULATED

Data on CO2 and water density and viscosity, and CO2 solubility, for the range of thermodynamic conditions encountered in the problem. Vertical profiles of gas saturation, fluid pressure, and dissolved CO2 mass fraction at different times. CO2 inventory in gas and liquid phases after 10^7 seconds. Mass flow rates of CO2 at the bottom and of water at the top vs. time (normalized for a 1 m thick section).

6. COMPARISON CRITERIA

Results should match to with +/- 5 %.

7. REFERENCES

Pruess, K. and J. García. Multiphase Flow Dynamics During CO2 Injection into Saline Aquifers, *Environmental Geology*, Vol. 42, pp. 282 - 295, 2002.

APPENDIX C

Code Intercomparison Problem 7: CO_2 Injection into a 2-D Layered Brine Formation[#]

1. INTRODUCTION AND GENERAL DESCRIPTION

This test problem is patterned after the CO_2 injection project at the Sleipner Vest field in the Norwegian sector of the North Sea, and is intended to investigate the dominant physical processes associated with the injection of supercritical CO_2 into a layered medium. Significant simplifications have been made, the most important of which is the assumption of isothermal conditions (37 ˚C, the ambient temperature of the formation). CO_2 injection rates (1,000,000 tonnes per year), system geometry, and system permeabilities correspond approximately to those at Sleipner, although no attempt was made to represent details of the permeability structure within the host formation. Injection of the supercritical CO_2, which is less dense than the saline formation waters into which it is injected, causes it to rise through the formation. Its rate of ascent, however, is limited by the presence of four relatively low permeability shales. The top and bottom of the formation is assumed to be impermeable. The only reactive chemistry considered in this problem is the dissolution of CO_2 in the aqueous phase.

2. LIST OF PROCESSES BEING STUDIED

a) Gravity-driven advection in response to strong vertical and lateral density gradients induced by the injection of CO_2 into saline formation water.
b) Density, viscosity, and solubility formulations of water and CO_2 as a function of pressure and temperature (P and T).

3. DEFINITION OF THE PROBLEM AND INPUT DATA

System Geometry:

The system is idealized as a two dimensional symmetric domain perpendicular to the horizontal injection well which has a screen length of 100 meters (Figure C.1). A one meter thick section perpendicular to the horizontal well is considered. The thickness of the formation at the injection site is 184 meters. The injection point is 940 meters below the sea floor, while the ocean depth at the site is 80 meters. The formation is assumed to consist of four lower permeability shale units 3 meters thick which are distributed within the high permeability sand. Each shale unit is separated by 30 meters. The well is 30 meters below the lowest shale unit, while the bottom of the aquifer is another 22 meters below the well.

[#] proposed by Carl Steefel; e-mail: CISteefel@lbl.gov

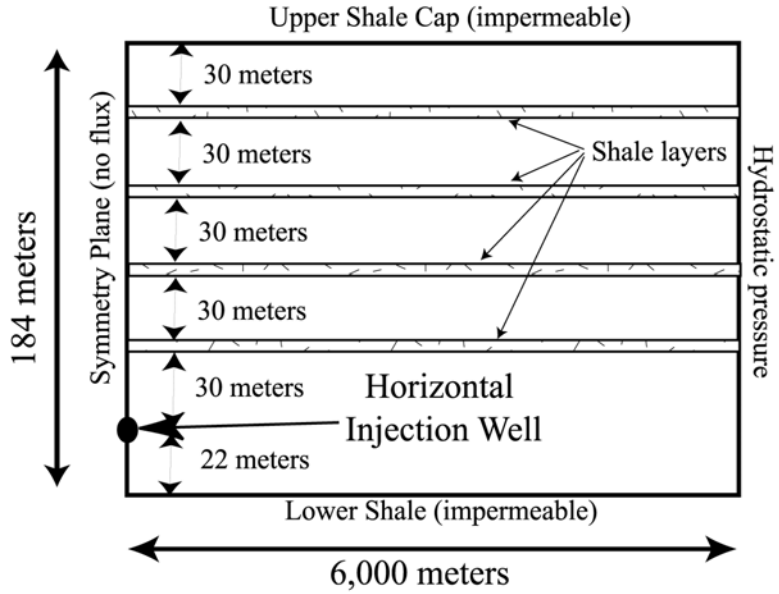

Figure C.1 Schematic representation of geometry for CO2 injection in Utsira Formation.

Boundary conditions:

No heat or mass flux is allowed across any of the boundaries except the vertical boundary 6,000 meters from the injection well. This boundary is fixed at hydrostatic pressure, thus allowing flow into and out of the domain so as to avoid overpressuring the formation. The 6,000 meter boundary is chosen, however, to be far enough from the injection well that the CO_2 does not reach this boundary after 2 years of injection.

Initial conditions (Table C.1):

a) T = 37 ˚C (isothermal throughout)
b) P = hydrostatic (approximately 110 bars at injection point, approximately 90 bars at top of formation).
c) CO_2 in the aqueous phase in equilibrium with a P_{CO2} of 0.5 bars, a typical value for sedimentary formation waters at the temperature we are considering.

Table C.1 Initial conditions and injection specifications

Pressure at well	110 bar
Temperature	37 ˚C
Salinity	3.2 wt.-% NaCl
CO2 injection rate	0.1585 kg/s in half space

Injection specifications (Table C.1):

a) Temperature = 37 ˚C
b) Injection rate: 31.7 kg/s over entire screen length (100 meters), corresponding to 0.317 kg/s for the 1 meter thick section considered. Because of symmetry, injection rate in half space is therefore 0.1585 kg/s.
c) Height of well cell: 1 meter.
d) Injection time scale: 2 years

Input data (Table C.2):

a) Capillary pressure and liquid relative permeability described with van Genuchten (1980) functions; gas relative permeability after Corey (1954). Porosity is 35% for sands, 10.25 % for shales.
b) Fully saturated permeability ($k = 3 \times 10^{-12}$ m^2 in sand layers, $10^{-14} m^2$ in shales)
c) Density, viscosity, and solubility in water of CO_2 as functions of P and T (Span and Wagner, 1996).
d) Vapor-liquid equilibrium properties of water.

4. PROBLEM VARIATIONS

Include non-isothermal effects by making the CO_2 injection temperature equal to 65 ˚C.

5. RESULTS TO BE CALCULATED

Liquid and gas saturations as a function of space and time. CO_2 concentration in the aqueous phase as a function of space. Gas and liquid fluxes.

6. COMPARISON CRITERIA

Results should match within +/- 5%.

IMPORTANT NOTICE

A first version of this test problem had specified that gas relative permeability was to be calculated from a van Genuchten function. In a workshop held in October 2001 in Berkeley, participants in the code intercomparison project agreed to change this specification to using a Corey (1954) curve instead, with parameters as given in Table C.2. In two subsequently issued laboratory reports with results of the code intercomparison project (Pruess and García, 2002; Pruess et al., 2002), the original van Genuchten specifications were inadvertently retained, even though all simulations had used the altered (Corey, 1954) specifications.

Table C.2 Hydrogeologic parameters

Permeability Porosity Aquifer thickness	Sands: $3x10^{-12}$ m^2; Shales: $10^{-14}m^2$ Sands: $\phi = 0.35$; Shales: $\phi = 0.1025$ 184 m
Relative permeability	
liquid: van Genuchten function (1980) $k_{rl} = \sqrt{S^*}\left\{1-\left(1-\left[S^*\right]^{1/\lambda}\right)^{\lambda}\right\}^2$ irreducible water saturation exponent	$S^* = \left(S_l - S_{lr}\right)/\left(1 - S_{lr}\right)$ $S_{lr} = 0.20$ $\lambda = 0.400$
gas: Corey (1954) $k_{rg} = \left(1-\hat{S}\right)^2\left(1-\hat{S}^2\right)$ irreducible water saturation irreducible gas saturation	$\hat{S} = \left(S_l - S_{lr}\right)/\left(1 - S_{lr} - S_{gr}\right)$ $S_{lr} = 0.20$ $S_{gr} = 0.05$
Capillary pressure	
van Genuchten function (1980) $P_{cap} = -P_0\left([S^*]^{-1/\lambda} - 1\right)^{1-\lambda}$ irreducible water saturation exponent strength coefficient	$S^* = \left(S_l - S_{lr}\right)/\left(1 - S_{lr}\right)$ $S_{lr} = 0.20$ $\lambda = 0.400$ Sand: $P_0 = 3.58$ kPa; Shale: $P_0 = 62.0$ kPa

7. REFERENCES

Corey, A.T. The Interrelation Between Gas and Oil Relative Permeabilities, *Producers Monthly*, 38-41, November 1954.

Pruess, K. and J. García. Solutions of Test Problems for Disposal of CO2 in Saline Aquifers, Lawrence Berkeley National Laboratory Report LBNL-51812, December 2002.

Pruess, K., J. García, T. Kovscek, C. Oldenburg, J. Rutqvist, C. Steefel and T. Xu. Intercomparison of Numerical Simulation Codes for Geologic Disposal of CO2, Lawrence Berkeley National Laboratory Report LBNL-51813, Berkeley, CA 94720, December 2002.

van Genuchten, M.Th. A Closed-Form Equation for Predicting the Hydraulic Conductivity of Unsaturated Soils, *Soil Sci. Soc. Am. J.*, Vol. 44, pp. 892 - 898, 1980.

Span, R. and W. Wagner. A New Equation of State for Carbon Dioxide Covering the Fluid Region from the Triple-Point Temperature to 100 K at Pressures up to 800 MPa, *J. Phys. Chem. Ref. Data*, Vol. 25, No. 6, pp. 1509 - 1596, 1996.